Universidad de A Coruña

# Synthesis and characterization of nano and microparticles of biopolymers for food packaging applications.

Yousof Farrag

Doctoral Thesis

2017

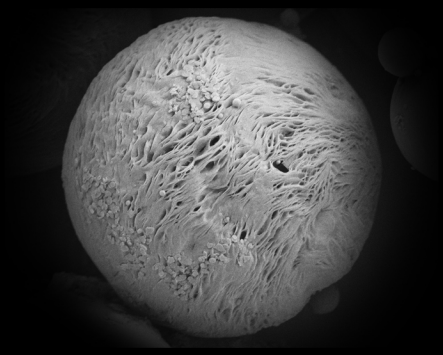

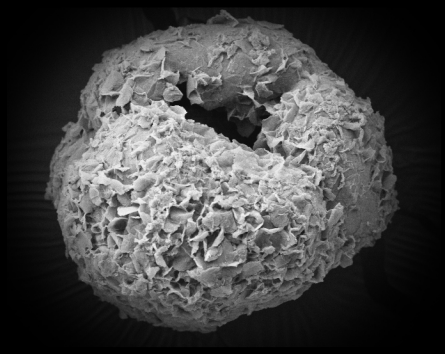

Departamento de Física y Ciencias de la Tierra

UNIVERSIDADE DA CORUÑA

Luis Fernando Barral Losada y Rebeca Bouza Padín, como directores de la Tesis Doctoral de Yousof Ramadan Farrag AbdEl Hafez, con NIE nº Y2216064M, autorizamos su presentación para depósito.

Luis F. Barral Losada

Rebeca Bouza Padín

# Synthesis and characterization of nano and microparticles of biopolymers for food packaging applications.

Author: Yousof Farrag

Doctoral Thesis UDC / 2017

Directors: Dr. Rebeca Bouza Padín

and

Dr. Luis Fernando Barral Losada

Doctoral program of Applied Physics

UNIVERSIDADE DA CORUÑA

**To my Parents**

# Acknowledgments

It is only my name will be written as the author of this work, but in fact many people deserve to have their names there, even before mine.

I would like to start thanking my parents. You have been by my side during all my entire life and especially during the master and the PhD research. You believed in me, supported and encouraged me with all that you could. Without you, all this work would not have been possible. No words would be sufficient to thank you. I love you so much. Thanks a lot, from all my heart.

I would like to express my gratitude to my supervisors: prof. Luis Barral and prof. Rebeca Bouza. Thank you for your confidence in me, supporting me, being patients with me, for all what I have learned from you and for motivating me especially in the difficult moments. Luis, you taught me a lot, at the scientific level and in general life aspects. I am eternally grateful to you for your continuous help and support. At the same time, you did encourage me to try and develop my own ideas. Thank you.

Nasim, thank you for supporting me during these years. You had to put up with me during very hard moments, thank you for your

patience and for all what you have done for me. I have to thank you also for translating the spanish parts of this thesis.

To my sisters Omima and Mariam, many thanks to you for your support. I am lucky to have you in my life.

I would like to acknowledge the help and support I received from the people of the (Centro de Investigación de Polímeros Avanzados, CIPA, Chile). Dr. Saddys Rodríguez-Llamazares, thank you for the time, the effort and the contributions to this work. To Walther Ide, Constanza Sabando and Natalia Pettinelli, thank you for your collaboration and for the effort you put into this work.

To prof. Tomas Torres, you opened to me the door to the investigation here in Spain. It is an honour to be your student. I am grateful for all what you have done for me.

To my friend Hytham Ahmad, it is really hard to find a sincere person like you in these days. You guided me to my first steps to the scientific research. Thank you.

Prof. Jorge Rubio, you led my first steps in the research laboratory. It is an honour to say that I have worked with you for three years. I learned a lot from you and you are being my reference. Thank you.

Prof. Enrique Lopez Cabarcos, thank you for your advices. I have learned a lot from our discussions. It was an honour working with you.

I would like to thank all the members of the group of polymers especially Sara, Belén, Maite, Jesús, María del Carmen, Javier and Joaquin. Thank you all for your support. My special thanks to the lab technician, Ángeles, for your effort and precise work.

I would not forget my friends and colleagues from the Complutense University of Madrid: Paulino, Marco, David, Diego, Ana and Monte. I spent an amazing time with you. I have learned a lot from all of you. Thank you.

Many thanks to everyone who helped me during this work. Belen Cuesta from CiMUS; Raquel Antón, the FESEM technician; Dr. Alberto Nuñez from the structural analysis unit of SAI, thank you all for your contributions.

Thanks to everyone who taught me even a letter in my life, to all my friends, teachers and all my family.

Finally, I would like to thank the Spanish Ministry of Economy and Finance for the grant BES-2014-069932 received during the thesis period (Ayudas para contratos predoctorales para

la formación de doctores) which is linked to the scientific project (MAT2013-41892-R, Project NanoCompBioPol). Also thanks to Nanobiofar research group in the Centre for Research in Molecular Medicine and Chronic Diseases (CiMUS), Universidade de Santiago de Compostela (USC) and to MatNaBio research group at the department of Physical-Chemistry II of the Faculty of Pharmacy of the Complutense University of Madrid (UCM) where some experiments were performed.

# Abstract

The main aim of this thesis is the preparation and characterization of nano and microparticles of selected biopolymers addressed for food packaging and active food packaging applications.

Two biopolymers have been selected for the nano and microparticles preparations: poly(3-hydroxybutyrate-co-3-hydroxyvalerate) (PHBV) and starch. The results for the PHBV showed spherical porous particles with wide variety of size distribution depending on the selected techniques and the procedure conditions. Starches from different botanical origins were used for preparing starch nanoparticles and starch/quercetin nanoparticles using the nanoprecipitation technique. The loading capacity, the release profile of the quercetin from the nanoparticles and therefore the antioxidant activity changed by changing the starch origin.

Starch microparticles with donut-shaped morphology were prepared from starches of two different botanical origins and then loaded to thermoplastic starch (TPS) films. The TPS loaded with microparticles showed better thermal stability, less water vapour and oxygen transmission rates. The donut-shaped microparticles were

also used as a carrier for quercetin within TPS films. The quercetin kept releasing during 4 to 11 days depending on the starch origin.

The produced nano and microparticles provide many possibilities for improving some properties of the biopolymeric packaging films with the capacity for active delivery function for reasonable periods.

# Resumen

El objetivo de esta tesis es la preparación y caracterización de nano y micropartículas de biopolímeros para su uso en envases y embalajes alimentarios convencionales y activos.

Se seleccionaron dos biopolímeros: Poli(3-hidroxibutirato-co-3-hidroxivalerato) (PHBV) y almidón. Para el PHBV, los resultados mostraron partículas esféricas y porosas con una amplia variedad en la distribución de tamaños, en función de la técnica utilizada y las condiciones de preparación. Se han utilizado también almidones de diferentes orígenes botánicos en la preparación de las nanopartículas tanto de almidón solo como de almidón cargado con quercetina. La capacidad de carga, el perfil de liberación y el consiguiente cambio en la actividad antioxidante de la quercetina varía según el origen del almidón.

Se prepararon micropartículas con forma de donut de dos almidones de diferente origen para su uso como relleno en filmes de almidones termoplásticos (TPS). Estos TPS cargados con las micropartículas mostraron mejor estabilidad térmica y menores tasas de transmisión de vapor de agua y oxígeno. Estas micropartículas se utilizaron también como portadores de quercetina dentro de los TPS.

Las nano y micropartículas producidas proporcionan muchas posibilidades para mejorar algunas de las propiedades de los biofilmes usados en la industria de envase y embalaje alimentario y les confieren capacidad de liberación de compuestos activos durante periodos razonables.

# Resumo

O obxectivo desta tese é a preparación e caracterización de nano e micropartículas de biopolímeros para o seu uso en envases e embalaxes alimentarios convencionais e activos.

Seleccionáronse dous biopolímeros: Poli(3-hidroxibutirato-co-3-hidroxivalerato (PHBV) e amidón. No caso do PHBV, os resultados amosaron partículas esféricas e porosas cunha ampla variedade na distribución de tamaños en función da técnica utilizada e as condicións de preparación.

Tamén, utilizáronse amidóns de orixes botánicas diferentes na preparación das nanopartículas, tanto as de só amidón como as de amidón cargado con quercetina. A capacidade de carga, o perfil de liberación e o cambio na actividade antioxidante da quercetina varía segundo a orixe do amidón.

Ademais preparáronse micropartículas coa forma de donut de dous amidóns de orixe botánica diferente para o seu uso como recheo en filmes de amidóns termoplásticos TPS. Estes amosaron mellor estabilidade térmica e menores taxas de transmisión de vapor de auga e osíxeno. Estas micropartículas usáronse tamén como portadores de quercetina dentro dos filmes de TPS.

As nano e micropartículas producidas proporcionan moitas posibilidades de mellora de algunha das propiedades dos biofilmes empregados na industria do envase e embalaxe alimentario, conferíndolles capacidade de liberación de compostos activos durante períodos razoables de tempo.

# Table of contents

# List of figures

# List of tables

# Abbreviations

| | |
|---|---|
| ABS | Acrylonitrile-butadiene-styrene |
| CNC | Cellulose nanocrystals |
| DLS | Dynamic light scattering |
| DNA | Deoxyribonucleic acid |
| DSC | Differential scanning calorimetry |
| FESEM | Field emission scanning electron microscopes |
| GHG | Greenhouse gases |
| HDPE | High-density polyethylene (HDPE) |
| HV | Hydroxyvalerate |
| LDPE | Low-density polyethylene |
| OTR | Oxygen transmission rate |
| PBS | Polybutylene succinate |
| PCL | Polycaprolactone |
| PES | Polyester |
| PET | Polyethylene terephthalate |
| PHAs | Polyhydroxyalkanoates |
| PHB | Polyhydroxybutyrate |
| PHBV | Poly(3-hydroxybutyrate-co-3-hydroxyvalerate) |
| PLA | Polylactic acid |
| PP | Polypropylene |
| PS | Polystyrene |
| PUR | Polyurethane |
| PVA | Poly(vinyl alcohol) |
| PVC | Polyvinyl chloride |
| PVD | Physical vapour deposition |
| RNA | Ribonucleic acid |
| SDSC | Step-scan differential scanning calorimetry |

| | |
|---|---|
| SEM | Scanning electron microscopy |
| SLS | Static light scattering |
| TGA | Thermogravimetric analysis |
| TPS | Thermoplastic starch |
| WAXRD | Wide angle X-ray diffraction |
| WVTR | Water vapour transmission rate |
| XRD | X-ray diffraction |

# 1. Introduction

## 1. Plastics

Plastics are materials that can be shaped by applying heat or pressure. Most plastics are made from polymeric synthetic resins, although a few are based on natural substances (Daintith, 2008). They are normally organic polymers of high molecular weight and the majority are derived from petroleum sources. A polymer is a substance that has large molecules consisting of repeated units. The most common plastics that are used today include (in order of the european demand) polypropylene (PP), low-density polyethylene (LDPE), high-density polyethylene (HDPE), polyvinyl chloride (PVC), polyurethanes (PU), polyethylene terephthalate (PET), polystyrene (PS) and polyester (PES). Between these plastics, LDPE, PP, HDPE, PET have major applications in the food packaging area. Table 1.1 resumes the main applications of the most common plastics.

*Table 1.1 Common plastics and their major applications* (Encyclopædia Britannica, 2017).

| Polymer family and type | Typical products and applications |
|---|---|
| High-density polyethylene (HDPE) | Milk bottles, wire and cable insulation, toys |
| Low-density polyethylene (LDPE) | Packaging film, grocery bags, agricultural mulch |
| Polypropylene (PP) | Bottles, food containers, toys |
| Polystyrene (PS) | Eating utensils, foamed food containers |
| Acrylonitrile-butadiene-styrene (ABS) | Appliance housings, helmets, pipe fittings |
| Polyvinyl chloride, unplasticized (PVC) | Pipe, conduit, home siding, window frames |
| Polyethylene terephthalate (PET) | Transparent bottles, recording tape |
| Polyester (unsaturated) (PES) | Boat hulls, automobile panels |
| Polyurethane (PUR) | Flexible and rigid foams for upholstery, insulation |

The world production and demand of plastics has been increasing over the last 65 years. In 2015, the global production of primary plastics from fossil origin was around 400 million tonnes (mt) in comparison with 300 mt in 2005. The packaging industry shared around 36% of the plastic market in 2015 being the largest

plastic market. However, packaging sector generated about 47% of the total plastic wastes in the same year as most of the packaging plastics leave use at the same production year. Between 1950 and 2015, over 8300 mt of primary plastics were produced, of that only 10% have been recycled and 9% have been incinerated. Around 60% of those plastics (4900 mt) were discarded and accumulated in landfills or in the natural environment (Geyer, Jambeck, & Law, 2017). Sunlight is fragmenting these discarded plastics into small particles of few millimetres or micrometres that spread all over the planet reaching even the oceans and threatens the marine ecosystems (Andrady, 2015). These facts are making scientific and the industrial communities more and more concerned about the environmental and the health impact of the fossil based plastics. In addition to the environmental issues, on the long term the conventional plastics are facing the challenge of being produced from a limited resource which is fossil oil and gas. Several strategies are being applied to solve these issues and to manage the plastic wastes. These strategies include plastic recycling and the use of energy recovery processes. Even so, more than 30% of the European plastic wastes of 2014 still

went to landfill (PlasticsEurope, 2016). The percentage of the recycling during the same year did not exceed 24% while 18% of the plastic wastes were incinerated for energy recovery (Geyer et al., 2017). Meanwhile, the concerns about the plastic safety and sustainability is driving the scientific and industrial community to develop sustainable and renewable alternatives to the fossil plastics.

Bio-based plastics are being extensively studied in the last years to evaluate their possible applications as a sustainable replacement of the conventional plastics (Chandra & Rustgi, 1998). In addition, they provide an alternative renewable resource while the fossil resources are limited. Some bioplastics that are produced by plants or bacteria have the potential to reduce the greenhouse gases (GHG) emissions by temporary fixation and removal of the $CO_2$ from the atmosphere. The fixed $CO_2$ is released at the end of the bioplastic life cycle leaving valuable biomasses that can be reused for growing other plants that close the energy cycle and make it more efficient.

## 2. Bioplastics and biopolymers

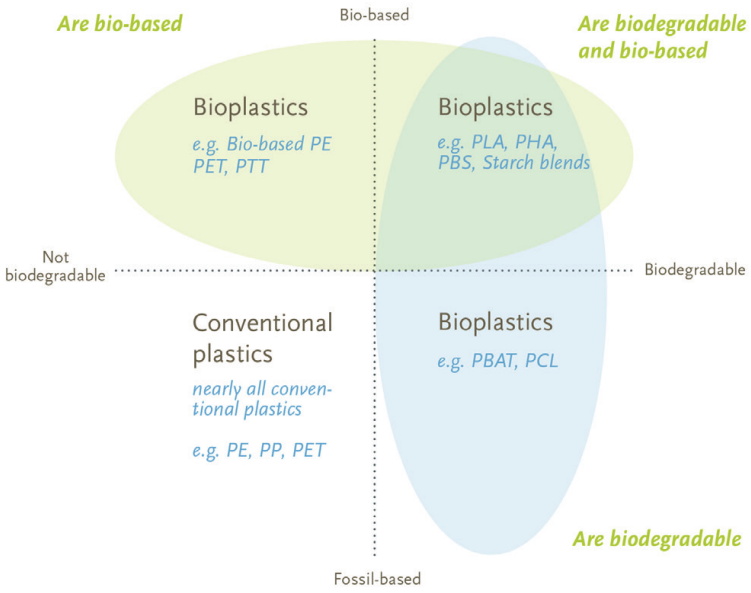


*Figure 1.1 Plastic types as a function of natural sources and biodegradability* (European bioplastics, 2017b).

According to the European bioplastics association, the term "bioplastics" includes bio-based plastics and biodegradable plastics or both. Bioplastics can be produced from biomass (bio-based) or from fossil oil and gas (fossil-based). Bio-based plastics are plastics that are derived totally or partly from biomass (Oever, Molenveld, Zee, & Bos, n.d.). Biodegradable plastics are those plastics that can be metabolized to water, naturally occurring gases as carbon dioxide ($CO_2$) and biomass with the help of microorganisms [Figure 1.1].

Those bio-based and biodegradable polymers that are produced naturally by living organisms are considered biopolymers. Table 1.2 resumes the classification and some examples of the bio-based plastics according to their origin.

*Table 1.2 Classification and examples of bio-based plastics according to their origin*

| Bio-based plastics | | | |
|---|---|---|---|
| Natural synthesis (biopolymers) | | | Chemical synthesis |
| Plant source | Animal Source | Microorganism | From biomass |
| • Cellulose<br>• Starch<br>• Lignin<br>• Pectin | • Chitin<br>• Chitosan | • Polyesters: PHAs as PHB[1], PHBV[2].<br>• Carbohydrates as Pullulan | • PLA[3]<br>• Bio-based PBS[4] |

[1] Polyhydroxybutyrate.
[2] Poly(3-hydroxybutyrate-co-3-hydroxyvalerate).
[3] Polylactic Acid.
[4] Polybutylene succinate.

Biopolymers are wide variety of polymers that include polynucleotides (DNA and RNA), polypeptides, polysaccharides and natural polyesters. Among them, polyesters and polysaccharides are of a potential importance for the bio-based plastic industry especially for the food packaging sector.

2.*1. Polyhydroxyalkanoates (PHAs)*

PHAs are linear polyesters that are produced by some microorganisms to store carbon and energy for metabolizing them in absence of external carbon source. These polymers are accumulated in the cytoplasm of the cell forming up to 95% of the dry cell weight. The biopolymers can be extracted with a solvent then precipitated from water as a white powder (Stevens, 2003). Some PHAs are produced commercially by large scale fermentation in bioreactors.

PHAs can be produced as homopolymers or copolymers depending on the cultivation conditions. The general chemical structure of the homo PHAs is presented in Figure 1.2. They are thermoplastics, i.e. can be repeatedly softened by heating and hardened again on cooling. They can be processed using the conventional processing equipment of plastics. The mechanical and the barrier properties of the PHAs depend on their chemical composition. The major commercial product of PHAs is poly(3-hydroxy)butyrate PHB (m = 1 and R = methyl, see Figure 1.2).

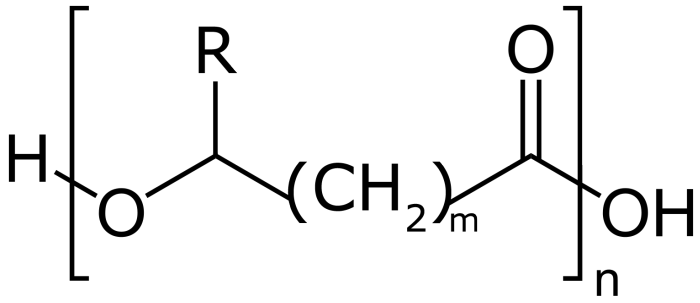


*Figure 1.2 General chemical structure of PHAs*

PHAs are biocompatible biopolymers and some of them have biomedical applications. The biocompatibility of a material deals with how the tissue reacts to foreign materials and the ability of a material to perform with an appropriate host response in a specific application (Kumar et al., 2003). They are also completely biodegradable biopolymers where the biodegradation depends on copolymer composition, molecular weight, degree of crystallinity and the size and shape of the article (Stevens, 2003).

### *2.2. Polysaccharides*

A polysaccharide is any of a group of carbohydrates comprising long chains of monosaccharide (simple sugar) molecules

(Daintith, 2008). Monosaccharides units are connected through glycosidic bonds [Figure 1.3].

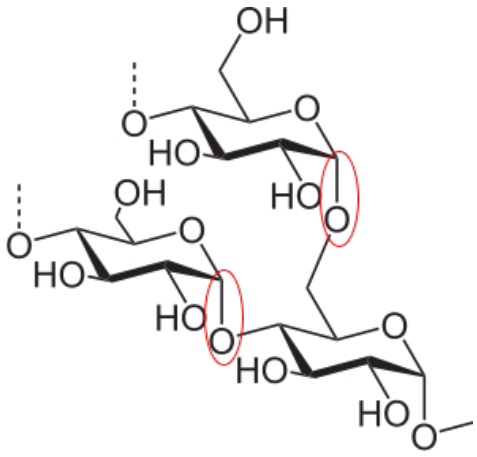


*Figure 1.3 Glycosidic bonds in an amylopectin molecule.*

The polysaccharide biopolymer can be linear (as cellulose, alginates and amylose in starch) or highly branched (as amylopectin in starch). Different polysaccharides have different functions in the producing living organisms that can be resumed in energy storage or structure functions. The difference in the chemical structure (monosaccharide unit type, chemical bonds, branching and the complexity of the molecule) leads to different physical and chemical properties of polysaccharides. Cellulose, the most abundant organic polymer on earth, is one of the structural polysaccharides. It consists of long unbranched glucose units and is responsible for providing

the rigidity of the cell wall of many plants, algae and some fungi. It also has wide industrial applications as paper, textile, food and pharmaceutical industries. Starch is one of the most important polysaccharides for many industries and represents energy source for the humans as the most common carbohydrate in human diets. More detailed information about starch will be given later in this chapter.

## 3. Biopolymers for food packaging

"Today, there is pretty much nothing that bioplastics can't do. For almost every conventional plastic material and application, there is a bioplastic alternative available that offers the same or in some cases even better properties and functionalities" saying the European bioplastics association (European bioplastics, 2017a). Bioplastics have found their ways to be applied in several areas such as packaging industry, building and constructions, textiles, and as biomedical scaffolds and stents (Ahmad, Williams, Doublier, Durand, & Buleon, 1999).

Although the market of bioplastics is still young and shares only around 1% of the global plastic market, the demand on the bioplastics is rising and new bioplastic products are developed continuously every year. The growth of the bioplastic market is reaching between 20% and 100% per year (European bioplastics, 2016). The production of some bioplastics like the polyhydroxyalkanoates PHAs is expected to quadruple by 2021. As in the case of conventional plastics, packaging is the largest field of applications for the bioplastics with around 39% of the total bioplastic markets in 2016 [Figure 1.4].

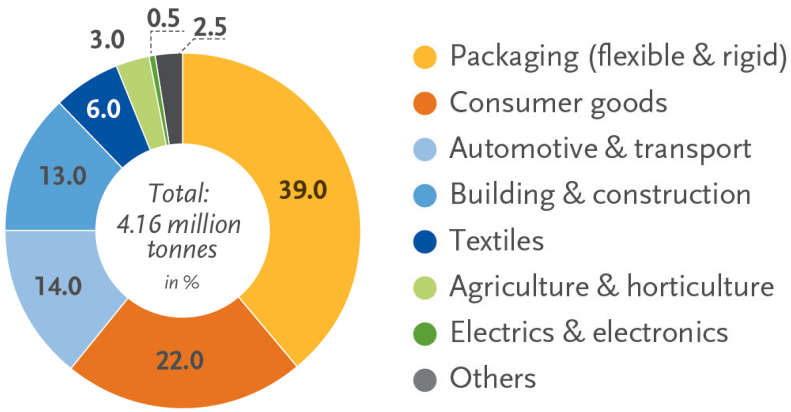


*Figure 1.4 Global production capacities of bioplastics by market segment* (European bioplastics, 2016).

Despite these very promising data, the introduction of the biopolymers and the bio-based biodegradable polymers to the market is facing major limitations especially processing and performance limitations (Rhim, Park, & Ha, 2013). Most biopolymers have relatively poor mechanical properties and low heat distortion temperature. The barrier properties of these polymers are also weak especially for water vapour (Mihindukulasuriya & Lim, 2014). Nowadays, almost 77% of the bioplastics used in the industry are bio-based/non-biodegradable plastics such as polyurethanes and bio-based polyethylene PE and bio-based poly(ethylene terephthalate) (PET) (European bioplastics, 2017a). PLA and PHB are examples of bio-based polymers and biopolymers respectively which their brittleness and poor mechanical properties have limited their uses for various applications as homopolymers (Bugnicourt, Cinelli, Lazzeri, & Alvarez, 2014; Castro-Aguirre, Iñiguez-Franco, Samsudin, Fang, & Auras, 2016; Notta-Cuvier et al., 2014). Table 1.3 presents some thermal and mechanical parameters of some common bio and conventional plastics in food packaging.

*Table 1.3 Thermal and mechanical properties of some common bio and conventional plastics in food packaging Sources:* (Avella, Martuscelli, & Raimo, 2000; Encyclopædia Britannica, 2017; Stevens, 2003).

| Polymer | Glass transition temperature (°C) | Melting temperature (°C) | Tensile strength (MPa) | Elongation at break (%) | Flexural modulus (GPa) |
|---|---|---|---|---|---|
| HDPE | −120 | 137 | 20–30 | 10–1,000 | 1–1.5 |
| LDPE | −120 | 110 | 8–30 | 100–650 | 0.25–0.35 |
| PP | −20 | 176 | 30–40 | 100–600 | 1.2–1.7 |
| PHB | 9 | 175 | 45 | 4 | 3.8 |
| PHBV (20% HV) | -5 | 114 | 26 | 27 | 1.9 |
| PLA | 63 | 135 | 110-145 | 100-160 | 3.3-3.8 |

In order to improve the processability and the properties of the biopolymers, several approaches have been followed including the addition of plasticizers, chemical modifications and physical blending with other biopolymers. The plasticizer is a substance added to the polymer to make it flexible. It exchanges intermolecular bonds among the polymer chains to bond between the macromolecules and the small molecular weight compound thus promote conformational changes resulting in increased

deformability (Imre & Pukánszky, 2013). The use of plasticizers improves the mechanical properties and decrease the glass transitions and the melting points of polymers improving their processability (Mousa, Dong, & Davies, 2016). Physical blending is the simple mixing of polymers during melt state when no chemical reaction is taking place. Several studies were published reporting blends of several biopolymers including blending of starch with PLA, PHB, PCL; PHB with PHBV, PCL and polysaccharides among many other blends (Avella et al., 2000; Imre & Pukánszky, 2013). Despite these approaches, the properties of the biopolymers in general are still not satisfactory and find difficulties in industrial applications (Rhim et al., 2013).

One of the promising strategies to improve and tune the physical properties of the biopolymers is the addition of fillers to the polymer matrix. Those biomaterials containing two or more phases in which one is a biopolymeric continuous phase and the other is a filler dispersed phase are called biocomposites (Mihindukulasuriya & Lim, 2014). A wide variety of materials have been used as fillers for plastics for enhancing their mechanical properties such as carbon

black, talc, glass and silica (Andrady, 2015). Recently, many of nano and microparticles have been reported as fillers improving mechanical and barrier properties of different biopolymeric films. For example, cellulose nanocrystals and microcrystals, metallic nanoparticles and nanoclays (Montero, Rico, Rodríguez-Llamazares, Barral, & Bouza, 2016; Rhim et al., 2013; Rico, Rodríguez-Llamazares, Barral, Bouza, & Montero, 2016). Using small particles with such a high surface area and high aspect ratio even in relatively low concentrations (provided they are well-dispersed in polymer matrix) can achieve superior enhancement of the biopolymer properties in comparison with conventional larger sized fillers. Malmir et al. have reported recently the use of cellulose nanocrystals (CNC) to decrease the water vapour and the oxygen transmission rates through PHBV films (Malmir, Montero, Rico, Barral, & Bouza, 2017). CNC have also reported to improve the mechanical properties of various polymers and biopolymers such as starch, PLA, PHBV, poly(vinyl alcohol) (PVA) and polycaprolactone (PCL) (Imre & Pukánszky, 2013; Montero et al., 2016; Oksman et al., 2016; Yu, Yan, & Yao, 2014).

In addition to enhancing the physical properties, nano and microfillers can provide another functions for active food packaging applications. In general, active packaging is a packaging system that directly interact with the enclosed food and affect its quality without a specific trigger (Brockgreitens & Abbas, 2016). For example silver nanoparticles, nano ZnO coated particles and TiO nanoparticles are being investigated for their known antimicrobial properties (Bodaghi, Mostofi, Oromiehie, Ghanbarzadeh, & Hagh, 2015; Esmailzadeh, Sangpour, Shahraz, Hejazi, & Khaksar, 2016; He & Hwang, 2016). Polymeric nano and microparticles can also act as carriers for other substrates such as antioxidants, antimicrobials and antifungal agents which can be slowly released through the polymeric packaging films. Many biopolymers were selected for the preparation of nano and microparticles depending on the desired application and the biopolymer properties. Nano and microparticles have been prepared from polysaccharides (cellulose, starch, chitosan and pectin etc.), proteins (as gelatine and whey protein) and polyesters (such as PHB and PHBV) (Joye & McClements, 2014). In this thesis, PHBV (12% HV) and starches from different origins

have been selected for the preparation of the desired nano and microparticles. The obtained particles are aimed to be embedded in biopolymeric films to produce new biocomposite materials with better properties and active functions.

## 4. Materials and characterization techniques

### *4.1. Materials*

#### *4.1.1. Poly(3-hydroxybutyrate-co-3-hydroxyvalerate)*

Poly(3-hydroxybutyrate-co-3-hydroxyvalerate) (PHBV) is a hydrophobic copolymer of hydroxybutyrate (HB) and hydroxyvalerate (HV) in different molar ratios (Bakare et al. 2016) [Figure 1.5]. It belongs to the polyhydroxyalkanoates (PHAs) family of aliphatic polyesters that are produced naturally mainly by some bacteria as a carbon and energy source (Laycock, Halley, Pratt, Werker, & Lant, 2014). It is a completely biodegradable (Bordes et al. 2009; Wang et al. 2013) and biocompatible biopolymer (Shishatskaya et al. 2004) which is produced either by microorganisms or genetically modified plants (Baran et al. 2002). PHBV is soluble in chloroform and dichloromethane at room temperature. It is also soluble in toluene and dimethylformamide at high temperatures (80 ºC to 90 ºC). It has many applications in the fields of medicine (Meng et al. 2008), tissue engineering (Williams et al. 1999; Bai et al. 2015), drug delivery (Durán et al. 2008; Vilos

et al. 2013) and in packaging industry as a substitute to traditional non-biodegradable plastics (Chandra and Rustgi 1998; Bittmann et al. 2013; Farmahini-Farahani et al. 2015; Pawar et al. 2015).

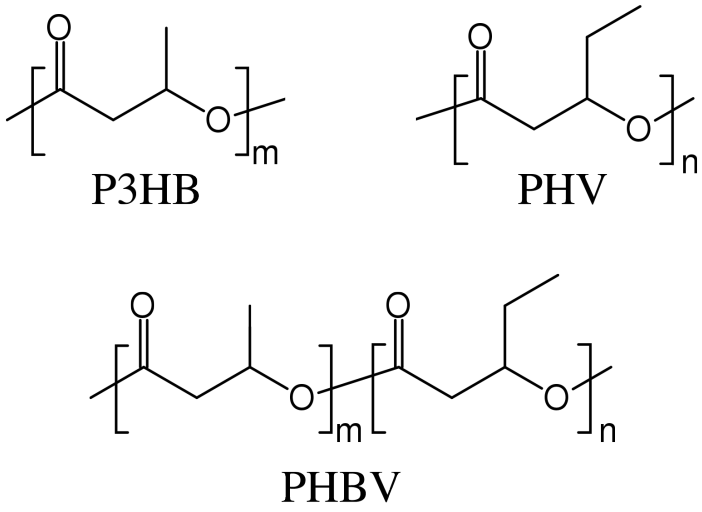


*Figure 1.5 Schematic representation of the chemical structure of PHBV*

The incorporation of the HV with the PHB polymer lead to a decrease in the crystallinity and the melting point. The melting point can be decreased from 175 ºC to 97 ºC by increasing the HV fraction up to 34% (Javadi, Pilla, Gong, & Turng, 2011). Gunaratne et al. have studied the crystallinity and the melting temperatures of PHBV with 5, 8, 12% of HV in addition to homopolymer PHB, the results are resumed in Table 1.4 (Gunaratne & Shanks, 2005).

*Table 1.4 Melting temperatures and degree of crystallinity of PHB and different types of PHBV.*

| % of HV | $T_m$[1] | Degree of crystallinity[2] (%) |
|---|---|---|
| 0 | 172.4 | 66 |
| 5 | 163.2 | 30 |
| 8 | 156.5 | 22 |
| 12 | 157.1 | 17 |

[1] Melting temperature determined by step-scan differential scanning calorimetry (SDSC)

[2] Determined by wide angle X-ray diffraction (WAXRD)

The PHBV copolymer has improved mechanical properties over the PHB homopolymers. By increasing the HV content, the polymer become less brittle and more flexible with decreasing the elasticity modulus and increase in the elongation % (Avella et al., 2000). The decreased in the melting point help in avoiding degradation while processing.

### *4.1.2. Starch*

Starch is the second most abundant biopolymer on the planet after cellulose. It is produced by most of the green plants to store energy. The low cost and the wide availability of the starch make it one of the most interesting candidates as a biodegradable,

biocompatible natural polymer. Starch is being widely used in food industries, paper making and as excipient in the pharmaceutical industry (Chiu & Solarek, 2009; Mason, 2009). In addition, starch is gaining an increasing attention in the packaging industry for its potential applications in the fields of food packaging, edible films and composting bags (J. Castaño et al., 2014; J. Castaño, Bouza, Rodríguez-Llamazares, Carrasco, & Vinicius, 2012). Starches from different botanical sources have different ratios and molecular weights of amylose and amylopectin and different crystalline structures that lead to different physical properties and thus different processability and possible applications (Johanna Castaño et al., 2017; Kim, Park, & Lim, 2015; Srichuwong, Sunarti, Mishima, Isono, & Hisamatsu, 2005; Young, 1984).

At molecular level, starch is mainly a polymer of glucose units that are connected together forming two macromolecules: amylose which is a helical α-(1–4) –linked D-glucose units [Figure 1.6], and amylopectin which is a highly-branched macromolecule of α-(1→4)-linked D-glucose units joined by frequent α-(1→6) branch

points [Figure 1.7]. Minor components of the starch granules include lipids (including phospholipids and free fatty acids), phosphate monoester and proteins/enzymes. The native starch granules are semi-crystalline granules built up of alternative amorphous and crystalline shells of 100 to 400 nm (Pérez, Baldwin, & Gallant, 2009). The main crystalline structure types of the granules are named A- and B- types. The structure of A-type starch crystals is a very compact left handed six folded double helix structure with no space for water or any other molecules in the centre. The B-type crystalline structure is also left handed six folded double helix structure but with more loosely packing. The double helices are connected via hydrogen bonds that form a channel through the hexagonal arrangement. This channel is filled with water molecules making a water column in the centre of the hexagonal arrangement. The crystalline structure thought to have an important contribution in the starch properties such as the gelatinization temperature and the swelling properties (Pérez et al., 2009; van Soest, Hulleman, de Wit, & Vliegenthart, 1996).

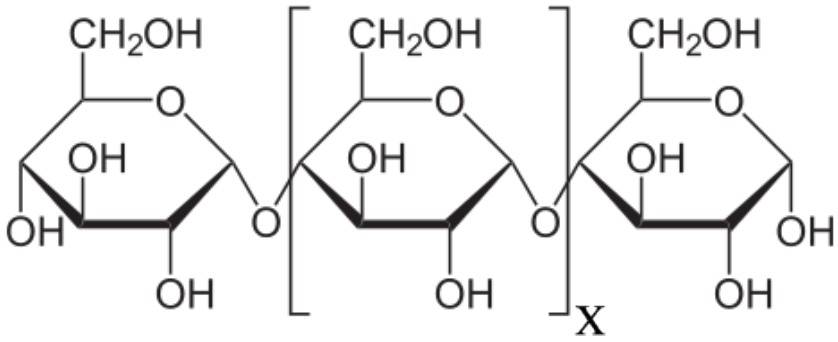


*Figure 1.6 Schematic representation of amylose.*

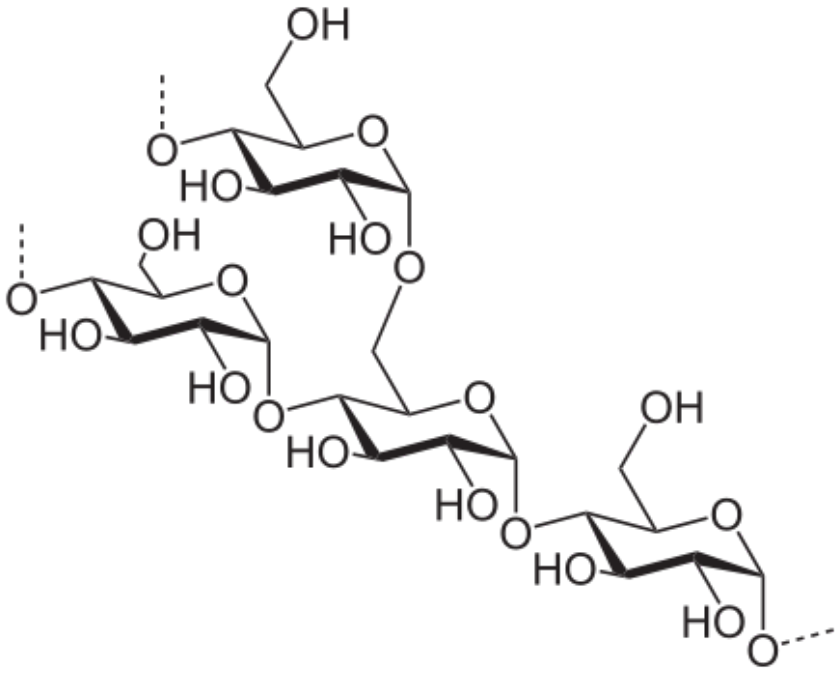


*Figure 1.7 Schematic representation of amylopectin.*

*4.1.3. Quercetin*

Quercetin (3,3',4',5,7-pentahydroxyflavone; IUPAC name: 2-(3,4-dihydroxyphenyl)-3,5,7-trihydroxy-4H-chromen-4-one) is a naturally occurring flavonoid which is the major representative of flavonol subclass (H. Li et al., 2009) [Figure 1.8]. It is found in many leaves, fruits and vegetables such as onions, apples and tea among other plants (Bose, Du, Takhistov, & Michniak-Kohn, 2013; Jeszka-Skowron, Krawczyk, & Zgoła-Grześkowiak, 2015). Quercetin, among other flavonoids, has been extensively studied during the last years for its antioxidant, anti-inflammatory and anti-cancer activities (Guazelli et al., 2013; H. Li et al., 2009; Lightfoot Vidal et al., 2016; Mohan, Anandan, & Rajendran, 2016; G. Wang, Wang, Chen, Du, & Li, 2016).

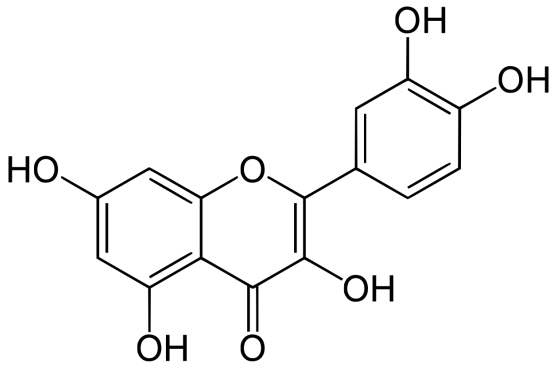


*Figure 1.8 Skeletal formula of quercetin.*

Quercetin has a very low solubility in water. It is soluble in ethanol and most of organic solvents. Quercetin is also soluble in aqueous alkaline solution but it undergoes degradation in alkaline medium especially under light (Dechene, 1951; Jurasekova, Domingo, Garcia-Ramos, & Sanchez-Cortes, 2014). Quercetin has a characteristic maximum absorbance peak at a wavelength 372 nm which can be easily detected by UV–visible spectroscopy.

### *4.2. Characterization techniques*

#### *4.2.1. Scanning electron microscopy (SEM)*

Scanning electron microscopy (SEM) is an electron microscope where the electron beam is produced by an electron gun and accelerated using voltage from 1 to 30 kV. The electrons interact with the surface atoms of the scanned materials and the detector collects the signals of the secondary electrons emitted by the surface atoms excited by the electron beam [Figure 1.9]. Other types of signals like backscattered electrons or X-rays can be detected too (Kelsall, Hamley, & Geoghegan, 2015).

The electron gun is normally of Tungsten or Lanthanum Hexaboride ($LaB_6$) filament which needs to be heated for emitting electrons. The field emission scanning electron microscopes (FESEM) are equipped with a field emission gun that provides better quality images, higher resolution and higher brightness. The resolution of the obtained images depends on many factors such as the type of the electron gun, the applied voltage and the metal coating, in some ultra-high resolution FESEM the resolution can reach below 1 nm at 30 kV.

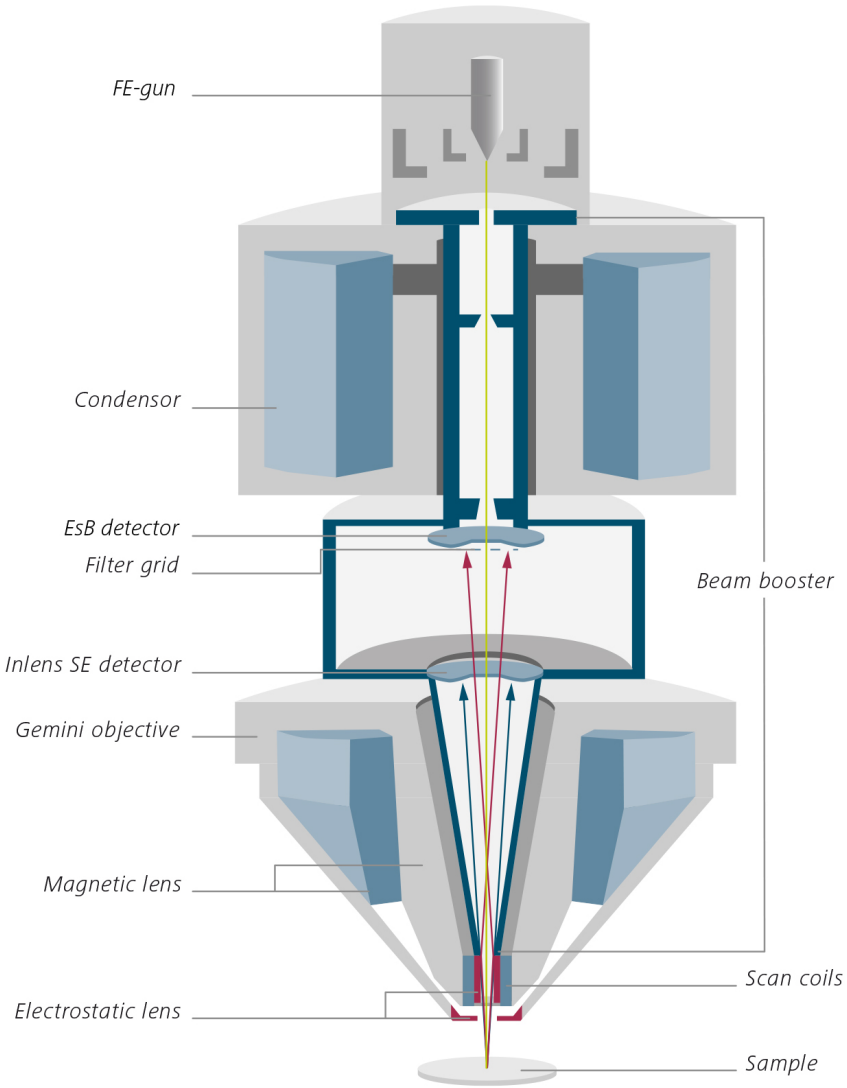


*Figure 1.9 Diagram of FESEM.*

The samples which are non-conductive (like polymeric samples) need to be coated with an electrically conductive metal such as gold (Au), silver (Ag), platinum (Pt) and iridium (Ir) before

being scanned by SEM. The technique used for this coating is a physical vapour deposition technique (PVD) called sputter coating. In this technique, a metal surface (target) is positioned as cathode and is eroded when bombarded with heavy fast inert gas ions (usually Ar) in conditions of gaseous glow discharge between an anode and cathode. As a result, the metal sputtered atoms will be deposited as a very thin even layer (few nanometres) on the surface of the sample. The sputter coating prevents the charging of the sample with the electron beam, improves the secondary electron emission, i.e. increases the signal to noise ratio, reduces the beam penetration and provide a protection for the beam sensitive materials.

*4.2.2. Dynamic light scattering (DLS)*

DLS is a non-invasive, easy and one of the most common techniques for the determination of the size distribution of small particles in solution of a suspension. The DLS measures the fluctuation of the light scattering intensities of the particles in solution observed over a short period of time. The particles are

illuminated with a laser beam of a determined wavelength and the fluctuation of the light scattered is detected by a fast photon detector placed at a known angle. The laser used for DLS is normally of 632.8 nm or 532 nm. The continuous Brownian motion of the particles makes the scattering intensities to fluctuate continuously. Particles with different sizes have different Brownian motion speed, i.e. different translational diffusion coefficient (D). In case of small particles, the fluctuations of the scattered light are fast but of low amplitude and for large molecules vice versa (Braun, Cherdron, Rehahn, Ritter, & Voit, 2005). The DLS is measuring what called the hydrodynamic diameter of the particles $d_h$, which is the diameter of the particles as well as the surrounding molecules of the solvent shell. The hydrodynamic diameter ($d_h$) is determined using the Stokes-Einstein Equation (1.1):

$$d_h = \frac{kT}{3\pi\eta D} \qquad (1.1)$$

where T is the measurement temperature, $\eta$ is the viscosity of the medium, k is the Boltzmann constant and D is the translational diffusion coefficient.

*4.2.3. Static light scattering (SLS)*

Unlike the DLS, the SLS technique depends on the measurement of the light scattering intensity at one or more angles. A laser beam is used for the illumination of the sample and usually several detectors are collecting the scattered light at different angles. This technique is useful for the determination of the weight-average molecular weight of polymers and for measuring the particle size in the range from tens of nanometres to few millimetres. The amount and the concentration required for performing the measurements are much higher in comparison with DLS.

*4.2.4. Thermogravimetric analysis (TGA)*

TGA is a widely used technique for studying the thermal stability of materials. In this method, the weight of the sample is measured continuously while increasing the temperature in an environment of a certain gas. A typical thermogravimetric analyser consists of a highly precision balance with a sample pan inside a furnace that can reach high temperatures (up to 1500 ºC for some TGAs). The sample used for TGA is normally of few milligrams.

The furnace must be controlled through a software to insure the required rate for increasing the temperature. The thermal analysis can be done in an environment of different gases like $N_2$, $O_2$, air, argon and others. The weight of the sample (or the percentage of the initial sample weight) is plotted against the temperature making the TGA curves. The first derivation of the TGA curves is used for more in-depth understanding and analysis. The TGA is useful for the determination of decomposition temperature and the weight changes during the decomposition reaction. It is also used for tracking volatile rates of liquid mixtures or the percentage of water in some hydrophilic polymers.

*4.2.5. Differential scanning calorimetry (DSC)*

Differential scanning calorimetry (DSC) is a thermo-analytical technique where the thermal transitions during the change of temperature are analysed. The DSC is normally equipped with two identically positioned platforms, one for a sample pan and the other for a reference pan. The sample has to be measured precisely (few mg) and the pans have to be identical of well-known heat capacity.

A software must control the temperature of both pans to be almost identical through the experiment which is done normally under inert atmosphere. During the experiment, both sample and reference pans are heated up (or cooled down) at the same rate. The amount of heat required for each of the sample and reference pans to reach the same temperature is recorded. As the sample pan contains the sample material while the reference is empty, more heat is required to heat the sample pan. The energy difference (ΔH) supplied to the sample or the reference is equal to the change in heat capacity ($C_p$) (Chartoff, Sircar, Chartoff, & Sircar, 2004). The thermal transition may be endothermic or exothermic transition depending on the change in heat capacity. Thus, DSC can be used to observe transitions such as melting, crystallization, glass transition $T_g$ and gelatinization temperature. It is used also for the determination of the amount and different types of waters in hydrogels.

*4.2.6. X-ray diffraction (XRD)*

X-ray diffraction (XRD) is the diffraction of X-rays by a crystal that is the bases of X-ray crystallography.

X-ray crystallography is the use of X-ray diffraction to determine the structure of crystals or molecules. The technique involves directing a beam of X-rays at a crystalline sample and recording the diffracted X-rays on a photographic plate. The diffraction pattern consists of a pattern of spots on the plate, and the crystal structure can be worked out from the positions and intensities of the diffraction spots. X-rays are diffracted by the electrons in the molecules and if molecular crystals of a compound are used, the electron density distribution in the molecule can be determined (Daintith, 2008).

The two British scientists William Henry Bragg and his son William Lawrence Bragg have shared Nobel Prize of physics in 1915 for developing Bragg's law [Equation 1.2] that explains relationship between the scattering pattern and the crystalline structure.

$$n\lambda = 2dsin\theta \qquad (1.2)$$

Where n is a positive integer, λ is the wavelength of the incident beam, d is the inter-planar distance and θ is the scattering angle [Figure 1.10].

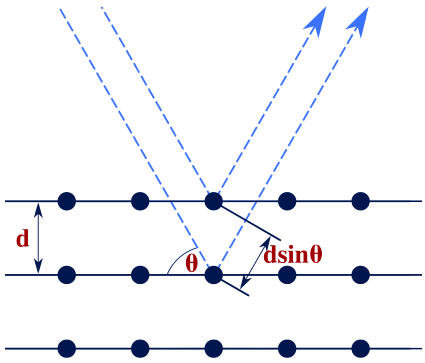


*Figure 1.10 Diagram of bragg's diffraction.*

*4.2.7. Ultraviolet–visible spectroscopy (UV–vis)*

It is an important optical method for used for quantitative determination of some analytes. It is based on the principle that electronic transitions in molecules occur in the visible and ultraviolet regions of the electromagnetic spectrum, and that a given transition occurs at a characteristic wavelength (Daintith, 2008). The analysis is typically carried out in highly diluted solutions; however, it is possible to perform the analysis for thin films as well (Braun et al., 2005). UV-vis spectrophotometer is the instrument that measures

the intensity of the light beam after passing through the sample and compares it with the intensity of the light passing through the reference. The absorbance (A) is calculated through the software based on Beer-Lambert Law Equation (1.3):

$$A = \log \frac{I_0}{I} = \varepsilon l c \qquad (1.3)$$

Where $I_0$ is the intensity of the light after passing through the reference, I is the intensity of the light beam after passing through the sample length l, c is the molar concentration of the sample and ε is the molar absorption coefficient. The sample length l is normally the length of the cuvette where the sample solution is placed. The Beer–Lambert law means that the intensity of light passing through a sample diminishes exponentially with the concentration and the thickness of the sample (Daintith, 2008). If the sample thickness is fixed (length of the cuvette), the absorbance will be directly proportional to the concentration of the sample. The concentration of the sample can be easily calculated by measuring its absorbance and using a calibration curve.

*4.2.8. Water vapour transmission rate (WVTR)*

The steady-state transport properties of water vapour in barrier polymers are characterized by water vapour transmission rate (WVTR) (Dhoot et al., 2002). This parameter is critical for many industries especially for packaging of food and medications. Many equipment are available for performing this measurement.

The equipment used in this thesis is a single cell water vapour transmission rate (WVTR) testing system for films. In this system, the film is put between two cell sides, one represents a dry cell side and the other is the test gas side where the water vapour source is placed [Figure 1.11]. WVTR is calculated by counting the passed water vapour molecules through the film every 30 min. The water vapour molecules are carried to the counting side of the equipment by nitrogen gas which is purged continuously during the test. WVTR can be presented as grams of water transmitted through the film divided by the area and the time ($g/m^2$.day).

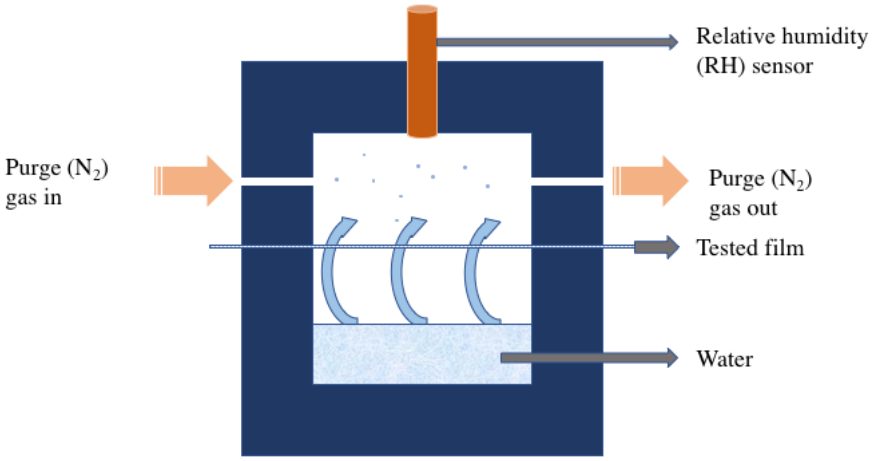


*Figure 1.11 Diagram of a WVTR testing cell.*

### *4.2.9. Oxygen transmission rate (OTR)*

In this technique, the volume of oxygen gas passed through a given area of the polymeric film during a certain period of time is measured. As well as WVTR, this is an important parameter especially for the packaging materials of foods and pharmaceuticals.

The equipment used in this thesis for the measurement of OTR is of a single cell where pure nitrogen gas is routed to one side of the film until a stable zero has been established. Following that, pure oxygen gas is introduced into the other side of the film. Oxygen molecules diffusing through the film are conveyed to the sensor by

the carrier gas and then calculated (Dhoot et al., 2002) [Figure 1.12]. OTR can be presented as volume of the oxygen gas transmitted through the film divided by the area and the time ($cm^3/m^2$.day).

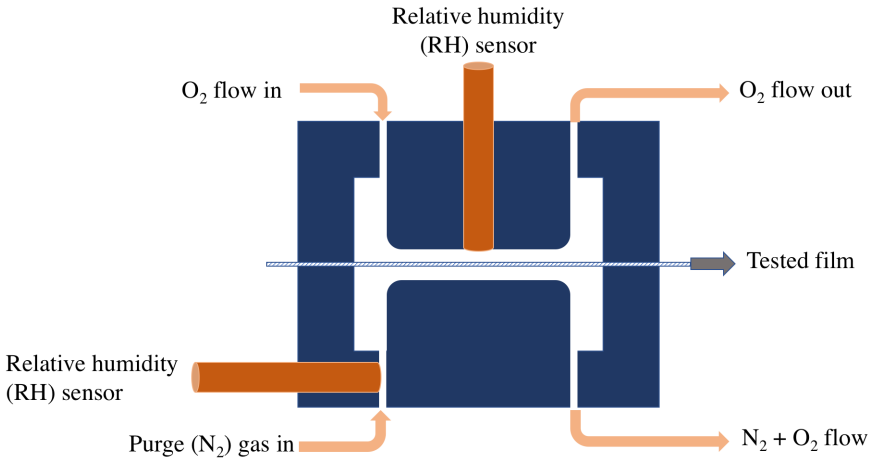


*Figure 1.12 Diagram of an OTR testing cell.*

The DSC, TGA, UV-vis, WVTR and OTR measurements of this thesis were performed in our laboratory (the laboratory of polymers, Escuela Universitaria Politécnica, Ferrol).

The DLS measurements were performed in the laboratory of Nanobiofar research group in the Centre for Research in Molecular Medicine and Chronic Diseases (CiMUS), University of Santiago de Compostela (USC) and in the laboratory of MatNaBio research group at the department of Physical-Chemistry II of the Faculty of Pharmacy of the Complutense University of Madrid (UCM).

All the FESEM micrographs were done in the Electronic and Confocal Microscopy unit of the (Rede de Infraestruturas de Apoio á Investigación e ao Desenvolvemento Tecnolóxico (RIAIDT)) of the University of Santiago de Compostela.

The SLS and XRD measurements were performed in the structural analysis unit (Unidad de Análisis Estructural) of the Research Support Services (Servizos de Apoio á Investigación) of the University of a Coruña (UDC).

## Objectives of the Thesis

The general objective of this thesis is the synthesis and characterization of nano and microparticles of biopolymers for food packaging applications.

For achieving this objective, we have developed four specific objectives as following:

1. Select an easy and appropriate technique for obtaining the desired nano and microparticles from both biopolymers: PHBV and starches from different botanical sources.
2. Characterization of the obtained nano and microparticles of both biopolymers.
3. Study the possibility of loading some of these nano and microparticles with natural antioxidants. Evaluate the loading percentage, antioxidant activity and the release kinetics.
4. Incorporation of some of the prepared nano or microparticles into biopolymeric films. Study the effect of this incorporation on the properties of the films related to the desired application in the food packaging area.

## Structure of the Thesis

The objectives of this thesis were developed as a part of the scientific project "Development of new materials based on polymeric bionanocomposites from natural resources [NanoCompBioPol]" funded by the Spanish Ministry of Economy and Finance. The thesis presents the part of the project that corresponds to the development of nano and microparticles from biopolymers and provides some possible applications for this particles in the food packaging area. The details of the thesis are presented in five main chapters preceded by an introduction chapter and followed by a general conclusions chapter as following:

**Chapter 1**. Introduction

In this chapter, light has been thrown on the actual state of the bioplastics and the biopolymers in the market. The difference between bioplastics, bio-based plastics, biodegradable polymer and biopolymers were discussed. The chapter is pointing out some poor properties of the biopolymers and the usage of fillers strategy as a solution.

It also introduces the main materials and characterization techniques used in this thesis.

**Chapter 2**. Preparation and characterization of nano and microparticles of poly(3-hydroxybutyrate-co-3-hydroxyvalerate) (PHBV) via emulsification / solvent evaporation and nanoprecipitation techniques.

This chapter describes the preparation and the characterization of nano and microparticles of poly(3-hydroxybutyrate-co-3-hydroxyvalerate) via two different preparation techniques: emulsification/solvent evaporation and nanoprecipitation and studies the effect of various conditions of preparation on the size and the morphology of the produced particles.

**Chapter 3**. Preparation of starch nanoparticles loaded with quercetin using nanoprecipitation technique.

This chapter discusses the preparation of starch nanoparticles from three different origins (pea, corn and potato) loaded with quercetin. It analyses the effect of the

starch origin on the quercetin loading percentage, the release kinetics and the antioxidant activity of the produced nanoparticles.

**Chapter 4**. Preparation of donut-shaped starch microparticles by aqueous-alcoholic treatment

This chapter reports a simple technique for the preparation of donut-shaped starch microparticles by thermal aqueous-alcoholic treatment.

**Chapter 5**. Starch edible films loaded with donut-shaped starch microparticles.

This chapter describes the preparation of thermoplastic starch edible films (TPS) loaded with donut-shaped starch microparticles from two different botanical origins. The chapter also discusses the improvement of the thermal and barrier properties of the starch films due to the incorporation of the donut-shaped starch microparticles.

**Chapter 6**. Starch edible films loaded with donut-shaped starch-quercetin microparticles: characterization and release kinetics.

Starch edible films loaded with donut-shaped starch-quercetin microparticles were prepared from two different botanical origins (pea and corn). The quercetin loading percentage and therefore the antioxidant activity for the microparticles was studied. The quercetin release kinetics through the starch films was studied in addition to the thermal stability of the films.

**Chapter 7**. General conclusions.

This chapter resumes the conclusions of each individual chapter and presents some general conclusions.

Each of the five main chapters was written in an independent way for its posterior planned publication. Each of these chapters is divided in an introduction, materials and methods section, results and discussion section and conclusions section. The references were presented separately for the introduction and for each individual chapter.

All figures as well as the tables of this thesis were indexed in two separated lists before the introduction chapter. The figures and

the tables were named using 2 numbers separated by a dot (.). The first number is the chapter number, while the second is the figure or the table number in a continuous order from the beginning to the end of the thesis.

## References

Ahmad, F. B., Williams, P. A., Doublier, J. L., Durand, S., & Buleon, A. (1999). Physico-chemical characterisation of sago starch. Carbohydrate Polymers, 38(4), 361–370. http://doi.org/10.1016/S0144-8617(98)00123-4

Andrady, A. L. (2015). Plastics and Environmental Sustainability. Plastics and Environmental Sustainability. http://doi.org/10.1002/9781119009405

Avella, M., Martuscelli, E., & Raimo, M. (2000). Review Properties of blends and composites based on poly(3-hydroxy)butyrate (PHB) and poly(3-hydroxybutyrate-hydroxyvalerate) (PHBV) copolymers. Journal of Materials Science, 35(3), 523–545. http://doi.org/10.1023/A:1004740522751

Bodaghi, H., Mostofi, Y., Oromiehie, A., Ghanbarzadeh, B., & Hagh, Z. G. (2015). Synthesis of clay-TiO2 nanocomposite thin films with barrier and photocatalytic properties for food packaging application. Journal of Applied Polymer Science, 132(14), 4–11. http://doi.org/10.1002/app.41764

Bose, S., Du, Y., Takhistov, P., & Michniak-Kohn, B. (2013). Formulation optimization and topical delivery of quercetin from solid lipid based nanosystems. International Journal of Pharmaceutics, 441(1–2), 56–66. http://doi.org/10.1016/j.ijpharm.2012.12.013

Braun, D., Cherdron, H., Rehahn, M., Ritter, H., & Voit, B. (2005). Polymer Synthesis : Theory and Practice. New York. http://doi.org/10.1002/pi.1938

Brockgreitens, J., & Abbas, A. (2016). Responsive Food Packaging: Recent Progress and Technological Prospects. Comprehensive Reviews in Food Science and Food Safety, 15(1), 3–15. http://doi.org/10.1111/1541-4337.12174

Bugnicourt, E., Cinelli, P., Lazzeri, A., & Alvarez, V. (2014). Polyhydroxyalkanoate (PHA): Review of synthesis, characteristics, processing and potential applications in packaging. Express

Polymer Letters, 8(11), 791–808. http://doi.org/10.3144/expresspolymlett.2014.82

Castaño, J., Bouza, R., Rodríguez-Llamazares, S., Carrasco, C., & Vinicius, R. V. B. (2012). Processing and characterization of starch-based materials from pehuen seeds (Araucaria araucana (Mol) K. Koch). Carbohydrate Polymers, 88(1), 299–307. http://doi.org/10.1016/j.carbpol.2011.12.008

Castaño, J., Rodríguez-Llamazares, S., Contreras, K., Carrasco, C., Pozo, C., Bouza, R., … Giraldo, D. (2014). Horse chestnut (Aesculus hippocastanum L.) starch: Basic physico-chemical characteristics and use as thermoplastic material. Carbohydrate Polymers, 112, 677–685. http://doi.org/10.1016/j.carbpol.2014.06.046

Castaño, J., Rodríguez-Llamazares, S., Sepúlveda, E., Giraldo, D., Bouza, R., & Pozo, C. (2017). Morphological and structural changes of starch during processing by melt blending. Starch - Stärke, 68, 1–9. http://doi.org/10.1002/star.201600247

Castro-Aguirre, E., Iñiguez-Franco, F., Samsudin, H., Fang, X., & Auras, R. (2016). Poly(lactic acid)—Mass production, processing, industrial applications, and end of life. Advanced Drug Delivery Reviews, 107, 333–366. http://doi.org/10.1016/j.addr.2016.03.010

Chandra, R., & Rustgi, R. (1998). Biodegradable polymers. Progress in Polymer Science, 23(7), 1273–1335. http://doi.org/10.1016/S0079-6700(97)00039-7

Chartoff, R. P., Sircar, A. K., Chartoff, R. P., & Sircar, A. K. (2004). Thermal Analysis of Polymers. In Encyclopedia of Polymer Science and Technology. Hoboken, NJ, USA: John Wiley & Sons, Inc. http://doi.org/10.1002/0471440264.pst367

Chiu, C. wai, & Solarek, D. (2009). Modification of Starches. Starch (Third Edit). Elsevier Inc. http://doi.org/10.1016/B978-0-12-746275-2.00017-3

Daintith, J. (2008). Dictionary of Chemistry (6th Edition). Oxford University Press, 289. http://doi.org/10.1016/B978-0-08-011600-6.50016-4

Dechene, E. B. (1951). The relative stability of rutin and quercetin in alkaline solution. Journal of the American Pharmaceutical Association., 40(10), 495–497. http://doi.org/10.1002/jps.3030401005

Dhoot, S. N., Freeman, B. D., Stewart, M. E., Dhoot, S. N., Freeman, B. D., & Stewart, M. E. (2002). Barrier Polymers. In Encyclopedia of Polymer Science and Technology. Hoboken, NJ, USA: John Wiley & Sons, Inc. http://doi.org/10.1002/0471440264.pst025

Encyclopædia Britannica. (2017). Plastic. In Encyclopædia Britannica. Encyclopædia Britannica, inc. Retrieved from https://www.britannica.com/science/plastic

Esmailzadeh, H., Sangpour, P., Shahraz, F., Hejazi, J., & Khaksar, R. (2016). Effect of nanocomposite packaging containing ZnO on growth of Bacillus subtilis and Enterobacter aerogenes. Materials Science and Engineering C, 58, 1058–1063. http://doi.org/10.1016/j.msec.2015.09.078

European bioplastics. (2016). Bioplastic market data. European Bioplastics, 4. Retrieved from http://docs.european-bioplastics.org/publications/EUBP_Bioplastics_market_data_report_2016.pdf

European bioplastics. (2017a). Bioplastics: facts and figures. European Bioplastics, 26. Retrieved from http://docs.european-bioplastics.org/publications/EUBP_Facts_and_figures.pdf

European bioplastics. (2017b). Frequently asked questions on bioplastics. European Bioplastics, 26. Retrieved from http://docs.european-bioplastics.org/publications/EUBP_FAQ_on_bioplastics.pdf

Geyer, R., Jambeck, J. R., & Law, K. L. (2017). Production, use, and fate of all plastics ever made. Science Advances, 3(7), e1700782. http://doi.org/10.1126/sciadv.1700782

Guazelli, C. F. S., Fattori, V., Colombo, B. B., Georgetti, S. R., Vicentini, F. T. M. C., Casagrande, R., … Verri, J. W. A. (2013). Quercetin-loaded microcapsules ameliorate experimental colitis in

mice by anti-inflammatory and antioxidant mechanisms. Journal of Natural Products, 76(2), 200–208. http://doi.org/10.1021/np300670w

Gunaratne, L. M. W. K., & Shanks, R. A. (2005). Multiple melting behaviour of poly(3-hydroxybutyrate-co-hydroxyvalerate) using step-scan DSC. European Polymer Journal, 41, 2980–2988. http://doi.org/10.1016/j.eurpolymj.2005.06.015

He, X., & Hwang, H. M. (2016). Nanotechnology in food science: Functionality, applicability, and safety assessment. Journal of Food and Drug Analysis, 24(4), 671–681. http://doi.org/10.1016/j.jfda.2016.06.001

Imre, B., & Pukánszky, B. (2013). Compatibilization in bio-based and biodegradable polymer blends. European Polymer Journal, 49(6), 1215–1233. http://doi.org/10.1016/j.eurpolymj.2013.01.019

Javadi, A., Pilla, S., Gong, S., & Turng, L.-S. (2011). Biobased and Biodegradable PHBV-Based Polymer Blends and Biocomposites : Properties and Applications. In Handbook of Bioplastics and Biocomposites Engineering Applications (pp. 372–396). Hoboken, NJ, USA: John Wiley & Sons, Inc. http://doi.org/10.1002/9781118203699.ch14

Jeszka-Skowron, M., Krawczyk, M., & Zgoła-Grześkowiak, A. (2015). Determination of antioxidant activity, rutin, quercetin, phenolic acids and trace elements in tea infusions: Influence of citric acid addition on extraction of metals. Journal of Food Composition and Analysis, 40, 70–77. http://doi.org/10.1016/j.jfca.2014.12.015

Joye, I. J., & McClements, D. J. (2014). Biopolymer-based nanoparticles and microparticles: Fabrication, characterization, and application. Current Opinion in Colloid & Interface Science, 19(5), 417–427. http://doi.org/10.1016/j.cocis.2014.07.002

Jurasekova, Z., Domingo, C., Garcia-Ramos, J. V, & Sanchez-Cortes, S. (2014). Effect of pH on the chemical modification of quercetin and structurally related flavonoids characterized by optical (UV-visible and Raman) spectroscopy. Physical Chemistry

Chemical Physics, 16(25), 12802–12811. http://doi.org/10.1039/c4cp00864b

Kelsall, R. W., Hamley, I. W., & Geoghegan, M. (Eds.). (2015). Nanoscale Science and Technology. Wiley.

Kim, H. Y., Park, S. S., & Lim, S. T. (2015). Preparation, characterization and utilization of starch nanoparticles. Colloids and Surfaces B: Biointerfaces, 126, 607–620. http://doi.org/10.1016/j.colsurfb.2014.11.011

Kumar, N., Ezra, A., Ehrenfroind, T., Krasko, M. Y., Domb, A. J., Kumar, N., … Domb, A. J. (2003). Biodegradable polymers, medical applications. In Encyclopedia of Polymer Science and Technology. Hoboken, NJ, USA: John Wiley & Sons, Inc. http://doi.org/10.1002/0471440264.pst027

Laycock, B., Halley, P., Pratt, S., Werker, A., & Lant, P. (2014). The chemomechanical properties of microbial polyhydroxyalkanoates. Progress in Polymer Science, 39(2), 397–442. http://doi.org/10.1016/j.progpolymsci.2013.06.008

Li, H., Zhao, X., Ma, Y., Zhai, G., Li, L., & Lou, H. (2009). Enhancement of gastrointestinal absorption of quercetin by solid lipid nanoparticles. Journal of Controlled Release, 133(3), 238–244. http://doi.org/10.1016/j.jconrel.2008.10.002

Lightfoot Vidal, S., Rojas, C., Bouza Padin, R., Perez Rivera, M., Haensgen, A., Gonzalez, M., & Rodriguez-Llamazares, S. (2016). Synthesis and characterization of polyhydroxybutyrate-co-hydroxyvalerate nanoparticles for encapsulation of quercetin. Journal of Bioactive and Compatible Polymers, 31(5), 439–452. http://doi.org/10.1177/0883911516635839

Malmir, S., Montero, B., Rico, M., Barral, L., & Bouza, R. (2017). Morphology, thermal and barrier properties of biodegradable films of poly (3-hydroxybutyrate-co-3-hydroxyvalerate) containing cellulose nanocrystals. Composites Part A: Applied Science and Manufacturing, 93, 41–48. http://doi.org/10.1016/j.compositesa.2016.11.011

Mason, W. R. (2009). Starch Use in Foods. Starch (Third Edit). Elsevier Inc. http://doi.org/10.1016/B978-0-12-746275-2.00020-3

Mihindukulasuriya, S. D. F., & Lim, L. T. (2014). Nanotechnology development in food packaging: A review. Trends in Food Science and Technology, 40(2), 149–167. http://doi.org/10.1016/j.tifs.2014.09.009

Mohan, L., Anandan, C., & Rajendran, N. (2016). Drug release characteristics of quercetin-loaded TiO nanotubes coated with chitosan. International Journal of Biological Macromolecules, 4–9. http://doi.org/10.1016/j.ijbiomac.2016.04.034

Montero, B., Rico, M., Rodríguez-Llamazares, S., Barral, L., & Bouza, R. (2016). Effect of nanocellulose as a filler on biodegradable thermoplastic starch films from tuber, cereal and legume. Carbohydrate Polymers. http://doi.org/10.1016/j.carbpol.2016.10.073

Mousa, M. H., Dong, Y., & Davies, I. J. (2016). Recent advances in bionanocomposites: Preparation, properties, and applications. International Journal of Polymeric Materials and Polymeric Biomaterials, 65(5), 225–254. http://doi.org/10.1080/00914037.2015.1103240

Notta-Cuvier, D., Odent, J., Delille, R., Murariu, M., Lauro, F., Raquez, J. M., … Dubois, P. (2014). Tailoring polylactide (PLA) properties for automotive applications: Effect of addition of designed additives on main mechanical properties. Polymer Testing, 36, 1–9. http://doi.org/10.1016/j.polymertesting.2014.03.007

Oever, M. Van Den, Molenveld, K., Zee, M. Van Der, & Bos, H. (n.d.). Bio-based and biodegradable plastics – Facts and Figures.

Oksman, K., Aitomäki, Y., Mathew, A. P., Siqueira, G., Zhou, Q., Butylina, S., … Hooshmand, S. (2016). Review of the recent developments in cellulose nanocomposite processing. Composites Part A: Applied Science and Manufacturing, 83, 2–18. http://doi.org/10.1016/j.compositesa.2015.10.041

Pérez, S., Baldwin, P. M., & Gallant, D. J. (2009). Structural features of starch granules I. Starch (Third Edit). Elsevier Inc. http://doi.org/10.1016/B978-0-12-746275-2.00005-7

PlasticsEurope. (2016). Plastic - the Facts 2016, 38. Retrieved from http://www.plasticseurope.es/Document/plastics---the-facts-2016-15787.aspx?FolID=2

Rhim, J.-W., Park, H.-M., & Ha, C.-S. (2013). Bio-nanocomposites for food packaging applications. Progress in Polymer Science, 38(10–11), 1629–1652. http://doi.org/10.1016/j.progpolymsci.2013.05.008

Rico, M., Rodríguez-Llamazares, S., Barral, L., Bouza, R., & Montero, B. (2016). Processing and characterization of polyols plasticized-starch reinforced with microcrystalline cellulose. Carbohydrate Polymers, 149, 83–93. http://doi.org/10.1016/j.carbpol.2016.04.087

Srichuwong, S., Sunarti, T. C., Mishima, T., Isono, N., & Hisamatsu, M. (2005). Starches from different botanical sources I: Contribution of amylopectin fine structure to thermal properties and enzyme digestibility. Carbohydrate Polymers, 60(4), 529–538. http://doi.org/10.1016/j.carbpol.2005.03.004

Stevens, E. S. (2003). Environmentally Degradable Plastics. In Encyclopedia of Polymer Science and Technology. Hoboken, NJ, USA: John Wiley & Sons, Inc. http://doi.org/10.1002/0471440264.pst482

van Soest, J. J. G., Hulleman, S. H. D., de Wit, D., & Vliegenthart, J. F. G. (1996). Crystallinity in starch bioplastics. Industrial Crops and Products, 5(1), 11–22. http://doi.org/10.1016/0926-6690(95)00048-8

Wang, G., Wang, J. J., Chen, X. L., Du, L., & Li, F. (2016). Quercetin-loaded freeze-dried nanomicelles: Improving absorption and anti-glioma efficiency in vitro and in vivo. Journal of Controlled Release, 235, 276–290. http://doi.org/10.1016/j.jconrel.2016.05.045

Young, A. H. (1984). Chapter VIII – Fractionation of starch. In Starch: Chemistry and Technology (Second edi, pp. 249–283). http://doi.org/10.1016/B978-0-12-746270-7.50014-8

Yu, H., Yan, C., & Yao, J. (2014). Fully biodegradable food packaging materials based on functionalized cellulose nanocrystals/poly(3-hydroxybutyrate-co-3-hydroxyvalerate) nanocomposites. RSC Adv., 4(104), 59792–59802. http://doi.org/10.1039/C4RA12691B

## 2. Preparation and characterization of nano and microparticles of poly(3-hydroxybutyrate-co-3-hydroxyvalerate) (PHBV) via emulsification / solvent evaporation and nanoprecipitation techniques

## 1. Introduction

Polymeric nano and microparticles have many applications in different areas such as drug delivery systems, biosensors, analytical and catalysis agents, tissue engineering and for environmental applications (Joye & McClements, 2014; Lassalle & Ferreira, 2007; Retama, Mecerreyes, Lopez-Ruiz, & Lopez-Cabarcos, 2005; Rico et al., 2016). Many methods are being followed to prepare polymeric particles from a lot of polymers based on both chemical and physical behaviour of the polymers and their monomers (Rao & Geckeler, 2011; Vauthier & Bouchemal, 2009). Studying the factors that affect the morphological, chemical and physical properties of the produced particles is a key step for controlling the production of the particles and addressing their appropriate applications.

One of the most common techniques for the preparation of polymeric nano and microparticles is emulsification/solvent evaporation (Amperiadou & Georgarakis, 1995; Park & Kim, 2004; Yang, Chung, & Ping Ng, 2001). It is based on making an oil in water emulsion of polymer solution in an aqueous solution

containing a surfactant. The formation of the stable emulsion is followed by evaporation of the polymer solvent which is usually a volatile organic solvent. The emulsion is made by simple magnetic or mechanical stirring. The stirring could be followed by a further step of sonication (Musyanovych, Schmitz-Wienke, Mailänder, Walther, & Landfester, 2008). The emulsification can be performed also by ultrasonication using a high-power ultrasound (Iqbal, Valour, Fessi, & Elaissari, 2015; Lu et al., 2012). The incorporated surfactant stabilizes the emulsion, while its concentration affects the size of the droplet of the emulsion. The evaporation of the solvent is carried out by mild heating for several hours or under low pressure leaving behind polymeric nano and microparticles suspended in the aqueous phase (Lionzo, Ré, Guterres, & Pohlmann, 2007).

Nanoprecipitation is an easy technique for the preparation of polymeric nanoparticles (Drozdek & Bazylińska, 2016; Schubert, Delaney, Jr, & Schubert, 2011). It involves the selection of an appropriate anti-solvent which has to be miscible with the polymer solvent but not a solvent for the polymer. Water is the most commonly used anti-solvent. However, other solvents like organic

solvents and saline solutions can also be used (Galindo-Rodriguez, Alle, Fessi, & Doelker, 2004; Schubert et al., 2011). The precipitation of the particles of the polymer occurs when they are exposed to the anti-solvent by slow addition of one phase in the other while sonication or stirring or both. Nanoprecipitation does not require the use of surfactants. However, they could be added to the anti-solvent to stabilize the nanoparticles in some cases (Bilati, Allémann, & Doelker, 2005). The polymer nature, polymer solvent and polymer concentration, solvent/non solvent ratio, interactions and the way of addition are very important for the success of nanoprecipitation process and to get the desired size and morphology of the particles (Legrand et al., 2007).

Polyhydroxyalkanoates (PHAs) are a family of aliphatic polyesters that are produced naturally by some bacteria as a carbon and energy source (Laycock et al., 2014). They attracted the attention of the scientific community in the last years as an alternative to the petroleum source plastics with less environmental impact (Bittmann, Bouza, Barral, Castro-Lopez, & Dopico-Garcia, 2015; Ding, Roether, Boccaccini, & Schubert, 2014; Kennouche et

al., 2016; Poletto et al., 2008). Poly(3-hydroxybutyrate-co-3-hydroxyvalerate) (PHBV) is a copolymer of hydroxybutyrate (HB) and hydroxyvalerate) (HV) in different molar ratios (Bakare et al., 2016). It is a completely biodegradable (Bordes, Pollet, & Avérous, 2009; B. Wang et al., 2013) and biocompatible biopolymer (Shishatskaya, Volova, Puzyr, Mogilnaya, & Efremov, 2004) which is produced either by microorganisms or genetically modified plants (Baran, Ozer, & Hasirci, 2002). It has many applications in the fields of medicine (Meng et al., 2008), tissue engineering (Bai, Dai, & Li, 2015; Williams, Martin, Horowitz, & Peoples, 1999), drug delivery (Durán, Alvarenga, Da Silva, Melo, & Marcato, 2008; Vilos et al., 2013) and in packaging industry as a substitute to traditional non-biodegradable plastics (Bittmann, Bouza, Barral, Diez, & Ramirez, 2013; Chandra & Rustgi, 1998; Farmahini-Farahani, Xiao, Khan, Pan, & Yang, 2015; Pawar, Misra, Bose, Chatterjee, & Mittal, 2015).

The work presented in this chapter on one hand introduces nanoprecipitation as a possible technique for the preparation of PHBV nano and microparticles which was not reported before. On the other hand, the chapter also studies the effect of the surfactant

type, surfactant concentration and polymer concentration on the size and the morphology of the produced nano and microparticles of PHBV via the traditional emulsification/solvent evaporation method (Bouza et al., 2016; Q. Chen et al., 2016; W. Li et al., 2014; Lightfoot Vidal et al., 2016; Pacheco, Amaral, Reis, Marques, & Correlo, 2015; Pich, Schiemenz, Corten, & Adler, 2006; Pramual et al., 2016).

The morphology and the size of the nano and microparticles of PHBV produced via both techniques were analysed using field emission scanning electron microscope (FESEM), static mode light scattering (SLS) and dynamic light scattering (DLS).

The produced nano and microparticles of PHBV are intended basically to be used as reinforcement fillers of biopolymer packaging matrices made of different types of biomaterials such as PHBV and different types of starch. For that use, nanoprecipitation shows advantages with respect to emulsification/solvent evaporation method; as an easy, reproducible, low cost and a high yield technique.

## 2. Materials and methods

### *2.1. Materials and reagents*

Poly(3-hydroxybutyrate-co-3-hydroxyvalerate) with 12% hydroxyvalerate (HV) content (PHBV) Mw: 240,000, was supplied by Goodfellow Cambridge limited, UK. Sodium dodecyl sulphate (SDS), chloroform, dichloromethane, ethanol, methanol and dimethylformamide (DMF) were purchased from Scharlau, Spain. Polyvinyl alcohol (PVA) 86.7-88.7 mol% hydrolysis Mw: 31,000 (Mowiol® 4-88) and sodium chloride were purchased from Sigma Aldrich, Germany. All chemicals were used without further purification. The water used in both techniques and washing was purified on a Milli-Q ultrapure system (Millipore, Molsheim, France).

### *2.2. Preparation of the particles via emulsification/solvent evaporation*

PHBV was dissolved in dichloromethane in different concentrations using sonication, or both sonication and heating at 40 ºC for high concentrations. The aqueous phase was prepared with

two different surfactants viz. SDS and PVA to study their effect. The SDS was added to water and the mixing was performed at room temperature. Heating at 90 ºC with continuous stirring was necessary for making PVA solution. PHBV solution was poured on the aqueous solutions. The emulsion was formed by either stirring or ultrasonication with a high-power ultrasound. The stirring was performed for 1h using magnetic or mechanical stirrer. The ultrasonication was performed for 20 min using an ultrasonic processor SONOPULS HD 3200 (Bandelin electronics, Germany) equipped with a titanium microtip of 13 mm diameter. The ultrasonic power is up to 200 W and the processing frequency is 20 kHz. The organic solvent was evaporated by stirring overnight at 40 ºC. The particles were collected in the aqueous solution, washed several times with deionized water, and then lyophilized to be characterized. Lyophilisation was performed with a Lyoquest-85 (Azbil Telstar Technologies, S. L. U., Spain) at 0.2 mbar for at least 3 days.

*Table 2.5 Preparation conditions of PHBV particles via emulsification/solvent evaporation.*

| No | PHBV concentration % w/v | Surfactant | Surfactant concentration % w/v | Conditions |
|---|---|---|---|---|
| 1ES | 1 | SDS | 0.3 | Stirring for 1h |
| 2ES | | | 1 | |
| 3ES | | | 2 | |
| 4ES | | | 5 | |
| 5ES | | | 10 | |
| 6ES | | | 15 | |
| 7ES | 0.1 | | 1 | |
| 8ES | | | 2 | |
| 9ES | | | 5 | |
| 10ES | | | 10 | |
| 11ES | 1 | | 1 | Ultrasonication for 20 min |
| 12ES | 1 | PVA | 4 | Stirring for 1h |
| 13ES | | | 5 | |
| 14ES | | | 10 | |
| 15ES | 0.5 | | 10 | |
| 16ES | 0.1 | | 10 | |
| 17ES | 1 | | 1 | Ultrasonication for 20 min |

In case of using SDS as surfactant, a first series of particles were prepared by adding 50 mL of 1% PHBV in dichloromethane to a 250 mL beaker containing 100 mL of water with different concentrations of SDS as is shown in Table 2.5 (samples 1ES-6ES). The beaker was tapped and stirred magnetically at 1000 rpm for 1h at room temperature to form a stable emulsion. The emulsion was

left overnight at 40 ºC with stirring for evaporating the dichloromethane. A second series of preparations was performed repeating the same previously mentioned procedure but with 0.1% PHBV in dichloromethane (samples 7ES-10ES).

The same procedure was repeated using different concentrations of PVA as surfactant [Table 2.5, samples 12ES-17ES]. In this case 100 mL of organic phase were added to 300 mL of aqueous phase, the stirring was performed with mechanical stirrer as the magnetic stirring is not adequate for the viscous PVA solution. Variation of the PVA concentration and the polymer concentration were performed to study the effect of those factors on the morphology and the size of the produced particles.

*2.3. Preparation of the particles via nanoprecipitation*

Different concentrations of PHBV in chloroform and dichloromethane were prepared as mentioned before. PHBV solution in DMF was prepared by heating in a water bath at 85 ºC for 2 h. The PHBV solution was dropped in the anti-solvent during

ultrasonication or mechanical stirring at room temperature. The organic solvent was evaporated and the particles were washed several times with water, or washed directly without evaporation in case of using DMF as the boiling point of DMF is higher than water. The collected particles were lyophilized to be characterized.

Many combinations of different conditions and concentrations have been tested to produce PHBV nanoparticles via nanoprecipitation. As PHBV was found to be soluble in few organic solvents, the major changes were applied to the anti-solvent and the addition process. Absolute ethanol; 80% ethanol/20% water; 70% ethanol/30% water; methanol; 90% methanol/10% water; 80% methanol/20% water; water; and 10% NaCl solution in water were tested as anti-solvents, the addition was accompanied with mechanical stirring, both mechanical stirring and conventional sonication in a sonication bath or ultrasonication. In the case of using DMF as a solvent, the polymer solution was cooled to room temperature then dropped on water applying both mechanical stirring and conventional sonication in an ice bath. Table 2.6 shows

the different procedures followed for the preparation of PHBV particles via nanoprecipitation.

*Table 2.6 Preparation conditions of PHBV particles via nanoprecipitation.*

| No | PHBV w/v % | Organic solvent | Surfactant concentration w/v % | Anti-solvent | Conditions |
|---|---|---|---|---|---|
| 1NE | 1 | Dichloromethane | | Ethanol | Stirring |
| 2NE | | | SDS 1% | | |
| 3NE | | | SDS 0.3% | | |
| 4NE | 0.4 | | | | |
| 5NE | 0.2 | | | | |
| 6NE | 0.1 | | | | |
| 7NE | 1 | | | 80% ethanol+20% water | |
| 8NE | | | | 70% ethanol+30% water | Ultrasonication 50% |
| 9NE | | | | | |
| 10NM | 0.1 | Chloroform | | Methanol | Stirring |
| 11NM | 1 | | | | |
| 12NM | 2 | | | | |
| 13NM | 0.1 | | | 90% methanol + 10% water | |
| 14NM | 1 | | | | |
| 15NM | 2 | | | | |
| 16NM | 0.1 | | | 80% methanol + 20% water | |
| 17NM | 1 | | | | |
| 18NM | 2 | | | | |
| 19NM | 0.1 | | | 70% methanol + 30% water | |
| 20NM | 1 | | | | |
| 21NM | 2 | | | | |
| 22NW | 0.5 | DMF | | Water | Stirring + Sonication |
| 23NW | 0.25 | | | | |
| 24NW | 0.1 | | | 10% NaCl water solution | |

*2.4. Characterization*

The morphology of the particles was characterized using a Carl Zeiss ultra plus field emission scanning electron microscope (FESEM) operated at 3 kV (Carl Zeiss, Germany). The particles were previously sputter-coated with iridium using QUORUM Q150T-S turbo-pumped sputter coater (Quorum Technologies Ltd, UK).

The size of the particles was determined using static mode light scattering (SLS) Saturn DigiSizer II 5205 (Micromeritics Instrument Corporation, U.S.A) and dynamic light scattering (DLS) Zetasizer 3000 (Malvern Instruments, UK). The size of the particles was measured while dispersed in deionized water.

## 3. Results and discussion.

*3.1. Emulsification/solvent evaporation*

Two groups of particles were produced via this method. In the preparation of the first group SDS was used as emulsifying agent, while PVA was used in the second one. The polymer concentration, the surfactant concentration and switching between stirring and

ultrasonication were performed in each group. The produced particles were collected and analysed to study the effect of those factors on their size and morphology.

### *3.1.1. Emulsification using SDS*

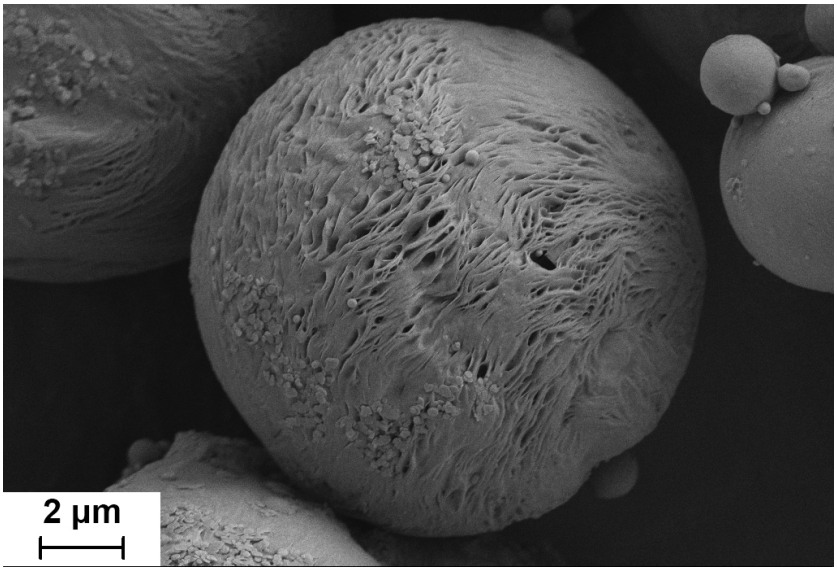


*Figure 2.13 Micrograph of a microparticle of PHBV prepared by emulsification/solvent evaporation method using 1% PHBV in dichloromethane and SDS as surfactant in a concentration of 1% (2ES).*

In general, spherical porous particles of PHBV were obtained via this preparation method [Figure 2.13]. Increasing the SDS concentration was accompanied with the decreasing of the size of the particles and a narrower size distribution. Although nanoparticles of PHBV can be obtained using SDS as surfactant,

those nanoparticles were always accompanied with relatively wide size range of microparticles except when very high SDS concentrations were used. The nanoparticles can be easily separated from the microparticles by filtration and ultra-filtration.

The analysis of the size of the particles by the static light scattering technique [Figure 2.14] shows that by using 0.3% surfactant concentration (a: 1ES), microparticles with wide size distribution were obtained, most of them are between 7-20 µm. This is higher than the size of the particles reported by Bouza et al. which ranges from 0.8-7 µm under the same preparation conditions (Bouza et al., 2016). By using 5% SDS concentration (d: 4ES), the size of the particles decreased to be in the range of 2-5 µm. Nanoparticles of PHBV appeared together with the microparticles starting from 2% SDS concentration (c: 3ES), The percentage of the nanoparticles increases with increasing the SDS concentration while its size remains around 350 nm independent on the surfactant concentration. Reaching a concentration of 15% SDS (f: 6ES), most of the particles were between 1-2 µm in addition to nanoparticles of 440 ± 134 nm.

Figure 2.15 shows the changes in the morphology and in the particle size distribution by changing the SDS concentration.

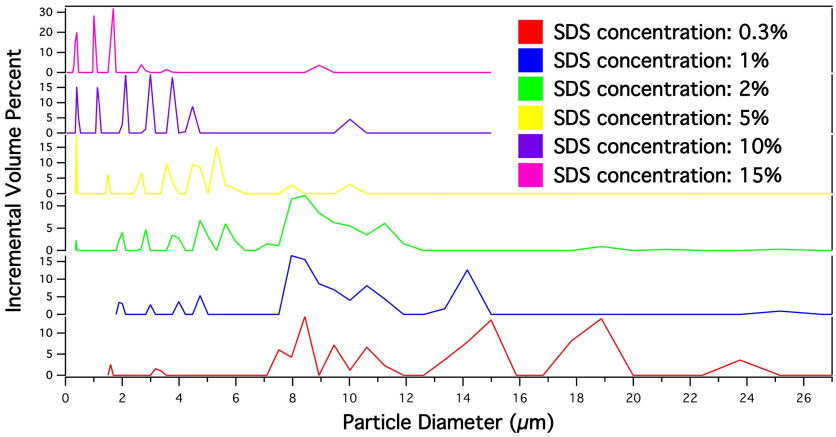


*Figure 2.14 Static light scattering plot. Particle diameter in μm vs incremental volume percent for different PHBV samples prepared by emulsification/solvent evaporation using different concentrations of SDS as surfactant and PHBV concentration of 1%.*

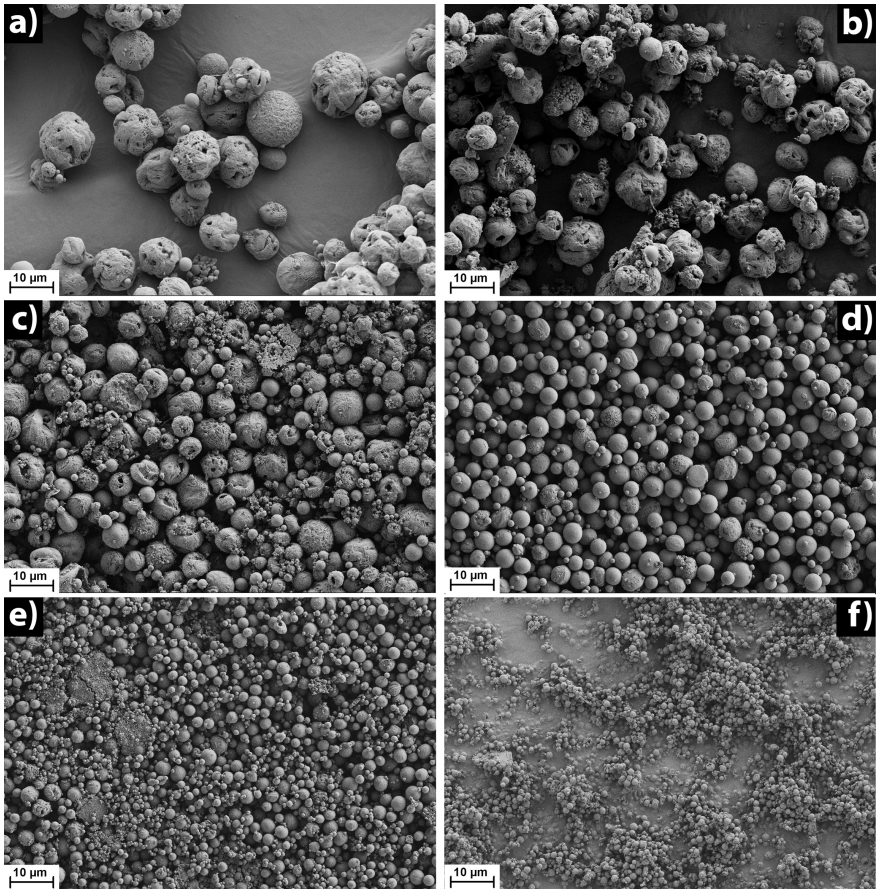


*Figure 2.15 Micrograph of nano and microparticles of PHBV prepared by emulsification/solvent evaporation method using 1% PHBV in dichloromethane and SDS as surfactant with concentrations: 0.3% (a: 1ES), 1% (b: 2ES), 2% (c: 3ES), 5% (d: 4ES), 10% (e: 5ES), 15% (f: 6ES).*

Figure 2.16 shows a comparison between two groups of particles that were prepared by the same conditions but varying the polymer concentration and the SDS concentration. The first group –

at the left side (a, c, e, g) - was prepared with 1% PHBV and various SDS concentrations (1, 2, 5 and 10 %), where the second group –at the right side (b, d, f, h) - was prepared using 0.1% PHBV with the same SDS concentrations. It was found that at low SDS concentration (1%), the size of the particles decreased by decreasing the polymer concentration and the particles are smoother with less pores (a, b). The polymer solution with lower concentration is less viscous which make it easier to be dispersed in small droplets (Freitas, Merkle, & Gander, 2005). The polymer concentration did not show a significant effect on the size of the particles at high SDS concentration (10%). Such a high surfactant concentration stabilizes the small emulsion microspheres and decrease its aggregation during the emulsification and solvent evaporation steps.

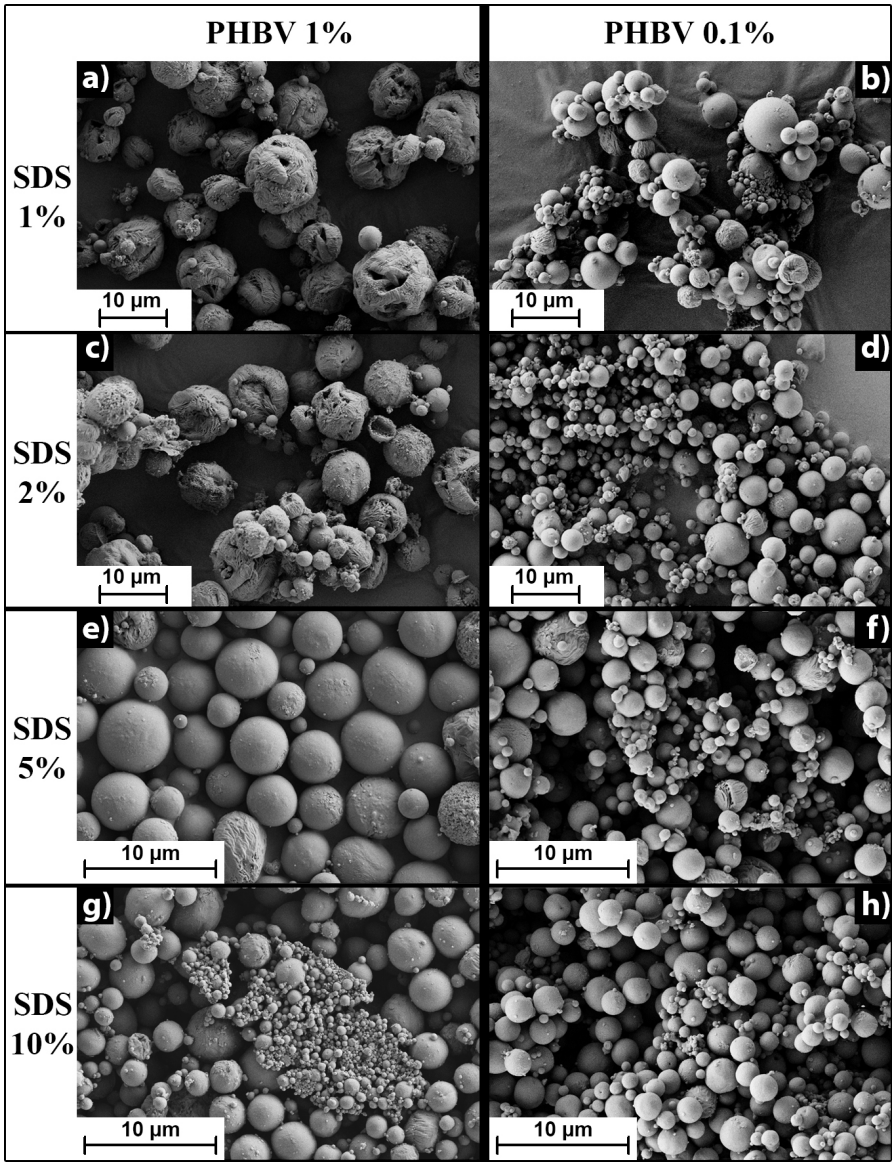


*Figure 2.16 Micrograph of nano and microparticles of PHBV prepared by emulsification/solvent evaporation method using SDS as surfactant with concentrations: 1% PHBV, 1% SDS (a: 2ES), 0.1% PHBV 1% SDS (b: 7ES), 1% PHBV 2% SDS (c: 3ES), 0.1% PHBV 2% SDS (d: 8ES), 1% PHBV 5% SDS (e: 4ES), 0.1% PHBV 5% SDS (f: 9ES), 1% PHBV 10% SDS (g: 5ES), 0.1% PHBV 10% SDS (h: 10ES).*

It seems that increasing the concentration of the surfactant has no significant effect on the size at a very low polymer concentration (0.1%) until reaching very high SDS concentration (10%). The produced particles in those series of preparation were microparticles between 2-10 µm with a population of nanoparticles of around 380 nm. When using a concentration of 10% SDS, the microparticles were between 1-2 µm while maintaining the same population of nanoparticles [Figure 2.17].

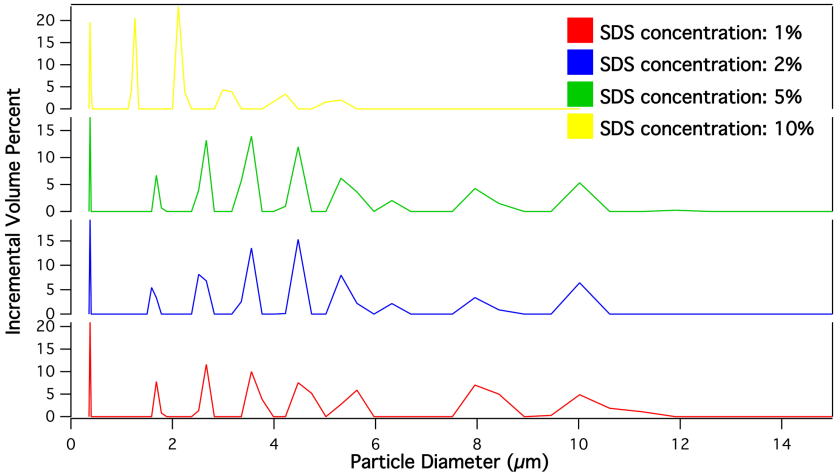


*Figure 2.17 Static light scattering plot. Particle diameter in µm vs incremental volume percent for different PHBV samples prepared by emulsification/solvent evaporation using different concentrations of SDS as surfactant and polymer concentration of 0.1%.*

*3.1.2. Emulsification using PVA*

As is shown in Figure 2.18 and Figure 2.19, when using 1% PHBV with a concentration of PVA (4%) porous particles with wide range of sizes were obtained. Most of the particles are microparticles of 7-18 µm together with a population of few micrometres 2-5 µm. By increasing PVA concentration to 5%, the produced particles were slightly smaller. The two populations of particles were still observed. More homogenous population of smoother and smaller microparticles were produced using 10% PVA, the size of the particles decreases to be between 1-3 µm, with much less pore sizes as is seen in Figure 2.19. Göz et al. have reported the production of nanoparticles of PHBV (12% mol HV) with size of 531 ± 150 nm using a high-speed homogenizer and a PVA concentration of 4%. Larger particles were formed in the form of coalescent globules using 10% of PVA, where no particles were obtained at PVA concentrations lower than 4% (Göz & Karakeçili, 2016).

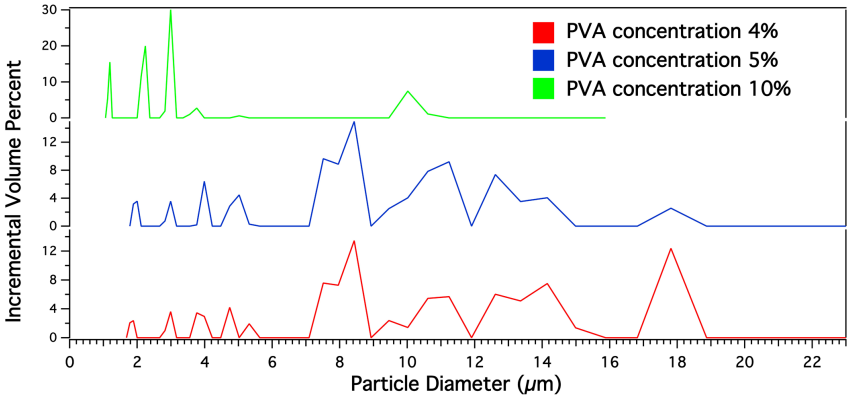


*Figure 2.18 Static light scattering plot. Particle diameter in μm vs incremental volume percent for different PHBV samples prepared by emulsification/solvent evaporation using different concentrations of PVA as surfactant and polymer concentration of 1%.*

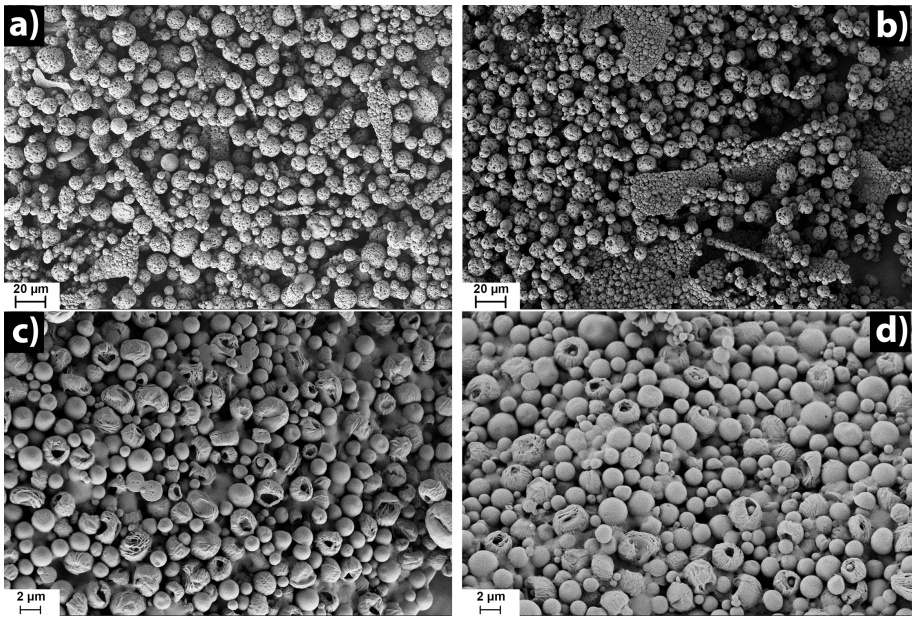


*Figure 2.19 Micrograph of nano and microparticles of PHBV prepared by emulsification/solvent evaporation method using PVA as surfactant with concentrations: 1% PHBV 4% / PVA (a: 12ES), 1% PHBV / 5%PVA (b: 13ES), 1% PHBV / 10% PVA (c: 14ES), 0.5% PHBV 10% PVA (d: 15ES).*

The analysis of the particles produced by various polymer concentrations shows that by decreasing the PHBV concentration to 0.5% while maintaining the PVA concentration at 10%, the particle size distribution decreased slightly. Most of particles were around 1-2 μm. Lowering the concentration of PHBV to 0.1% produced nanoparticles of around 380 nm in addition to microparticles of 1-2 μm [Figure 2.20]. Coimbra et al. (Coimbra, De Sousa, & Gil, 2008) have studied the effect of polymer concentration and the stabilizer concentration on the size of PHBV (6% mol HV) microparticles. They found that the polymer concentration is the only factor that significantly affect the size of the particles. They considered that the concentration of the surfactant has no effect on the mean particle size, which is not the case in our results.

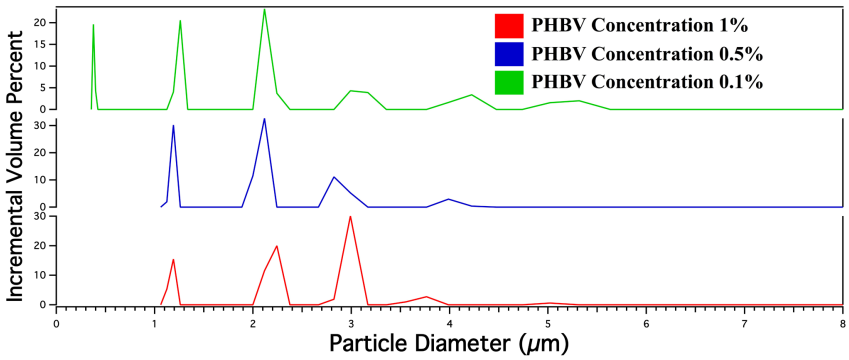


*Figure 2.20 Static mode light scattering plot. Particle diameter in μm vs incremental volume percent for different PHBV samples prepared by emulsification/solvent evaporation using solution of 10% PVA as surfactant and three different polymer concentrations.*

According to the showed results, mainly microparticles were obtained when using PVA as a surfactant and following the previously mentioned procedure. The size distribution of those microparticles can be controlled varying mainly PVA and the polymer concentration. Decreasing the polymer concentration or increasing the surfactant concentration gave smaller microparticles with a narrower size distribution range. Obtaining nanoparticles is possible using very low concentration of PHBV solution and high PVA concentration for making the emulsion. However, a filtration step is necessary to separate nanoparticles from microparticles.

The morphology of the polymeric particles depends on many factors like the solvent, the temperature during the preparation, the polymer composition and the crystallinity of the polymer (Gangrade & Price, 1991). PHBV is a highly crystalline polymer (ranging from 35% to 60%) (Lightfoot Vidal et al., 2016), therefore, its micro particles are rough and porous (W. Li et al., 2014). The roughness of the particles increases by increasing the molar fraction of (HV) within the copolymer (Murueva, Shishatskaya, Kuzmina, Volova, & Sinskey, 2013).The porosity was considered to be important for the encapsulation and the release behaviour of the particles (Grillo et al., 2011). Gnagrade et al. and Bouza et al. reported the decrease of size of the pores of the particles of PHBV by using dichloromethane instead of chloroform as a polymer solvent (Bouza et al., 2016; Gangrade & Price, 1991). Figure 2.15 shows that the size of the pores decreases by increasing the concentration of the surfactant. The pores almost disappeared and the particles are smooth at high SDS concentrations. Using lower polymer concentration resulted in the production of particles with much smoother surface and with less size and number of pores [Figure 2.16]. The microparticles produced

using SDS were smoother than those produced by PVA at the same surfactant concentration.

For establishing a comparison between the effect of both utilized surfactants, it can be said that at high concentration of surfactant (10%), PVA produces more homogenous and smaller microparticles. However, nanoparticles were obtained besides the microparticles when using SDS in the same concentration. More percentage of nanoparticles can be produced by increasing the SDS concentration and/or decreasing the polymer concentration. Obtaining only nanoparticles could be achieved simply by filtration the produced mixture of nano and microparticles. At low surfactant concentration (5%), the particles produced using SDS were smaller and the particle size distribution was narrower.

Another way to obtain a majority of nanoparticles is to use ultrasonication by a high-power ultrasound (Baran et al., 2002; Rodríguez-Contreras et al., 2013). Two samples were prepared by emulsification of 1% PHBV in 1% SDS and 1% PVA, respectively (11ES, 17ES). The ultrasonication was applied for 20 min at 50% power. Nanoparticles with a size of 398 ± 65 nm were obtained using

SDS, while with PVA the mean size was 297 ± 93 nm. The size distribution was significantly wider utilizing PVA [Figure 2.21]. Göz et al. (Göz & Karakeçili, 2016) and Lightfoot Vidal et al. (Lightfoot Vidal et al., 2016) have reported the use of the high-speed homogenizer for the preparation of nanoparticles of PHBV. The mean particle size of the nanoparticles obtained by Lightfoot Vidal et al. was around 611nm before filtration and 234 nm after filtration. The surfactant used was PVA 85,000–124,000 molecular weight in a concentration of 0.025%.

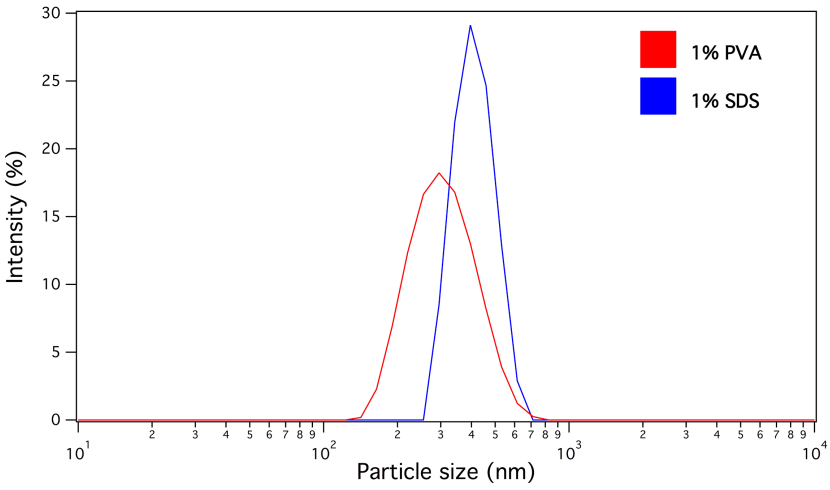


*Figure 2.21 Dynamic light scattering plot showing the size distribution of two PHBV samples prepared by emulsification/solvent evaporation of 1% PHBV in dichloromethane using two different surfactants, SDS (11ES) and PVA (17ES) applying the ultrasonication instead of stirring for emulsion preparation.*

*3.2. Nanoprecipitation*

Although the nanoprecipitation technique is one of the simplest way for the preparation of the nanoparticles, it is necessary to adjust many parameters to get the desired particles with proper size distribution and morphology and to evade any possible aggregation. The polymer concentration should be relatively low. The ratios between solvent / nonsolvent and nonsolvent / co-nonsolvent (if any) must be in the acceptable range. The addition process and the stirring or sonication rate and power have considerable impact on the whole process (Schubert et al., 2011).

*3.2.1. Ethanol as anti-solvent*

Different experiments were performed using different PHBV solution concentrations in dichloromethane as a polymer solvent, and absolute ethanol as an anti-solvent. The polymer solution was dropped on the anti-solvent solution considering that the ratio between dichloromethane and ethanol should not reach 7:3, by passing this ratio the mixture of dichloromethane and ethanol can

dissolve the particles (Poletto et al., 2008). The addition was accompanied with mechanical stirring at 300 rpm.

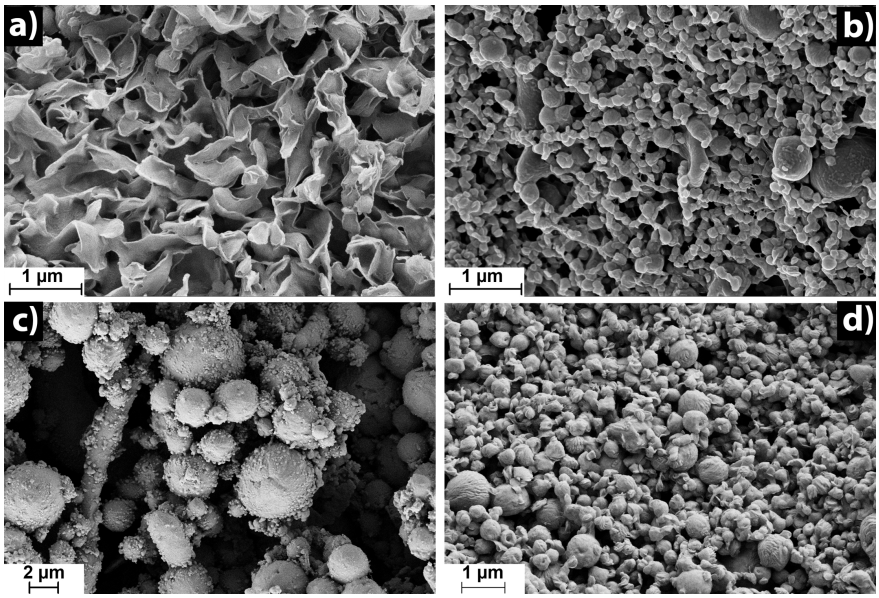


*Figure 2.22 Micrograph of nano and microparticles of PHBV prepared by nanoprecipitation method using 1% PHBV in dichloromethane and a mixture of ethanol and water as anti-solvent: 100% ethanol (a: 1NE), 80% ethanol/20% water (b: 7NE), 70% ethanol/30% water (c: 8NE), 70% ethanol/30% water applying ultrasonication (d: 9NE).*

Although ethanol was used successfully for the production of PLA and PLGA nanoparticles (Bilati et al., 2005), the result with PHBV was non homogenous sheet-like nano structures which tend to aggregate [Figure 2.22a: 1NE]. The size of those sheet-like structures is reduced by decreasing the polymer concentration in dichloromethane. The addition of SDS as a surfactant to the anti-

solvent has no significant effect on the size or the morphology of the nanostructures.

The polarity of the ethanol was increased by the addition of water (Wyman, 1931). The water / ethanol ratio should not exceed 3:7. A solution of ethanol with more than 30% of water is not miscible with dichloromethane and will make an emulsion upon stirring instead of the desired diffusion.

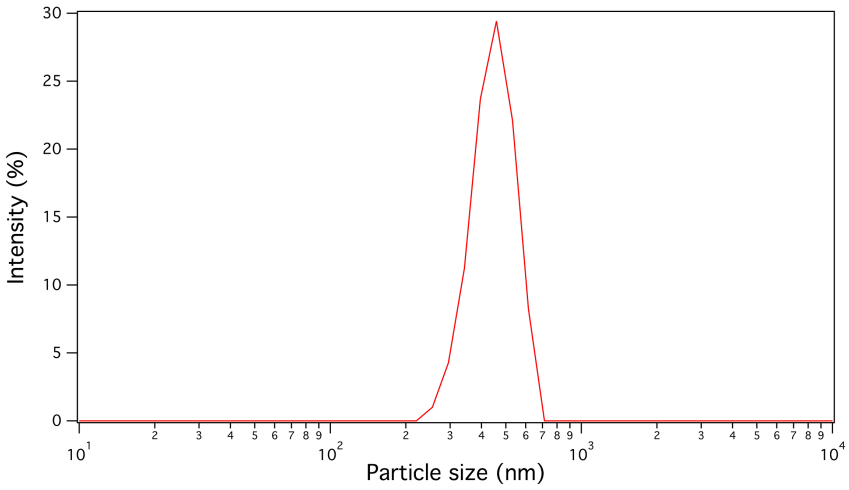


*Figure 2.23 Dynamic light scattering plot showing the size distribution of PHBV nanoparticles prepared by nanoprecipitation of 1% PHBV in dichloromethane using 70% ethanol/30% water applying ultrasonication (9NE).*

More rounded shaped nanoparticles and small microparticles in addition to some oval and nonuniform particles were obtained by the dropwise addition of 50 mL of 1% PHBV solution in

dichloromethane to 300 mL of an anti-solvent solution of 80% ethanol / 20% water under mechanical stirring at 300 rpm (7NE). Increasing the water ratio to 30% in the nonsolvent gave spherical, more rounded and separated nanoparticles with few small microparticles [Figure 2.22b-d: 7NE, 8NE, 9NE]. Better spherical nanoparticles of 400 ± 81 nm [Figure 2.23] were got by switching to ultrasonication instead of mechanical stirring.

*3.2.2. Methanol as anti-solvent*

Another series of nanoprecipitation were performed where 50 mL of 0.1, 1 and 2 % PHBV solution in chloroform were dropped on 300 mL of methanol applying stirring at 300 rpm. As in the case of ethanol, the same non-homogenous sheet-like nano structures were obtained. Bilati et al. have reported the successful use of methanol as anti-solvent for PLA and PLGA (Bilati et al., 2005).

Introducing water with methanol as an anti-solvent mixture with higher polarity (Akerlof, 1932) has changed significantly the morphology of the produced particles. However, water percentage in the nonsolvent should not exceed approximately 66.6% because a

mixture of methanol with more water percentage is immiscible with chloroform. Anti-solvent mixtures of methanol / water ratios of 90% / 10%; 80% / 20% and 70% / 30% were tested in this study [Table 2.6]. It is important to select the appropriate polymer concentration with each methanol/water ratio to get the desired size and morphology of the particles. Figure 2.24 shows the morphology of some of the particles got by this method of preparation.

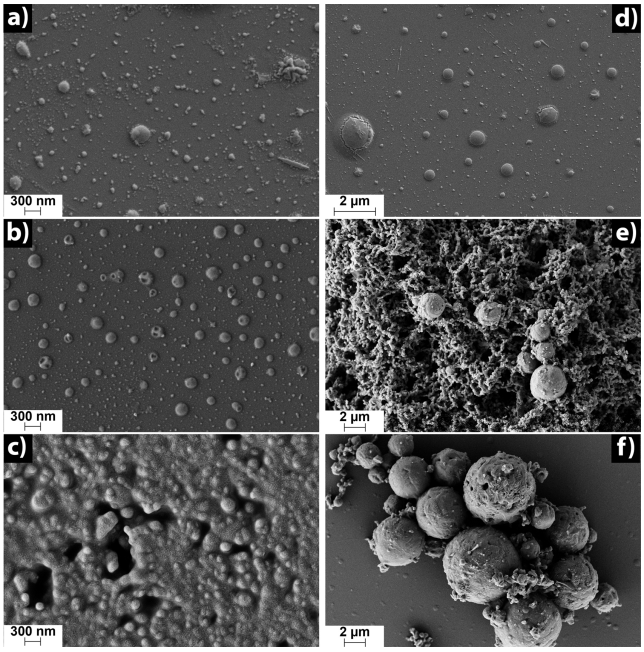


*Figure 2.24 Micrograph of nano and microparticles of PHBV prepared by nanoprecipitation method using: 0.1% PHBV / 90% methanol + 10% water (a: 13NM), 0.1% PHBV / 80% methanol+20% water (b: 16NM), 0.1% PHBV / 70% methanol+30% water (c: 19NM), 1% PHBV / 90% methanol + 10% water (d: 14NM), 1% PHBV /80% methanol+20% water (e: 17NM), 1% PHBV / 70% methanol+30% water (f: 20NM).*

Semi spherical nanoparticles with a size of 431 ± 102 nm were produced by dropping 0.1% PHBV solution on anti-solvent mixtures of 90% / 10% methanol / water (13NM). Increasing the polymer concentration to 1% produced a mixture of nano and small microparticles with the same morphology (14NM). The particles tend to aggregate when the PHBV concentration reaches 2% (15NM). Increasing water percentage to 20% while maintaining the polymer concentration at 0.1% leads to better spherical small nanoparticles in addition to decreasing the size of the particles to 162 ± 32 nm (16NM). However, microparticles and aggregations of nanoparticles started to appear with 1% and 2% PHBV (17NM, 18 NM). The size continued to decrease by increasing the water percentage in the anti-solvent mixture. A solution of 0.1% PHBV when dropped on a mixture of 70% methanol/30% water produced nanoparticles with size of 150 ± 58 nm (19NM), while increasing the PHBV concentration to 1% and 2% gave less aggregations and more spherical microparticles (20NM, 21NM).

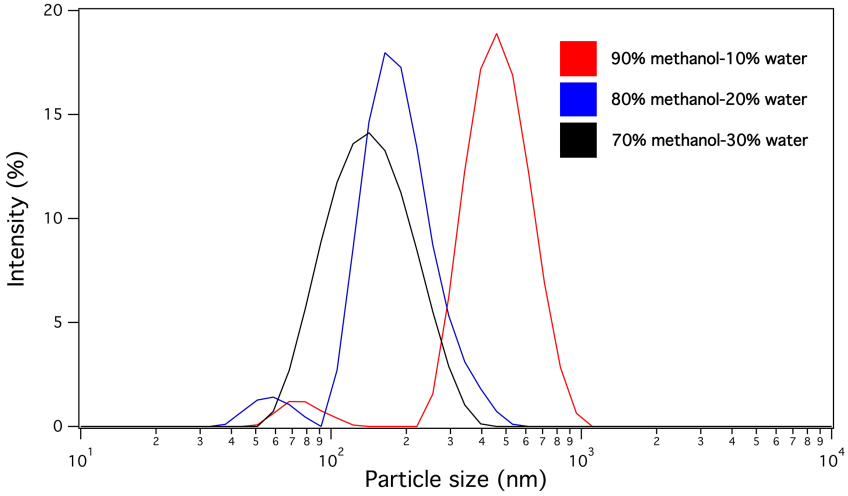


*Figure 2.25 Dynamic light scattering plot showing the size distribution of PHBV particles prepared by nanoprecipitation of 0.1% PHBV in dichloromethane using different mixtures of methanol and water as anti-solvents.*

It can be established that for getting nanoparticles, it is necessary to add water to methanol as anti-solvent mixture in addition to use very low PHBV concentration. Increasing water percentage decreases the size of the nanoparticles produced [Figure 2.26] while in case of the production of microparticles, it is recommended to use higher concentration of PHBV and high percentage of water with methanol.

*3.2.3. Water as anti-solvent*

It is not possible to make nanoprecipitation in water in case of dissolving the polymer in dichloromethane or chloroform. In this case DMF was used as a solvent capable to dissolve PHBV and at the same time it is miscible with water. Few nanoparticles appear within bigger PHBV nonuniform structures [Figure 2.26a: 22NW]. More spherical nanoparticles were produced using 10% NaCl solution in water as anti-solvent [Figure 2.26b: 24NW]. NaCl decreases the polarity of water (Gadani, Rana, Bhatnagar, Prajapati, & Vyas, 2012; Shcherbakov, Artemkina, & Korotkova, 2014), resulting in production of more spherical nanoparticles of around 200 nm.

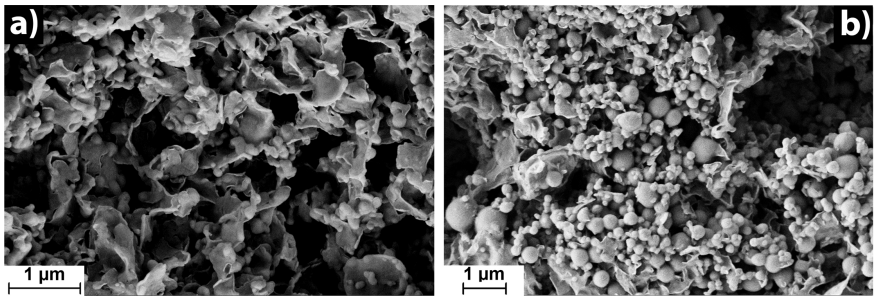


*Figure 2.26 Micrograph of nano and microparticles of PHBV prepared by nanoprecipitation method using 0.5% PHBV in DMF as solvent and water as anti-solvent (a: 22NW), 0.1% PHBV in DMF as solvent and 10% NaCl solution in water as anti-solvent (b: 24NW).*

It can be assumed that the interaction between the solvent and the anti-solvent plays a very important role –with other factors- in controlling the morphology and the size of the produced particles in nanoprecipitation where the polarity of both - solvent and the anti-solvent - are the main dominant of this interaction. In more specific words, adjusting the polarity of the anti-solvent is a key point for the success of this technique, especially for a polymer like the PHBV which has a very limited range of solvents. The addition of water to both ethanol and methanol increases the polarity of the anti-solvent mixture, while the salt addition to water decreases the dielectric constant of the anti-solvent solution reaching the adequate point for the formation of the nanoparticles.

## 4. Conclusions

PHBV nano and microparticles have been prepared through both emulsification/solvent evaporation and nanoprecipitation methods. The morphology and the size of the produced particles were controlled varying the procedure conditions. In case of emulsification/solvent evaporation, spherical porous particles of

PHBV were obtained with wide size distribution. The size, porosity and the size distribution of the particles could be controlled by controlling the surfactant type, the surfactant concentration, the polymer concentration and the emulsification method. Decreasing the polymer solution concentration or increasing the surfactant concentration gave smaller microparticles with narrower size distribution range. The surfactant concentration has more influence on the size of the particles at higher polymer concentration. Introducing the ultrasonication was necessary to obtain majority of nanoparticles.

Smaller nanoparticles and microparticles have been obtained using the nanoprecipitation technique, which has not been reported before for this polymer. The interaction between the solvent and the nonsolvent plays a crucial role in the morphology of the produced particles. In general, controlling the polarity of the anti-solvent is crucial for obtaining more spherical nano and microparticles. The polarity of water was reduced through increasing the ionic strength by adding salt. In case of ethanol and methanol, water was added to increase the anti-solvent polarity. The water percentage should be

adjusted to assure the miscibility of both solvent and anti-solvent. Nanoprecipitation as a possible technique for preparation of PHBV nanoparticles is more simple, cheaper and time saving for a high yield production.

## References

Akerlof, G. (1932). Dielectric constants of some organic solvent-water mixtures at various temperatures. Journal of the American Chemical Society, 54(11), 4125–4139. http://doi.org/10.1021/ja01350a001

Amperiadou, A., & Georgarakis, M. (1995). Controlled release salbutamol sulphate microcapsules prepared by emulsion solvent-evaporation technique and study on the release affected parameters. International Journal of Pharmaceutics, 115(1), 1–8. http://doi.org/10.1016/0378-5173(95)00223-6

Bai, J., Dai, J., & Li, G. (2015). Electrospun composites of PHBV/pearl powder for bone repairing. Progress in Natural Science: Materials International, 25(4), 327–333. http://doi.org/10.1016/j.pnsc.2015.07.004

Bakare, R., Hawthrone, S., Vails, C., Gugssa, A., Karim, A., Stubbs, J., & Raghavan, D. (2016). Antimicrobial and cell viability measurement of bovine serum albumin capped silver nanoparticles (Ag/BSA) loaded collagen immobilized poly(3-hydroxybutyrate-co-3-hydroxyvalerate) (PHBV) film. Journal of Colloid and Interface Science, 465, 140–148. http://doi.org/10.1016/j.jcis.2015.11.041

Baran, E. T., Ozer, N., & Hasirci, V. (2002). Poly(hydroxybutyrate-co-hydroxyvalerate) nanocapsules as enzyme carriers for cancer therapy: an in vitro study. Journal of Microencapsulation, 19(3), 363–376. http://doi.org/10.1080/02652040110105355

Bilati, U., Allémann, E., & Doelker, E. (2005). Development of a nanoprecipitation method intended for the entrapment of hydrophilic drugs into nanoparticles. European Journal of Pharmaceutical Sciences, 24(1), 67–75. http://doi.org/10.1016/j.ejps.2004.09.011

Bittmann, B., Bouza, R., Barral, L., Castro-Lopez, M., & Dopico-Garcia, S. (2015). Morphology and thermal behavior of poly (3-hydroxybutyrate- co -3-hydroxyvalerate)/poly(butylene adipate- co

-terephthalate)/clay nanocomposites. Polymer Composites, 36(11), 2051–2058. http://doi.org/10.1002/pc.23115

Bittmann, B., Bouza, R., Barral, L., Diez, J., & Ramirez, C. (2013). Poly(3-hydroxybutyrate- co -3-hydroxyvalerate)/clay nanocomposites for replacement of mineral oil based materials. Polymer Composites, 34(7), 1033–1040. http://doi.org/10.1002/pc.22510

Bordes, P., Pollet, E., & Avérous, L. (2009). Nano-biocomposites: Biodegradable polyester/nanoclay systems. Progress in Polymer Science, 34(2), 125–155. http://doi.org/10.1016/j.progpolymsci.2008.10.002

Bouza, R., del Mar Castro, M., Dopico-García, S., Victoria González-Rodríguez, M., Barral, L. F., & Bittmann, B. (2016). Polylactic acid and poly(3-hydroxybutyrate-co-3-hydroxyvalerate) nano and microparticles for packaging bioplastic composites. Polymer Bulletin, 73(12), 1–18. http://doi.org/10.1007/s00289-016-1687-2

Chandra, R., & Rustgi, R. (1998). Biodegradable polymers. Progress in Polymer Science, 23(7), 1273–1335. http://doi.org/10.1016/S0079-6700(97)00039-7

Chen, Q., Li, W., Yao, Q., Liang, R., Pérez-Garcia, R., Munoz, J., & Boccaccini, A. R. (2016). Multilayered drug delivery coatings composed of daidzein-loaded PHBV microspheres embedded in a biodegradable polymer matrix by electrophoretic deposition. Journal of Materials Chemistry B, 4(29), 5035–5045. http://doi.org/10.1039/C6TB00113K

Coimbra, P. A., De Sousa, H. C., & Gil, M. H. (2008). Preparation and characterization of flurbiprofen-loaded poly(3-hydroxybutyrate-co-3-hydroxyvalerate) microspheres. Journal of Microencapsulation, 25(3), 170–178. http://doi.org/10.1080/02652040701814140

Ding, Y., Roether, J. A., Boccaccini, A. R., & Schubert, D. W. (2014). Fabrication of electrospun poly (3-hydroxybutyrate)/poly (ε-caprolactone)/silica hybrid fibermats with and without calcium

addition. European Polymer Journal, 55, 222–234. http://doi.org/10.1016/j.eurpolymj.2014.03.020

Drozdek, S., & Bazylińska, U. (2016). Biocompatible oil core nanocapsules as potential co-carriers of paclitaxel and fluorescent markers: preparation, characterization, and bioimaging. Colloid and Polymer Science, 294(1), 225–237. http://doi.org/10.1007/s00396-015-3767-5

Durán, N., Alvarenga, M. A., Da Silva, E. C., Melo, P. S., & Marcato, P. D. (2008). Microencapsulation of antibiotic rifampicin in poly(3-hydroxybutyrate-co-3- hydroxyvalerate). Archives of Pharmacal Research, 31(11), 1509–1516. http://doi.org/10.1007/s12272-001-2137-7

Farmahini-Farahani, M., Xiao, H., Khan, A., Pan, Y., & Yang, Y. (2015). Preparation and characterization of exfoliated PHBV nanocomposites to enhance water vapor barriers of calendared paper. Industrial and Engineering Chemistry Research, 54(45), 11277–11284. http://doi.org/10.1021/acs.iecr.5b02734

Freitas, S., Merkle, H. P., & Gander, B. (2005). Microencapsulation by solvent extraction/evaporation: Reviewing the state of the art of microsphere preparation process technology. Journal of Controlled Release, 102(2), 313–332. http://doi.org/10.1016/j.jconrel.2004.10.015

Gadani, D. H., Rana, V. A., Bhatnagar, S. P., Prajapati, A. N., & Vyas, A. D. (2012). Effect of salinity on the dielectric properties of water. Indian Journal of Pure & Applied Physics, 50(June), 405–410.

Galindo-Rodriguez, S., Alle, E., Fessi, H., & Doelker, E. (2004). Physicochemical parameters associated with nanoparticle formation in the salting-out , nanoprecipitation methods. Pharmaceutical Research, 21(8), 1428–1439. http://doi.org/10.1023/B:PHAM.0000036917.75634.be

Gangrade, N., & Price, J. C. (1991). Poly(hydroxybutyrate-hydroxyvalerate) microspheres containing progesterone: preparation, morphology and release properties. Journal of

Microencapsulation, 8(2), 185–202. http://doi.org/10.3109/02652049109071487

Göz, E., & Karakeçili, A. (2016). Effect of emulsification-diffusion parameters on the formation of poly (3-hydroxybutyrate-co-3-hydroxyvalerate) particles. Artificial Cells, Nanomedicine, and Biotechnology, 44(1), 226–234. http://doi.org/10.3109/21691401.2014.937869

Grillo, R., Pereira, A. do E. S., de Melo, N. F. S., Porto, R. M., Feitosa, L. O., Tonello, P. S., … Fraceto, L. F. (2011). Controlled release system for ametryn using polymer microspheres: Preparation, characterization and release kinetics in water. Journal of Hazardous Materials, 186(2–3), 1645–1651. http://doi.org/10.1016/j.jhazmat.2010.12.044

Iqbal, M., Valour, J. P., Fessi, H., & Elaissari, A. (2015). Preparation of biodegradable PCL particles via double emulsion evaporation method using ultrasound technique. Colloid and Polymer Science, 293(3), 861–873. http://doi.org/10.1007/s00396-014-3464-9

Joye, I. J., & McClements, D. J. (2014). Biopolymer-based nanoparticles and microparticles: Fabrication, characterization, and application. Current Opinion in Colloid & Interface Science, 19(5), 417–427. http://doi.org/10.1016/j.cocis.2014.07.002

Kennouche, S., Le Moigne, N., Kaci, M., Quantin, J. C., Caro-Bretelle, A. S., Delaite, C., & Lopez-Cuesta, J. M. (2016). Morphological characterization and thermal properties of compatibilized poly(3-hydroxybutyrate-co-3-hydroxyvalerate) (PHBV)/poly(butylene succinate) (PBS)/halloysite ternary nanocomposites. European Polymer Journal, 75, 142–162. http://doi.org/10.1016/j.eurpolymj.2015.12.009

Lassalle, V., & Ferreira, M. L. (2007). PLA nano- and microparticles for drug delivery: An overview of the methods of preparation. Macromolecular Bioscience, 7(6), 767–783. http://doi.org/10.1002/mabi.200700022

Laycock, B., Halley, P., Pratt, S., Werker, A., & Lant, P. (2014). The chemomechanical properties of microbial polyhydroxyalkanoates. Progress in Polymer Science, 39(2), 397–442. http://doi.org/10.1016/j.progpolymsci.2013.06.008

Legrand, P., Lesieur, S., Bochot, A., Gref, R., Raatjes, W., Barratt, G., & Vauthier, C. (2007). Influence of polymer behaviour in organic solution on the production of polylactide nanoparticles by nanoprecipitation. International Journal of Pharmaceutics, 344(1–2), 33–43. http://doi.org/10.1016/j.ijpharm.2007.05.054

Li, W., Ding, Y., Rai, R., Roether, J. A., Schubert, D. W., & Boccaccini, A. R. (2014). Preparation and characterization of PHBV microsphere/45S5 bioactive glass composite scaffolds with vancomycin releasing function. Materials Science and Engineering C, 41, 320–328. http://doi.org/10.1016/j.msec.2014.04.052

Lightfoot Vidal, S., Rojas, C., Bouza Padin, R., Perez Rivera, M., Haensgen, A., Gonzalez, M., & Rodriguez-Llamazares, S. (2016). Synthesis and characterization of polyhydroxybutyrate-co-hydroxyvalerate nanoparticles for encapsulation of quercetin. Journal of Bioactive and Compatible Polymers, 31(5), 439–452. http://doi.org/10.1177/0883911516635839

Lionzo, M. I. Z., Ré, M. I., Guterres, S. S., & Pohlmann, A. R. (2007). Microparticles prepared with poly(hydroxybutyrate-co-hydroxyvalerate) and poly(ε-caprolactone) blends to control the release of a drug model. Journal of Microencapsulation, 24(2), 175–186. http://doi.org/10.1080/02652040701233556

Lu, R., Xu, B., Tao, K., Dou, H., Qiu, Y., Sun, K., … Sun, K. (2012). Structure and acoustical properties control of magnetite/PLA composite microbubbles. Colloid and Polymer Science, 290(1), 63–71. http://doi.org/10.1007/s00396-011-2523-8

Meng, W., Xing, Z. C., Jung, K. H., Kim, S. Y., Yuan, J., Kang, I. K., … Shin, H. I. (2008). Synthesis of gelatin-containing PHBV nanofiber mats for biomedical application. Journal of Materials Science: Materials in Medicine, 19(8), 2799–2807. http://doi.org/10.1007/s10856-007-3356-3

Murueva, A. V., Shishatskaya, E. I., Kuzmina, A. M., Volova, T. G., & Sinskey, A. J. (2013). Microparticles prepared from biodegradable polyhydroxyalkanoates as matrix for encapsulation of cytostatic drug. Journal of Materials Science: Materials in Medicine, 24(8), 1905–1915. http://doi.org/10.1007/s10856-013-4941-2

Musyanovych, A., Schmitz-Wienke, J., Mailänder, V., Walther, P., & Landfester, K. (2008). Preparation of biodegradable polymer nanoparticles by miniemulsion technique and their cell interactions. Macromolecular Bioscience, 8(2), 127–139. http://doi.org/10.1002/mabi.200700241

Pacheco, D. P., Amaral, M. H., Reis, R. L., Marques, A. P., & Correlo, V. M. (2015). Development of an injectable PHBV microparticles-GG hydrogel hybrid system for regenerative medicine. International Journal of Pharmaceutics, 478(1), 398–408. http://doi.org/10.1016/j.ijpharm.2014.11.036

Park, S.-J., & Kim, S.-H. (2004). Preparation and characterization of biodegradable poly(l-lactide)/poly(ethylene glycol) microcapsules containing erythromycin by emulsion solvent evaporation technique. Journal of Colloid and Interface Science, 271(2), 336–341. http://doi.org/10.1016/j.jcis.2003.08.067

Pawar, S. P., Misra, A., Bose, S., Chatterjee, K., & Mittal, V. (2015). Enzymatically degradable and flexible bio-nanocomposites derived from PHBV and PBAT blend: assessing thermal, morphological, mechanical, and biodegradation properties. Colloid and Polymer Science, 293(10), 2921–2930. http://doi.org/10.1007/s00396-015-3700-y

Pich, A., Schiemenz, N., Corten, C., & Adler, H. J. P. (2006). Preparation of poly(3-hydroxybutyrate-co-3-hydroxyvalerate) (PHBV) particles in O/W emulsion. Polymer, 47(6), 1912–1920. http://doi.org/10.1016/j.polymer.2006.01.038

Poletto, F. S., Fiel, L. A., Donida, B., Ré, M. I., Guterres, S. S., & Pohlmann, A. R. (2008). Controlling the size of poly(hydroxybutyrate-co-hydroxyvalerate) nanoparticles prepared by emulsification–diffusion technique using ethanol as surface

agent. Colloids and Surfaces A: Physicochemical and Engineering Aspects, 324(1), 105–112. http://doi.org/10.1016/j.colsurfa.2008.04.003

Pramual, S., Assavanig, A., Bergkvist, M., Batt, C. A., Sunintaboon, P., Lirdprapamongkol, K., … Niamsiri, N. (2016). Development and characterization of bio-derived polyhydroxyalkanoate nanoparticles as a delivery system for hydrophobic photodynamic therapy agents. Journal of Materials Science: Materials in Medicine, 27(2), 1–11. http://doi.org/10.1007/s10856-015-5655-4

Rao, J. P., & Geckeler, K. E. (2011). Polymer nanoparticles: Preparation techniques and size-control parameters. Progress in Polymer Science, 36(7), 887–913. http://doi.org/10.1016/j.progpolymsci.2011.01.001

Retama, J. R., Mecerreyes, D., Lopez-Ruiz, B., & Lopez-Cabarcos, E. (2005). Synthesis and characterization of semiconducting polypyrrole/polyacrylamide microparticles with GOx for biosensor applications. Colloids and Surfaces A: Physicochemical and Engineering Aspects, 270–271(270–271), 239–244. http://doi.org/10.1016/j.colsurfa.2005.06.007

Rico, M., Rodríguez-Llamazares, S., Barral, L., Bouza, R., & Montero, B. (2016). Processing and characterization of polyols plasticized-starch reinforced with microcrystalline cellulose. Carbohydrate Polymers, 149, 83–93. http://doi.org/10.1016/j.carbpol.2016.04.087

Rodríguez-Contreras, A., Canal, C., Calafell-Monfort, M., Ginebra, M. P., Julio-Moran, G., & Marqués-Calvo, M. S. (2013). Methods for the preparation of doxycycline-loaded phb micro- and nano-spheres. European Polymer Journal, 49(11), 3501–3511. http://doi.org/10.1016/j.eurpolymj.2013.08.010

Schubert, S., Delaney, Jr, J. T., & Schubert, U. S. (2011). Nanoprecipitation and nanoformulation of polymers: from history to powerful possibilities beyond poly(lactic acid). Soft Matter, 7(5), 1581–1588. http://doi.org/10.1039/c0sm00862a

Shcherbakov, V. V., Artemkina, Y. M., & Korotkova, E. N. (2014). Dielectric properties and high-frequency conductivity of the sodium chloride-water system. Russian Journal of Inorganic Chemistry, 59(9), 922–926. http://doi.org/10.1134/S0036023614090186

Shishatskaya, E. I., Volova, T. G., Puzyr, A. P., Mogilnaya, O. A., & Efremov, S. N. (2004). Tissue response to the implantation of biodegradable polyhydroxyalkanoate sutures. Journal of Materials Science: Materials in Medicine, 15(6), 719–728. http://doi.org/10.1023/B:JMSM.0000030215.49991.0d

Vauthier, C., & Bouchemal, K. (2009). Methods for the preparation and manufacture of polymeric nanoparticles. Pharmaceutical Research, 26(5), 1025–1058. http://doi.org/10.1007/s11095-008-9800-3

Vilos, C., Morales, F. A., Solar, P. A., Herrera, N. S., Gonzalez-Nilo, F. D., Aguayo, D. A., … Velasquez, L. A. (2013). Paclitaxel-PHBV nanoparticles and their toxicity to endometrial and primary ovarian cancer cells. Biomaterials, 34(16), 4098–4108. http://doi.org/10.1016/j.biomaterials.2013.02.034

Wang, B., Zhang, Y., Zhang, J., Gou, Q., Wang, Z., Chen, P., & Gu, Q. (2013). Crystallization behavior, thermal and mechanical properties of PHBV/graphene nanosheet composites. Chinese Journal of Polymer Science, 31(4), 670–678. http://doi.org/10.1007/s10118-013-1248-1

Williams, S. F., Martin, D. P., Horowitz, D. M., & Peoples, O. P. (1999). PHA applications: addressing the price performance issue: I. Tissue engineering. International Journal of Biological Macromolecules, 25(1), 111–121. http://doi.org/10.1016/S0141-8130(99)00022-7

Wyman, J. (1931). The dielectric constant of mixtures of ethyl alcohol and water from -5 To 40°. Journal of the American Chemical Society, 53(9), 3292–3301. http://doi.org/10.1021/ja01360a012

Yang, Y.-Y., Chung, T.-S., & Ping Ng, N. (2001). Morphology, drug distribution, and in vitro release profiles of biodegradable polymeric microspheres containing protein fabricated by double-emulsion solvent extraction/evaporation method. Biomaterials, 22(3), 231–241. http://doi.org/10.1016/S0142-9612(00)00178-2

## 3. Preparation of starch nanoparticles loaded with quercetin using nanoprecipitation technique.

## 1. Introduction

The field of nanotechnology and especially that of polymer nanoparticles is one of the most popular topics for current research and development playing a pivotal role in a wide spectrum of areas such as medicine, biotechnology, electronics and so on (Paul & Robeson, 2008; Rao & Geckeler, 2011). The growing availability of nanoparticles of precise and small size, customized surface, improved solubility, multiple functionality and shape, as well as their subsequent developments have contributed to the increasing interest in polymer nanoparticles (Balazs, Emrick, & Russell, 2006).

Many polymers such as polylactic acid (PLA), polyhydroxybutyrate-co-hydroxyvalerate (PHBV), polyethylene glycol (PEG) or polylactic-glycolic acid (PLGA) among others have been investigated for the preparation of nanoparticles with different characteristics (Bouza et al., 2016; Kumari, Yadav, & Yadav, 2010; Soppimath, Aminabhavi, Kulkarni, & Rudzinski, 2001). Likewise, nanoparticles obtained from biodegradable polymers have also aroused much attention in recent years. Natural polysaccharide polymers such as cellulose, chitosan, dextran, gelatin, alginate,

albumin and starch offer a possible alternative to the traditional non-biodegradable polymers (Bel Haaj, Magnin, Pétrier, & Boufi, 2013; Jones & McClements, 2010; Kim et al., 2015; Liu, Jiao, Wang, Zhou, & Zhang, 2008; Schlemmer & Sales, 2010).

Among them, starch is one of the natural occurring polymers which is biocompatible, biodegradable and shows bio-adhesion properties. Moreover, its abundance, low cost and wide availability make it one of the most promising natural polymers (Schlemmer & Sales, 2010; Singh, Singh, Kaur, Sodhi, & Gill, 2003; Y. Tan et al., 2009; Xie, Pollet, Halley, & Avérous, 2013). At a molecular level, starch is a heterogeneous polysaccharide that contains two glucosidic macromolecules amylose and amylopectin (Chin, Pang, & Tay, 2011; Lamanna, Morales, Garcia, & Goyanes, 2013). Being the second most abundant biomass material in nature, it is found in plant roots, stalks, crop seeds and staple crops such as rice, corn, wheat, tapioca and potato (Le Corre, Bras, & Dufresne, 2010). However, starch shows some limitations due to its poor solubility in cold water, its sensitivity to moisture and heat and its tendency to retrograde and reaching a high viscosity once it is gelatinized (J.

Castaño et al., 2014, 2012; A. M. Shi, Wang, Li, & Adhikari, 2013b). Therefore, some degree of modification is necessary, being starch nanoparticles one of the products of such modification (Marto et al., 2016). These nanoparticles were used to reinforce different kinds of matrices, such as starch, polyvinyl alcohol (PVA) and synthetic latex producing significant improvements in their mechanical and permeation properties as a consequence of the nanometric particle size (Lamanna et al., 2013; Nasseri & Mohammadi, 2014).

In order to achieve the properties of interest, the mode of preparation plays a vital role. Nanoparticles can be conveniently prepared either by emulsion polymerization, nanoencapsulation or nanoprecipitation among others (Le Corre et al., 2010; Rao & Geckeler, 2011; A. M. Shi, Li, Wang, Li, & Adhikari, 2011; A. M. Shi et al., 2013b). Nanoprecipitation involves the addition of a dilute solution of polymer to a non-solvent or vice versa, which leads to polymer precipitation on the nanoscale. The method is essentially based on the interfacial deposition of a polymer after displacement of a semi-polar solvent, miscible with water from a lipophilic solution. Rapid diffusion of the solvent into non-solvent phase

results in the decrease of interfacial tension between the two phases, which increases the surface area and leads to the formation of small droplets (Rao & Geckeler, 2011; Y. Tan et al., 2009).

Due to its simplicity and reproducibility, the nanoprecipitation technique has been used in the present work for the preparation of the starch nanoparticles. The starch nanoparticles were loaded with quercetin which is well-known for its high antioxidant activity. Quercetin (3,3',4',5,7-pentahydroxyflavone) is a naturally occurring flavonoid which is the major representative of flavonol subclass (H. Li et al., 2009). It is found in many leaves, fruits and vegetables such as onions, apples and tea among other plants (Bose et al., 2013; Jeszka-Skowron et al., 2015). Quercetin, among other flavonoids, has been extensively studied during the last years for its antioxidant, anti-inflammatory and anti-cancer activities (Guazelli et al., 2013; H. Li et al., 2009; Lightfoot Vidal et al., 2016; Mohan et al., 2016; G. Wang et al., 2016).

The aim of this work is to prepare nanoparticles from different botanical origin by nanoprecipitation. The effect of the origin on the morphology and the size of the produced nanoparticles

is studied. Quercetin is incorporated into the starch nanoparticles to provide biodegradable antioxidant starch-quercetin nanoparticles. The effect of the origin of the starch on the quercetin loading percentage, the antioxidant activity and the release kinetics are evaluated.

The incorporation of quercetin within the biopolymeric matrices is an interesting strategy to provide a protection for the packaged food as well as the biopolymeric packaging films from the oxidation problems (Benbettaïeb, Chambin, Karbowiak, & Debeaufort, 2016).

## 2. Materials and methods

### *2.1. Materials and reagents*

Pea, corn and potato starches were provided by Roquette Freres S. A. (France). The amylose content of the starches reported by the company was 35%, 25% and 20% respectively. Sodium hydroxide (NaOH) was provided by Probus, S.A (Spain). Urea (purity, ≥99.5%), methanol and hydrochloric acid (HCl) were purchased from Scharlau (Spain). Quercetin (purity ≥95%) and 1,1-

diphenyl-2-picrylhydrazyl radical (DPPH $^{*}$) were purchased from Sigma Aldrich (Germany). Water was purified using a Milli-Q Ultrapure water-purification system (Millipore, France).

*2.2. Preparation of starch nanoparticles*

Starch nanoparticles were prepared by nanoprecipitation under the following procedure. An aqueous solution of NaOH/urea/$H_2O$ at the ratio of 0.8:1:98.2 by weight was used as solvent system for the dissolution of starch. Starches from different origin were used for the preparation of the nanoparticles: pea, corn and potato. Concentrations of 5, 10, 20, and 30 mg/mL of each starch solution were prepared at ambient conditions. The starch powder was dissolved in the aqueous solution using a high-speed homogenizer (T 25 digital ULTRA-TURRAX, IKA, Germany) operating at a relatively low speed (4000 to 5000 rpm) to avoid the generation of excessive heat. The dissolution process continued for 30 min, then the solution was left for equilibration during the night at room temperature. Nanoprecipitation was performed as following: 55 mL 0.1 M HCl were added drop-wise through a needle connected

to a plastic reservoir into a 25 mL of starch solution placed into a 250 mL long glass beaker. Continuous stirring at 1000 rpm under ambient temperature was maintained during the addition process. The produced particles were washed several times with deionized water, freezed and lyophilised using a Lyoquest-85 (Azbil Telstar Technologies, S. L. U., Spain) at 0.2 mbar for 4 days.

*2.3. Morphology and size characterization*

The morphology of the starch nanoparticles was characterized using a Carl Zeiss ultra plus field emission scanning electron microscope (FESEM) operated at 3 kV (Carl Zeiss, Germany). The particles were previously sputter-coated with iridium using QUORUM Q150T-S turbo-pumped sputter coater (Quorum Technologies Ltd, UK).

The size of the particles was analysed while dispersed in deionized water and was determined using dynamic light scattering (DLS) Zetasizer Nano ZS equipment (Malvern Instruments, UK).

*2.4. Preparation of starch-quercetin nanoparticles*

Starch-quercetin nanoparticles were prepared by nanoprecipitation following the same procedure used for the starch nanoparticles preparation with few modifications. As quercetin is soluble in basic solutions, quercetin was dissolved in the NaOH/urea/$H_2O$ solution containing the starch in a concentration of 2 mg/mL. Starch concentration was maintained at 20 mg/mL. The addition of the 0.1 M HCl solution was performed at constant rate during 30 min using a diaphragm Liquid Dosing Pump SIMDOS 02 (KNF Neuberger, Switzerland). The produced particles were washed with 5 mL of 35% ethanol and centrifuged at 7500 rpm for 5 min and then were washed several times with deionized water. The nanoparticles were lyophilised at 0.2 mbar for 4 days.

*2.5. Determination of quercetin loading percentage*

The dried starch-quercetin nanoparticles obtained from the previously described method were weighed. Known quantities of the nanoparticles were re-dissolved in the NaOH/urea/$H_2O$ solution. The absorbance of the quercetin in the solution was determined

immediately with an UV-vis spectrophotometer SPECORD 200 PLUS (Analytikjena, Germany) at a wavelength of 312 nm. A series of standard solutions of quercetin in NaOH/urea/$H_2O$ were prepared for obtaining the calibration curve. Quercetin concentrations of (0.5, 1, 2, 2.5, 4, 5, 8, 10 mg/L) were used for making the calibration curve. The absorbances of the re-dissolved quercetin were measured after further dilution and then compared to the corresponding standard curve. The mentioned procedure was performed for three batches of starch-quercetin nanoparticles for each type of starch.

The loading of quercetin was calculated according to Equation 3.1 (Papadimitriou & Bikiaris, 2009).

$$Drug\ loading\ (\%) = \frac{weight\ of\ drug\ in\ nanoparticles}{weight\ of\ nanoparticles} \times 100 \quad (3.1)$$

*2.6. Antioxidant activity*

The antioxidant activities of the starch-quercetin nanoparticles were determined by the DPPH method. This experiment is based on measuring the scavenging capacity of the antioxidant toward the stable DPPH radical. Briefly, 2 µg of the freeze-dried starch-quercetin nanoparticles were suspended in 2 ml

of methanol. The suspensions were incubated overnight to insure the complete release of the quercetin from the nanoparticles. The suspensions afterwards were centrifuged and aliquots of (10, 20, 50, 100 µL) of the supernatant of each suspension were added to 1.5 mL of 0.1 mM DPPH solution in methanol. The total volume of each solution was completed to 2 mL using methanol. The mixtures were shaken and then were allowed to stand for 30 min at room temperature. A quercetin solution in methanol (0.5 mg/mL) was used as positive control. The absorbance of the DPPH radical at 517 nm was measured. The radical scavenging activity (RSA) was calculated according Equation 3.2 (Medina-Meza & Barbosa-Cánovas, 2015).

$$\text{RSA}\ (\%) = \frac{A_0 - A_S}{A_o} \times 100 \qquad (3.2)$$

Where $A_0$ is the absorbance of the DPPH in the absence of the antioxidants, $A_s$ is the absorbance of the samples. All the steps of the experiment were done away from light and using amber glassware. The measurements were performed in triplicate.

*2.7. In-vitro release in water/ethanol medium*

Few milligrams (between 1.2 and 2.5 mg) of the starch-quercetin nanoparticles were weighed and dispersed in 5 mL of 35% ethanol with gentle shaking and sonication for few seconds (a maximum of 10 s). The suspension was centrifuged at 9000 rpm for 4 min. Samples from the supernatant were collected at 5, 10, 20, 30, 60, 90, 120, 180 and 240 min. An amount of 35% ethanol equals to the taken sample was returned maintaining the volume at 5 mL. The amount of the quercetin in the release medium was determined using UV-vis spectroscopy at a wavelength 372 nm. A series of standard solutions of quercetin in 35% ethanol (1, 2, 4, 5, 10 mg/L) were used for calibration. The absorbances of the supernatant samples were measured after further dilution and then compared to the standard curve. The cumulative quercetin release was calculated. The experiment was repeated 3 times for each sample of the starch nanoparticles.

*2.8. Statistical analysis*

Statistical analysis was performed basically by means of Igor Pro 6.37 software. The Add-in program DDSolver was used for making the fitting calculations and for the calculation of the coefficient of determination $R^2$ and the AIC (Akaike's information criterion) (Y. Zhang et al., 2010).

## 3. Results and discussion

*3.1. Preparation of starch nanoparticles*

Nanoprecipitation technique consists of three basic components: the polymer, the polymer solvent and the non-solvent polymer. Starch is reported to be soluble in dimethyl sulfoxide (DMSO) and in highly alkaline solutions (Han & Lim, 2004; Snyder, Sowokinos, & Desborough, 1977). The NaOH/urea/$H_2O$ solvent system was chosen as to be an effective solvent for starch since it has been shown as an effectively solvent for cellulose (Cai et al., 2004; Cai & Zhang, 2006; Chang, Jian, Zheng, Yu, & Ma, 2010; Jin, Zha, & Gu, 2007). The presence of NaOH has been reported as a breaker of the intermolecular and intramolecular hydrogen bonding

of starch molecules (Han & Lim, 2004), while urea plays an important role in preventing self-association of starch molecules (Chin et al., 2011).

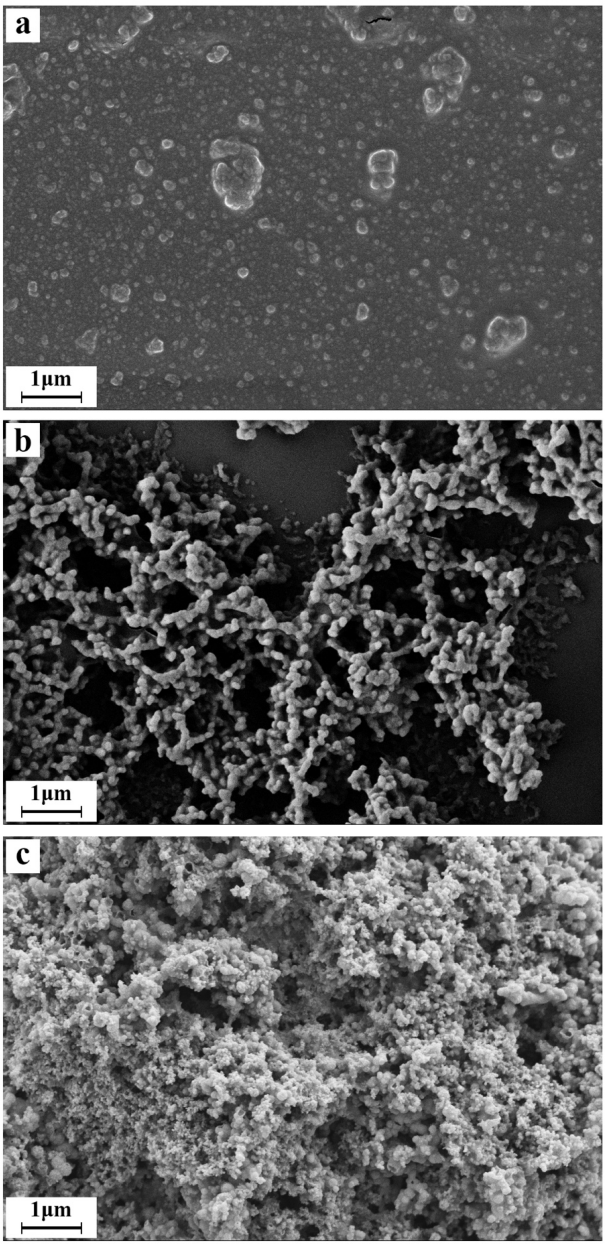


*Figure 3.27 Micrograph of pea (a), potato (b) and corn (c) starch nanoparticles prepared by nanoprecipitation of 20 mg/mL starch solution using 0.1M HCl as non-solvent.*

*Table 3.7 Dynamic light scattering data for different starch nanoparticles samples.*

| Sample | Starch concentration mg/mL | Z-Ave | PdI | Main peak intensity |
|---|---|---|---|---|
| Pea-1 | 5 | 92.4 | 0.268 | 119.3 |
| Pea-2 | 10 | 132.1 | 0.294 | 186.9 |
| Pea-3 | 20 | 165.3 | 0.467 | 285.2 |
| Pea-4 | 30 | 161.8 | 0.267 | 220.6 |
| Potato-1 | 5 | 91.2 | 0.276 | 136.7 |
| Potato-2 | 10 | 93.1 | 0.307 | 119.1 |
| Potato-3 | 20 | 137.8 | 0.358 | 215.2 |
| Potato-4 | 30 | 154.5 | 0.410 | 272.4 |
| Corn-1 | 5 | 174.7 | 0.354 | 271.6 |
| Corn-2 | 10 | 246.5 | 0.529 | 517.9 |
| Corn-3 | 20 | 214.3 | 0.531 | 389.4 |
| Corn-4 | 30 | 263.3 | 0.661 | 723.0 |

Previous papers have reported the use of absolute ethanol among other solvent/non-solvent systems for starch nanoprecipitation (Chin et al., 2011; El-Naggar, El-Rafie, El-sheikh, El-Feky, & Hebeish, 2015). Starch was reported to undergo partial precipitation at low pH (Byars, Fanta, & Kenar, 2013; Maslow & Davison, 1926), so starch nanoparticles could be obtained by gradually decreasing the pH under continuous stirring reaching pH 1. Dropping dilute HCl on the starch basic solutions with continuous

stirring produced spherical starch nanoparticles [Figure 3.27]. Table 3.7 provides the dynamic light scattering data of the produced nanoparticles. It can be seen that the size and the polydispersity of the nanoparticles increases by increasing the starch concentration.

*3.2. Preparation of starch-quercetin nanoparticles*

Quercetin is known to be soluble in organic solvents like ethanol, methanol, dimethyl formamide (DMF) or acetone and has a very low solubility in water (around 60 mg/L) (Chebil et al., 2007). However, quercetin is soluble in aqueous alkaline solutions and precipitates in aqueous acidic solutions. For the preparation of the starch-quercetin nanoparticles, the same nanoprecipitation procedure used for the preparation of the starch nanoparticles was followed taking advantage of the very limited solubility of quercetin in acidic aqueous medium. Quercetin was solubilized in the starch alkaline solution and precipitated with the starch by dropping 0.1M HCl on it.

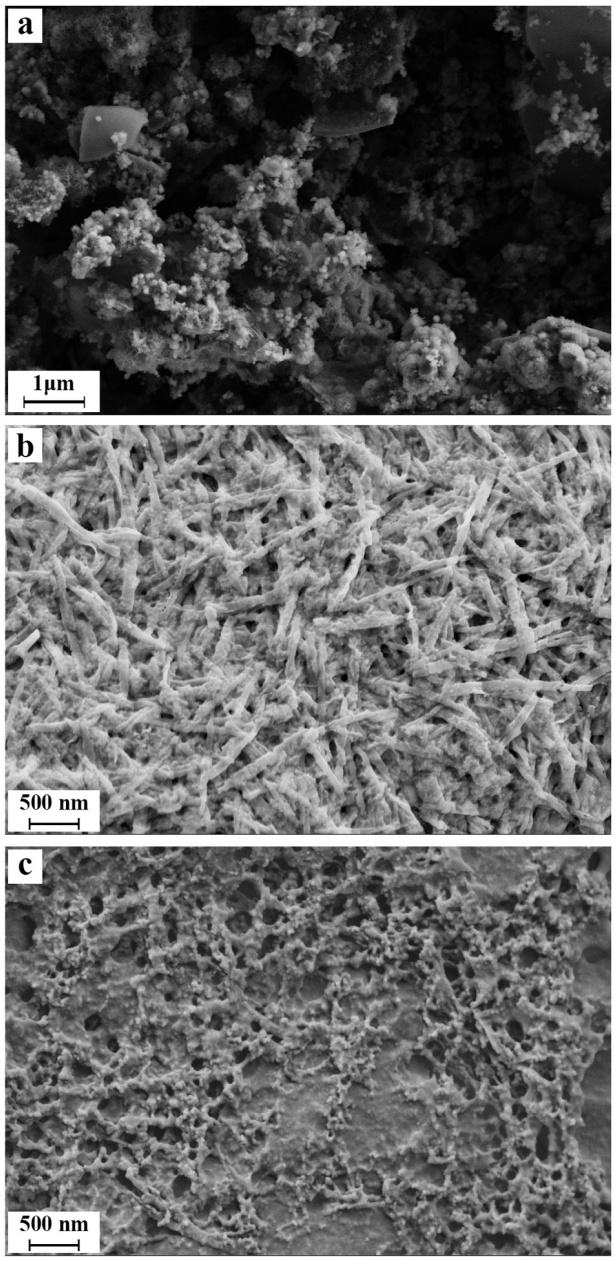


*Figure 3.28 Micrograph of pea (a), potato (b) and corn (c) starch-quercetin nanoparticles.*

The precipitated quercetin is thought to be entrapped within the precipitated starch molecules forming the starch-quercetin nanoparticles. The produced particles were washed with 5 mL of 35% ethanol to eliminate any quercetin that could be superficially adsorbed. The nanoprecipitation was performed just after the quercetin solubilisation to avoid the degradation of quercetin (Dechene, 1951; Jurasekova et al., 2014).

The morphologies of the produced nanoparticles have been affected by the introduction of the quercetin to the starch solution. Pea and corn starches have formed non-uniform shaped nanoparticles that tends to aggregate when lyophilised [Figure 3.28 a, c]. Nanofiber-like structures were obtained by using potato starch. The length of those fibers was around 500 nm [Figure 3.28 b].

*3.3. Quercetin loading and release profiles*

An experiment was performed to calculate the loading percentage of the starch-quercetin nanoparticles. The starch-quercetin nanoparticles were dissolved in NaOH/urea/$H_2O$ to insure the dissolution of all the amount of quercetin within the

nanoparticles. The absorbance was measured immediately after the dissolution of the particles to avoid the degradation of the quercetin in such a basic medium. Equation 3.1 was used to calculate the loading percentage. The loading percentage was found to be higher for the nanoparticles of potato and pea starch with a little difference (49 ± 3 and 44 ± 7, respectively). The corn starch has the minimum loading percentage of 20 ± 2. The different natures and amounts of amylopectins seem to be the cause of the differences in quercetin loading capacities. Amylopectin is the branched moiety of the starch molecules which thought to be more efficient in the immobilization of the quercetin molecules unlike the amylose which is a linear long and tough molecule (Jay lin Jane, 2009; Montero et al., 2016). Starches from different origins have different amylose/amylopectin ratios and different molecular weights of amylose and amylopectin. Young has reported the molecular weights of the amylopectins from pea, potato and corn starch of 5 x $10^8$ Da, 4.4 x $10^8$ Da and 4 x $10^8$ Da (Young, 1984). Although the pea starch contains an amylopectin of a molecular weight higher than that of the potato starch, the loading capacity of the potato starch was slightly higher, this might

be due to that the potato starch contains 80% amylopectin where the pea starch has a lower amount of amylopectin (65%). The low loading capacity of the corn starch seems to be a consequence of its low amylopectin molecular weight.

For understanding the release behaviour of the quercetin from the starch nanoparticles, the amount of the quercetin released was tracked using UV–vis spectroscopy. A solution of 35% ethanol in deionized water was used as a release medium. The solubility of the quercetin in such medium is 0.816 ± 0.110 mg/mL which insure the sink conditions (H. Li et al., 2009). The starch-quercetin nanoparticles were previously washed with 5 mL of the same solution to wash out the quercetin adsorbed on the surface of the nanoparticles.

Figure 3.29 shows the cumulative release profiles of quercetin from the starch-quercetin nanoparticles presented as the cumulative mMoles of quercetin released from each milligram of dried nanoparticles as a function of time in minutes. For all samples, the maximum amount of the released quercetin was reached after 3 h. This figure also shows that the cumulative amount of quercetin

released from corn starch nanoparticles is less than the other types of starch nanoparticles. Although the potato starch nanoparticles have a slightly higher loading capacity followed by the pea starch nanoparticles, their release profiles are almost the same. This difference in the release behaviour between the starch nanoparticles could be understood again according the difference in the botanical origin that influence the amylose/amylopectin nature and ratio.

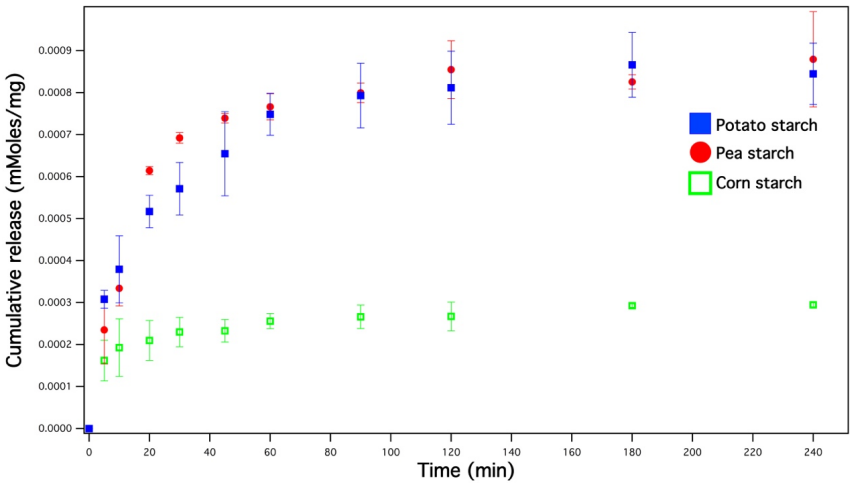


*Figure 3.29 Cumulative release profiles of quercetin from starch-quercetin nanoparticles from different origins.*

*3.4 Antioxidant activity*

DPPH radical solutions in organic solvents have a deep violet colour due to its odd electron and they show a strong absorption band at 517 nm. In the presence of antioxidants as quercetin, the DPPH radical is reduced, the odd electron is paired, the absorption is vanished and a progressive discoloration is observed (Jullian, Moyano, Yañez, & Olea-Azar, 2007; Kedare & Singh, 2011).

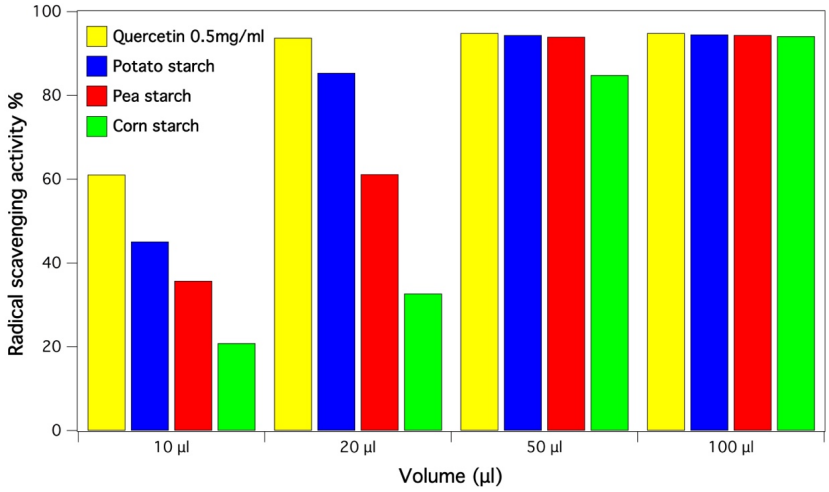


*Figure 3.30 Radical scavenging activity (%) for different volumes of the starch-quercetin nanoparticles suspensions and for the row quercetin solution as positive control.*

Figure 3.30 shows the radical scavenging activity (RSA) of the quercetin released from different starch-quercetin nanoparticles

compared to the RSA of a 0.5 mg/mL row quercetin solution in methanol. When 10 µL of the supernatant was diluted to 2 ml with DPPH methanolic solution (i.e. a final concentration of particles of 0.005 mg/mL), the potato starch-quercetin nanoparticles showed the highest RSA (45.1%) which is equivalent to 1.4 x $10^{-5}$ mMoles of quercetin, followed by the starch-quercetin nanoparticles from pea origin (35.7%) which is equivalent to 1.1 x $10^{-5}$ mMoles of quercetin. The corn starch-quercetin nanoparticles have showed 20.9% RSA at the same concentration (equivalent to 6.4 x $10^{-6}$ mMoles of quercetin). Increasing the concentration to 0.01 mg/mL (20 µL sample volume) lead to 85.4% and 61.2% RSA for potato starch-quercetin and pea starch-quercetin nanoparticles respectively, while the RSA of the corn starch-quercetin nanoparticles was 32.7%. At a concentration of 0.025 mg/mL (50 µL sample volume), the amount of quercetin released from both potato starch-quercetin and pea starch-quercetin nanoparticles was sufficient to reduce all the DPPH radical, while the RSA of the corn starch-quercetin nanoparticles was 85.0%. A 100 µL of the supernatant of the corn starch-quercetin nanoparticles suspension was required to reduce all

the DPPH radical. The antioxidant activities were clearly related to the quercetin loading percentages. The more loading percentage of quercetin, the more released quercetin in methanol which lead to higher radical scavenging activity.

*3.5. Mathematical models applied to the release profiles*

Various mathematical models have been developed to identify the drug release mechanism and to simulate the effect of different parameters on the release behaviour (Poletto, Jäger, Ré, Guterres, & Pohlmann, 2007). The release models of Peppas-Sahlin, Weibull, Korsmeyer-Peppas, Higuchi and Baker-Lonsdale are examples of the mathematical models used in the literature (Costa & Sousa Lobo, 2001; Shaikh, Kshirsagar, & Patil, 2015). The selection of the appropriate release model depends on the drug properties in addition to the matrix. Several mathematical models were applied to describe the release of the quercetin from the starch nanoparticles.

Table 3.8 shows the various parameters of the different release models in addition to the coefficient of determination $R^2$ and

the AIC. The experimental data showed the best fitting with Peppas-Sahlin followed by Weibull and then Korsmeyer-Peppas models. The applied models were presented graphically for the potato starch-quercetin release data as shown in Figure 3.31.

*Table 3.8 Parameters obtained by fitting the quercetin release profiles to different release models.*

| Model | Parameter | Pea starch | Potato starch | Corn starch |
|---|---|---|---|---|
| **Peppas-Sahlin** | $R^2$ | 0.994 | 0.997 | 0.997 |
| | AIC | 37.980 | 29.910 | 22.878 |
| | $k_1$ | 20.868 | 10.740 | 19.305 |
| | $k_2$ | -1.857 | -0.493 | -2.071 |
| | m | 0.325 | 0.457 | 0.226 |
| **Weibull** | $R^2$ | 0.994 | 0.984 | 0.997 |
| | AIC | 37.402 | 49.867 | 21.800 |
| | α | 2.845 | 5.033 | 4.379 |
| | β | 0.178 | 0.289 | 0.160 |
| | $T_i$ | 4.342 | 3.493 | 2.651 |
| **Korsmeyer-Peppas** | $R^2$ | 0.976 | 0.966 | 0.995 |
| | AIC | 51.299 | 56.493 | 25.911 |
| | k | 25.791 | 17.067 | 19.261 |
| | n | 0.161 | 0.240 | 0.146 |
| **Higuchi** | $R^2$ | 0.211 | 0.629 | 0.117 |
| | AIC | 87.719 | 80.627 | 80.265 |
| | k | 5.258 | 4.993 | 3.660 |

| | | | | |
|---|---|---|---|---|
| **Baker-Lonsdale** | $R^2$ | 0.480 | 0.783 | 0.289 |
| | AIC | 83.135 | 74.736 | 77.889 |

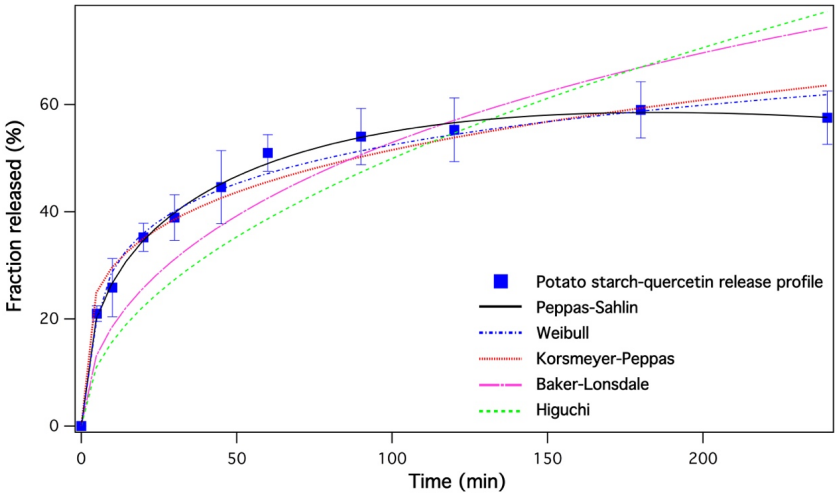


*Figure 3.31 Fit of various mathematical models to the experimental release data of the quercetin from the potato starch nanoparticles.*

The values of the coefficient of determination $R^2$ for Peppas-Sahlin model were between 0.994 and 0.997 for all the starch nanoparticles while the AIC values were lower in comparison with the values for the other models. This model describes the drug release from hydrophilic polymers with different geometric shapes. The model considers the release kinetics to be affected by two additive transport mechanisms: Fickian diffusional release and case-II relaxational contribution (Equation 3.3) (Peppas & Sahlin, 1989; Siepmann & Peppas, 2001).

$$\frac{M_t}{M_\infty} = k_1 t^m + k_2 t^{2m} \qquad (3.3)$$

Where $M_t$ is the amount of drug released at time t, $M_\infty$ is the amount of drug released at an infinite time, $k_1$ and $k_2$ are the release constants and m is the release exponent. According to Peppas and Sahlin, this equation is applicable for $M_t/M_\infty < 0.6$. The first term of the right-hand side of the Equation 3.3 represents the fickian diffusion contribution which occurs by the usual molecular diffusion of the drug due to a chemical potential gradient. The second term represents the case-II relaxational contribution associated with relaxation in hydrophilic polymers which swell in water or biological fluids (Peppas & Sahlin, 1989).

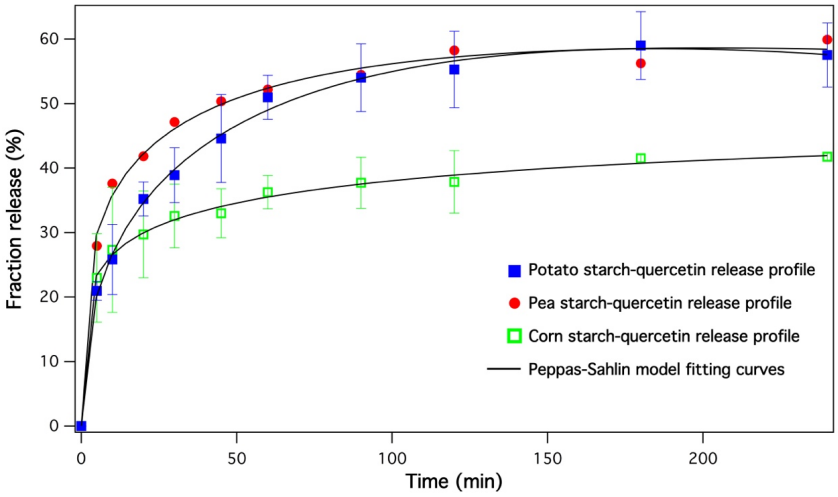


*Figure 3.32 Fit of the Peppas-Sahlin model to the experimental release data of quercetin from nanoparticles of starches from different botanical origin.*

Figure 3.32 shows the fitting curves of the quercetin release from the starch nanoparticles from different origin to the Peppas-Sahlin model. After 4 h, corn starch-quercetin nanoparticles released 41.7 % of the total amount of the loaded quercetin, where the fraction of quercetin released from the pea and the potato starch nanoparticles was 59.9% and 57.5% respectively. As shown in

Table 3.8, the values of $k_1$ (the fickian diffusion contribution constant) are of one order of magnitude more than $k_2$ (the case II relaxational contribution constant) for all the starch-quercetin

nanoparticles. This indicates that the release process is predominated mainly by fickian diffusion. The $k_2$ values were lower and have negative signs which makes the value of second part of the Equation 3.3 always negative. The same findings were reported before for the release profiles through some hydrophilic matrices. (Aguirre et al., 2016; Altimari et al., 2012; Maghsoodi & Barghi, 2011). These findings suggest that the case II relaxation interferes with the diffusion of the quercetin and slows it down (Ford et al., 1991). It has been suggested also that the negative $k_1$ or $k_2$ values should be interpreted as that their corresponding release component has no significant contribution in the release process compared to the other release component (Ferrero, Muñoz-Ruiz, & Jiménez-Castellanos, 2000; Ghosal & Ray, 2011; Maghsoodi & Barghi, 2011; Miranda, Millán, & Caraballo, 2006).

## 4. Conclusions

Starches from different botanical origin have been used for preparing starch nanoparticles using the nanoprecipitation technique. The starch nanoparticles were spherical and their sizes

depend on the starch concentration in the solution as well as the origin of the starch. The starch origin has a significant effect on the behaviour of starch at nanometric level as starches from different origin have different amylose/amylopectin ratio. Nanoparticles from different starches loaded with quercetin have been produced. The loading capacity, the release profile of the quercetin from the nanoparticles and therefore the antioxidant activity changed by changing the starch origin. The corn starch-quercetin nanoparticles were found to have the lowest loading percentage of quercetin, the lowest antioxidant activity and the lowest quercetin release kinetics. The nanoparticles of potato starch showed a slightly higher loading capacity than that of the pea starch nanoparticles. This might be due to the higher amylopectin content of the potato starch which thought to be more efficient in the immobilization of the quercetin molecules unlike the amylose which is a linear long and tough molecule. The nanoparticles of potato and pea starch showed similar fractions of quercetin released which is higher than that of corn starch. The release kinetics of the quercetin from the starch-quercetin

nanoparticles seem to be controlled mainly by Fickian diffusion which have been revealed applying the Peppas-Sahlin model.

## References

Aguirre, G., Villar-Alvarez, E., González, A., Ramos, J., Taboada, P., & Forcada, J. (2016). Biocompatible stimuli-responsive nanogels for controlled antitumor drug delivery. Journal of Polymer Science, Part A: Polymer Chemistry, 54(12), 1694–1705. http://doi.org/10.1002/pola.28025

Altimari, I., Spizzirri, U. G., Iemma, F., Curcio, M., Puoci, F., & Picci, N. (2012). pH-sensitive drug delivery systems by radical polymerization of gelatin derivatives. Journal of Applied Polymer Science, 125(4), 3006–3013. http://doi.org/10.1002/app.36234

Balazs, A. C., Emrick, T., & Russell, T. P. (2006). Nanoparticle polymer composites: where two small worlds meet. Science, 314(5802), 1107–1110. http://doi.org/10.1126/science.1130557

Bel Haaj, S., Magnin, A., Pétrier, C., & Boufi, S. (2013). Starch nanoparticles formation via high power ultrasonication. Carbohydrate Polymers, 92(2), 1625–1632. http://doi.org/10.1016/j.carbpol.2012.11.022

Benbettaïeb, N., Chambin, O., Karbowiak, T., & Debeaufort, F. (2016). Release behavior of quercetin from chitosan-fish gelatin edible films influenced by electron beam irradiation. Food Control, 66, 315–319. http://doi.org/10.1016/j.foodcont.2016.02.027

Bose, S., Du, Y., Takhistov, P., & Michniak-Kohn, B. (2013). Formulation optimization and topical delivery of quercetin from solid lipid based nanosystems. International Journal of Pharmaceutics, 441(1–2), 56–66. http://doi.org/10.1016/j.ijpharm.2012.12.013

Bouza, R., del Mar Castro, M., Dopico-García, S., Victoria González-Rodríguez, M., Barral, L. F., & Bittmann, B. (2016). Polylactic acid and poly(3-hydroxybutyrate-co-3-hydroxyvalerate) nano and microparticles for packaging bioplastic composites. Polymer Bulletin, 73(12), 1–18. http://doi.org/10.1007/s00289-016-1687-2

Byars, J. A., Fanta, G. F., & Kenar, J. A. (2013). Effect of

amylopectin on the rheological properties of aqueous dispersions of starch-sodium palmitate complexes. Carbohydrate Polymers, 95(1), 171–176. http://doi.org/10.1016/j.carbpol.2013.02.050

Cai, J., & Zhang, L. (2006). Unique gelation behavior of cellulose in NaOH/urea aqueous solution. Biomacromolecules, 7(1), 183–189. http://doi.org/10.1021/bm0505585

Cai, J., Zhang, L., Zhou, J., Li, H., Chen, H., & Jin, H. (2004). Novel fibers prepared from cellulose in NaOH/urea aqueous solution. Macromolecular Rapid Communications, 25(17), 1558–1562. http://doi.org/10.1002/marc.200400172

Castaño, J., Bouza, R., Rodríguez-Llamazares, S., Carrasco, C., & Vinicius, R. V. B. (2012). Processing and characterization of starch-based materials from pehuen seeds (Araucaria araucana (Mol) K. Koch). Carbohydrate Polymers, 88(1), 299–307. http://doi.org/10.1016/j.carbpol.2011.12.008

Castaño, J., Rodríguez-Llamazares, S., Contreras, K., Carrasco, C., Pozo, C., Bouza, R., … Giraldo, D. (2014). Horse chestnut (Aesculus hippocastanum L.) starch: Basic physico-chemical characteristics and use as thermoplastic material. Carbohydrate Polymers, 112, 677–685. http://doi.org/10.1016/j.carbpol.2014.06.046

Chang, P. R., Jian, R., Zheng, P., Yu, J., & Ma, X. (2010). Preparation and properties of glycerol plasticized-starch (GPS)/cellulose nanoparticle (CN) composites. Carbohydrate Polymers, 79(2), 301–305. http://doi.org/10.1016/j.carbpol.2009.08.007

Chebil, L., Humeau, C., Anthoni, J., Dehez, F., Engasser, J.-M., & Ghoul, M. (2007). Solubility of flavonoids in organic solvents. Journal of Chemical & Engineering Data, 52(5), 1552–1556. http://doi.org/10.1021/je7001094

Chin, S. F., Pang, S. C., & Tay, S. H. (2011). Size controlled synthesis of starch nanoparticles by a simple nanoprecipitation method. Carbohydrate Polymers, 86(4), 1817–1819. http://doi.org/10.1016/j.carbpol.2011.07.012

Costa, P., & Sousa Lobo, J. M. (2001). Modeling and comparison of dissolution profiles. European Journal of Pharmaceutical Sciences, 13(2), 123–133. http://doi.org/10.1016/S0928-0987(01)00095-1

Dechene, E. B. (1951). The relative stability of rutin and quercetin in alkaline solution. Journal of the American Pharmaceutical Association., 40(10), 495–497. http://doi.org/10.1002/jps.3030401005

El-Naggar, M. E., El-Rafie, M. H., El-sheikh, M. A., El-Feky, G. S., & Hebeish, A. (2015). Synthesis, characterization, release kinetics and toxicity profile of drug-loaded starch nanoparticles. International Journal of Biological Macromolecules, 81, 718–729. http://doi.org/10.1016/j.ijbiomac.2015.09.005

Ferrero, C., Muñoz-Ruiz, A., & Jiménez-Castellanos, M. R. (2000). Fronts movement as a useful tool for hydrophilic matrix release mechanism elucidation. International Journal of Pharmaceutics, 202(1–2), 21–28. http://doi.org/10.1016/S0378-5173(00)00407-5

Ford, J. L., Mitchell, K., Rowe, P., Armstrong, D. J., Elliott, P. N. C., Rostron, C., & Hogan, J. E. (1991). Mathematical modelling of drug release from hydroxypropylmethylcellulose matrices: Effect of temperature. International Journal of Pharmaceutics, 71(1–2), 95–104. http://doi.org/10.1016/0378-5173(91)90071-U

Ghosal, K., & Ray, S. D. (2011). Alginate/hydrophobic HPMC (60M) particulate systems: New matrix for site-specific and controlled drug delivery. Brazilian Journal of Pharmaceutical Sciences, 47(4), 833–844. http://doi.org/10.1590/S1984-82502011000400021

Guazelli, C. F. S., Fattori, V., Colombo, B. B., Georgetti, S. R., Vicentini, F. T. M. C., Casagrande, R., … Verri, J. W. A. (2013). Quercetin-loaded microcapsules ameliorate experimental colitis in mice by anti-inflammatory and antioxidant mechanisms. Journal of Natural Products, 76(2), 200–208. http://doi.org/10.1021/np300670w

Han, J. A., & Lim, S. T. (2004). Structural changes in corn starches

during alkaline dissolution by vortexing. Carbohydrate Polymers, 55(2), 193–199. http://doi.org/10.1016/j.carbpol.2003.09.006

Jane, J. lin. (2009). Structural features of starch granules II. Starch: Chemistry and Technology (Third Edit). Elsevier Inc. http://doi.org/10.1016/B978-0-12-746275-2.00006-9

Jeszka-Skowron, M., Krawczyk, M., & Zgoła-Grześkowiak, A. (2015). Determination of antioxidant activity, rutin, quercetin, phenolic acids and trace elements in tea infusions: Influence of citric acid addition on extraction of metals. Journal of Food Composition and Analysis, 40, 70–77. http://doi.org/10.1016/j.jfca.2014.12.015

Jin, H., Zha, C., & Gu, L. (2007). Direct dissolution of cellulose in NaOH/thiourea/urea aqueous solution. Carbohydrate Research, 342(6), 851–858. http://doi.org/10.1016/j.carres.2006.12.023

Jones, O. G., & McClements, D. J. (2010). Functional biopolymer particles: Design, fabrication, and applications. Comprehensive Reviews in Food Science and Food Safety, 9(4), 374–397. http://doi.org/10.1111/j.1541-4337.2010.00118.x

Jullian, C., Moyano, L., Yañez, C., & Olea-Azar, C. (2007). Complexation of quercetin with three kinds of cyclodextrins: An antioxidant study. Spectrochimica Acta - Part A: Molecular and Biomolecular Spectroscopy, 67(1), 230–234. http://doi.org/10.1016/j.saa.2006.07.006

Jurasekova, Z., Domingo, C., Garcia-Ramos, J. V, & Sanchez-Cortes, S. (2014). Effect of pH on the chemical modification of quercetin and structurally related flavonoids characterized by optical (UV-visible and Raman) spectroscopy. Physical Chemistry Chemical Physics, 16(25), 12802–12811. http://doi.org/10.1039/c4cp00864b

Kedare, S. B., & Singh, R. P. (2011). Genesis and development of DPPH method of antioxidant assay. Journal of Food Science and Technology, 48(4), 412–422. http://doi.org/10.1007/s13197-011-0251-1

Kim, H. Y., Park, S. S., & Lim, S. T. (2015). Preparation,

characterization and utilization of starch nanoparticles. Colloids and Surfaces B: Biointerfaces, 126, 607–620. http://doi.org/10.1016/j.colsurfb.2014.11.011

Kumari, A., Yadav, S. K., & Yadav, S. C. (2010). Biodegradable polymeric nanoparticles based drug delivery systems. Colloids and Surfaces B: Biointerfaces, 75(1), 1–18. http://doi.org/10.1016/j.colsurfb.2009.09.001

Lamanna, M., Morales, N. J., Garcia, N. L., & Goyanes, S. (2013). Development and characterization of starch nanoparticles by gamma radiation: Potential application as starch matrix filler. Carbohydrate Polymers, 97(1), 90–97. http://doi.org/10.1016/j.carbpol.2013.04.081

Le Corre, D., Bras, J., & Dufresne, A. (2010). Starch nanoparticles : A review. Biomacromolecules, 11(5), 1139–1153. http://doi.org/10.1021/bm901428y

Li, H., Zhao, X., Ma, Y., Zhai, G., Li, L., & Lou, H. (2009). Enhancement of gastrointestinal absorption of quercetin by solid lipid nanoparticles. Journal of Controlled Release, 133(3), 238–244. http://doi.org/10.1016/j.jconrel.2008.10.002

Lightfoot Vidal, S., Rojas, C., Bouza Padin, R., Perez Rivera, M., Haensgen, A., Gonzalez, M., & Rodriguez-Llamazares, S. (2016). Synthesis and characterization of polyhydroxybutyrate-co-hydroxyvalerate nanoparticles for encapsulation of quercetin. Journal of Bioactive and Compatible Polymers, 31(5), 439–452. http://doi.org/10.1177/0883911516635839

Liu, Z., Jiao, Y., Wang, Y., Zhou, C., & Zhang, Z. (2008). Polysaccharides-based nanoparticles as drug delivery systems. Advanced Drug Delivery Reviews, 60(15), 1650–1662. http://doi.org/10.1016/j.addr.2008.09.001

Maghsoodi, M., & Barghi, L. (2011). Polymer percolation threshold in multi-component HPMC matrices tablets. Advanced Pharmaceutical Bulletin, 1(1), 27–33. http://doi.org/10.5681/apb.2011.004

Marto, J., Gouveia, L. F., Gonçalves, L. M., Gaspar, D. P., Pinto,

P., Carvalho, F. A., … Almeida, A. J. (2016). A Quality by design (QbD) approach on starch-based nanocapsules: A promising platform for topical drug delivery. Colloids and Surfaces B: Biointerfaces, 143, 177–185. http://doi.org/10.1016/j.colsurfb.2016.03.039

Maslow, H., & Davison, W. (1926). The effect of the hydrogen-ion concentration upon the starch-liquefying activity of the amylase of Aspergillus oryzae. Journal of Biological Chemistry, 68, 83–93. Retrieved from http://www.jbc.org/content/68/1/83.short

Medina-Meza, I. G., & Barbosa-Cánovas, G. V. (2015). Assisted extraction of bioactive compounds from plum and grape peels by ultrasonics and pulsed electric fields. Journal of Food Engineering, 166, 268–275. http://doi.org/10.1016/j.jfoodeng.2015.06.012

Miranda, A., Millán, M., & Caraballo, I. (2006). Study of the critical points in lobenzarit disodium hydrophilic matrices for controlled drug delivery. Chemical & Pharmaceutical Bulletin, 54(5), 598–602. http://doi.org/10.1248/cpb.54.598

Mohan, L., Anandan, C., & Rajendran, N. (2016). Drug release characteristics of quercetin-loaded TiO nanotubes coated with chitosan. International Journal of Biological Macromolecules, 4–9. http://doi.org/10.1016/j.ijbiomac.2016.04.034

Montero, B., Rico, M., Rodríguez-Llamazares, S., Barral, L., & Bouza, R. (2016). Effect of nanocellulose as a filler on biodegradable thermoplastic starch films from tuber, cereal and legume. Carbohydrate Polymers. http://doi.org/10.1016/j.carbpol.2016.10.073

Nasseri, R., & Mohammadi, N. (2014). Starch-based nanocomposites: A comparative performance study of cellulose whiskers and starch nanoparticles. Carbohydrate Polymers, 106(1), 432–439. http://doi.org/10.1016/j.carbpol.2014.01.029

Papadimitriou, S., & Bikiaris, D. (2009). Novel self-assembled core-shell nanoparticles based on crystalline amorphous moieties of aliphatic copolyesters for efficient controlled drug release. Journal of Controlled Release, 138(2), 177–184.

http://doi.org/10.1016/j.jconrel.2009.05.013

Paul, D. R., & Robeson, L. M. (2008). Polymer nanotechnology: Nanocomposites. Polymer, 49(15), 3187–3204. http://doi.org/10.1016/j.polymer.2008.04.017

Peppas, N. A., & Sahlin, J. J. (1989). A simple equation for the description of solute release. III. Coupling of diffusion and relaxation. International Journal of Pharmaceutics, 57(2), 169–172. http://doi.org/10.1016/0378-5173(89)90306-2

Poletto, F. S., Jäger, E., Ré, M. I., Guterres, S. S., & Pohlmann, A. R. (2007). Rate-modulating PHBHV/PCL microparticles containing weak acid model drugs. International Journal of Pharmaceutics, 345(1–2), 70–80. http://doi.org/10.1016/j.ijpharm.2007.05.040

Rao, J. P., & Geckeler, K. E. (2011). Polymer nanoparticles: Preparation techniques and size-control parameters. Progress in Polymer Science, 36(7), 887–913. http://doi.org/10.1016/j.progpolymsci.2011.01.001

Schlemmer, D., & Sales, M. J. A. (2010). Thermoplastic starch films with vegetable oils of Brazilian Cerrado: Thermal characterization. Journal of Thermal Analysis and Calorimetry, 99(2), 675–679. http://doi.org/10.1007/s10973-009-0352-5

Shaikh, H. K., Kshirsagar, R. V, & Patil, S. G. (2015). Mathematical models for drug release characterization : A review. World Journal of Pharmacy and Pharmaceutical Sciences, 4(4), 324–338.

Shi, A. M., Li, D., Wang, L. J., Li, B. Z., & Adhikari, B. (2011). Preparation of starch-based nanoparticles through high-pressure homogenization and miniemulsion cross-linking: Influence of various process parameters on particle size and stability. Carbohydrate Polymers, 83(4), 1604–1610. http://doi.org/10.1016/j.carbpol.2010.10.011

Shi, A. M., Wang, L. J., Li, D., & Adhikari, B. (2013). Characterization of starch films containing starch nanoparticles Part 1: Physical and mechanical properties. Carbohydrate

Polymers, 96(2), 593–601. http://doi.org/10.1016/j.carbpol.2012.12.042

Siepmann, J., & Peppas, N. A. (2001). Modeling of drug release from delivery systems based on hydroxypropyl methylcellulose (HPMC). Advanced Drug Delivery Reviews, 48(2–3), 139–157. http://doi.org/10.1016/j.addr.2012.09.028

Singh, N., Singh, J., Kaur, L., Sodhi, N. S., & Gill, B. S. (2003). Morphological, thermal and rheological properties of starches from different botanical sources. Food Chemistry, 81(2), 219–231. http://doi.org/10.1016/S0308-8146(02)00416-8

Snyder, J. C., Sowokinos, J. R., & Desborough, S. L. (1977). Rapid extraction and solubilization of potato starch with dimethylsulfoxide. American Potato Journal, 54(11), 513–517. http://doi.org/10.1007/BF02852218

Soppimath, K. S., Aminabhavi, T. M., Kulkarni, A. R., & Rudzinski, W. E. (2001). Biodegradable polymeric nanoparticles as drug delivery devices. Journal of Controlled Release, 70(1–2), 1–20. http://doi.org/10.1016/S0168-3659(00)00339-4

Tan, Y., Xu, K., Li, L., Liu, C., Song, C., & Wang, P. (2009). Fabrication of size-controlled starch-based nanospheres by nanoprecipitation. ACS Applied Materials and Interfaces, 1(4), 956–959. http://doi.org/10.1021/am900054f

Wang, G., Wang, J. J., Chen, X. L., Du, L., & Li, F. (2016). Quercetin-loaded freeze-dried nanomicelles: Improving absorption and anti-glioma efficiency in vitro and in vivo. Journal of Controlled Release, 235, 276–290. http://doi.org/10.1016/j.jconrel.2016.05.045

Xie, F., Pollet, E., Halley, P. J., & Avérous, L. (2013). Starch-based nano-biocomposites. Progress in Polymer Science, 38(10–11), 1590–1628. http://doi.org/10.1016/j.progpolymsci.2013.05.002

Young, A. H. (1984). Chapter VIII – Fractionation of starch. In Starch: Chemistry and Technology (Second edi, pp. 249–283). http://doi.org/10.1016/B978-0-12-746270-7.50014-8

Zhang, Y., Huo, M., Zhou, J., Zou, A., Li, W., Yao, C., & Xie, S. (2010). DDSolver: an add-in program for modeling and comparison of drug dissolution profiles. The AAPS Journal, 12(3), 263–271. http://doi.org/10.1208/s12248-010-9185-1

# 4. Preparation of donut-shaped starch microparticles by aqueous-alcoholic treatment

## 1. Introduction

Starch is a natural polymer of glucose that is widely available, biodegradable and biocompatible. Depending on the botanical source, the starch granules are typically of many micrometres in size and of different shapes. There are several strategies to increase the surface area of starch granules and thereby their processability and performance. For example, in the acid hydrolysis treatment the particle size of starch is reduced and its degree of crystallinity is increased, which leads to a decrease of the swelling power and pasting temperature and retards the development of viscosity (Gonçalves, Noreña, da Silveira, & Brandelli, 2014). Starch structures with a high area to volume ratio, i.e. micro/nanoparticles, have been used as a carrier to modulate the release of active compounds (El-Feky, El-Rafie, El-Sheikh, El-Naggar, & Hebeish, 2015). The size and the shape of the micro/nanoparticles as well as their properties and release characteristics depends on the preparation method (Xie et al., 2013).

A granular cold water soluble starch has been used as a solid biodegradable matrix to encapsulate substances, such as ethylene (Shi, Fu, Tan, Huang, & Zhang, 2017), atrazine (J. Chen & Jane, 1995), and fatty acids (Lay Ma, Floros, & Ziegler, 2011). These microparticles generally are obtained by an alcoholic-alkaline treatment, where the sodium hydroxide disrupts the intermolecular hydrogen bonds of starch macromolecules, while ethanol inhibits the swelling of the granules (J. Chen & Jane, 1994). Although the overall integrity of the granules is preserved, the starch granules are completely deformed and the size is increased after the treatment.

In this chapter, a simple and novel method for the preparation of donut-shaped microparticles is described, in which heated starch slurry is precipitated by addition of ethanol. The morphology, structure, thermal and swelling properties of the microparticles were studied. The produced microparticles are intended to be used mainly as a carrier of active compounds or filler for bioplastics; both uses could be combined for active food packaging applications.

## 2. Materials and methods

### *2.1. Materials and reagents*

Corn starch composed of 25% of amylose was supplied by Roquette Freres S. A. (France). Ethanol was purchased from Scharlau (Spain).

### *2.2. Preparation of starch microparticles*

The microparticles preparation from corn starch granules was performed according to the method proposed by Ma et al. with modifications (Ma, Jian, Chang, & Yu, 2008). In short, 8 g of starch were added to 150 mL of Milli-Q water. The mixture was heated at 66 ºC, below the gelatinization temperature, under constant stirring at 500 rpm for 1 h. Then, 150 mL of absolute ethanol were added to the starch slurry during 75 min (2 mL/min) using a diaphragm pump (SIMDOS 02, KNF Neuberger, Switzerland). The suspension of starch microparticles was cooled to room temperature, and other 150 mL of ethanol were added dropwise under constant stirring at a flow rate of 3 mL/min. Finally, the microparticles were washed with

ethanol to remove water and then dried in a forced air circulation oven at 50 °C.

*2.3. Scanning electron microscopy (SEM)*

The morphology of the starch microparticles was characterized using a Carl Zeiss ultra plus field emission scanning electron microscope (FESEM) operated at 3 kV (Carl Zeiss, Germany). The particles were previously sputter-coated with iridium using a QUORUM Q150T-S turbo-pumped sputter coater (Quorum Technologies Ltd, UK).

*2.4. X-ray diffraction (XRD)*

The XRD spectra were recorded using a Bruker Endeavour diffractometer (model D4/max-B, Germany) with Cu Kα radiation (40 kV and 20 mA). The measurements were taken over a 2Θ range of 5-35° at steps of 0.02° and 1s time step.

*2.5. Differential scanning calorimetry (DSC)*

The gelatinization properties of starch microparticles and the corn starch granules were determined in triplicate by a Pyris-1 DSC (Perkin Elmer, Norwalk, CT, USA). About 2.0 mg of the starch sample (dry basis) were weighed in an aluminium pan and 6.0 µL of deionized water were added. The DSC scans were performed from 40 ºC to 120°C under $N_2$ atmosphere (20 mL/min) at 5 °C/min. An empty pan was used as reference. Onset ($T_o$), gelatinization (Tg), and conclusion (Tc) temperatures, as well as the enthalpy of gelatinization (ΔHg) were determined.

*2.6. Solubility and swelling properties*

Solubility index (%) and swelling power (g/g) were measured in triplicate using the method reported by (J. Castaño et al., 2014). Briefly, suspensions of starch microparticles and granules were heated separately at 60°C for 30 min followed by centrifugation at 4400 rpm for 30 min. The supernatant was decanted and dried overnight at 70°C. The dried soluble solid was weighed to determine the solubility index (Equation 4.1).

$$\text{Solubility index (\%)} = \frac{\text{Weight of the dried soluble starch}}{\text{Total weight of the starch}} \times 100 \quad (4.1)$$

The solid residue of centrifugation was weighed for the determination of the swelling power (Equation 4.2).

$$\text{Swelling power} = \frac{\text{Weight of solid residue}}{\text{Total weight of the starch}} \quad (4.2)$$

## 3. Results and discussion

### *3.1. Scanning electron microscopy (SEM)*

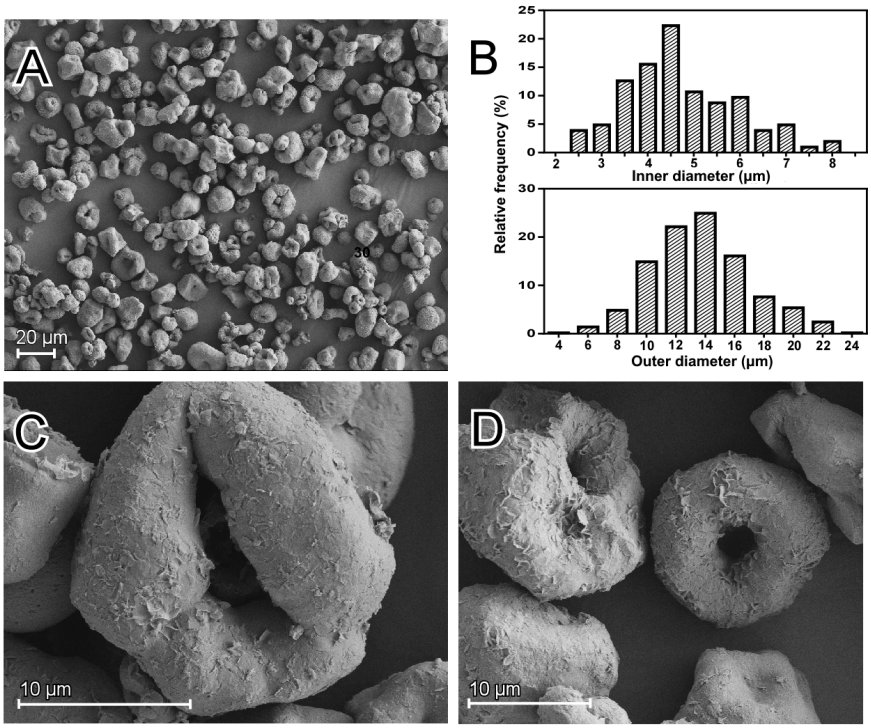


*Figure 4.33: Representative SEM images (A, C, D) and size distribution of outer and inner diameter (B) of donut-shaped microparticles.*

The thermal treatment of the starch slurry followed by the addition of ethanol as precipitant produced donut-shaped microparticles as can be observed in Figure 4.33A. The size of the particles, measured directly from the SEM micrographs using the ImageJ software, was in the same range of the corn starch granules

(5 - 25 μm). The size distribution of the microparticles in Figure 4.33B showed a defined peak centred at 14.1 μm and a range between 4.6 and 24.1 μm. The distribution of the size of the central hole of the donut-like structure showed a defined peak at 4.6 μm and ranged from 2.3 to 8.2 μm. The shape of the central hole depended on the microparticle size. The central hole of particles lower than 12 μm was round [Figure 4.33D], whereas for larger particles the hole appeared deformed and collapsed [Figure 4.33C]. Almost all the microparticles displayed a central hole, although in some cases the hole was not well formed and the particles only exhibited a deep-concave geometry [Figure 4.33D]. The donut-shaped microparticles presented a rough surface with a lamella structure similar to normal corn starch granules after chemical surface gelatinization with a degree of 84% (Pan & Jane, 2000). The morphology of the microparticles suggests that the supra-macromolecular packing of granules did not completely break down after the thermal treatment. An analogous morphology was described for granular cold water soluble starch prepared by an alcoholic-alkaline method at ambient pressure (Majzoobi, Kaveh, Blanchard, & Farahnaky, 2015).

However, the central cavity of these particles was not well defined and their surface was smooth. Another difference between donut microparticles and granular cold water soluble starch is their size. The last one is approximately 2 - 4 times larger than the size of the original starch (L. Shi, Fu, Tan, Huang, & Zhang, 2017).

It is also noteworthy that the obtained donut microparticles maintained their morphology after more than 18 month of storage and after re-dispersion in ethanol.

*3.2. X-ray diffraction (XRD)*

In order to investigate the structural changes of the donut-shaped microparticles with respect to corn starch granules their X-ray patterns were analysed. The starch granules had A-type crystallinity, showing well defined diffraction peaks at around 15°, 17°, 18° and 23° [Figure 4.34]. These peaks almost disappeared for the microparticles. However, two broad peaks at 13° and 20° were observed which are characteristics of a V-type single helix crystalline arrangement (L. Shi et al., 2017). During the swelling of the granules, the uncoiling or dissociation of the double helix

structure of amylopectin happened, and the order of the crystalline lamella was destroyed. Ethanol restricts the swelling of the granules and forms inclusion complexes with amylose and long branch chains of amylopectin, generating the V-type single helix structure. Jane et al. (J. Jane, Craig, Seib, & Hoseney, 1986) reported similar X-ray diffraction patterns for cold water soluble corn starch and proposed that during heating of the dispersion of corn starch in aqueous alcohol, the double helical structure of both amylose and amylopectin were converted into a single helix.

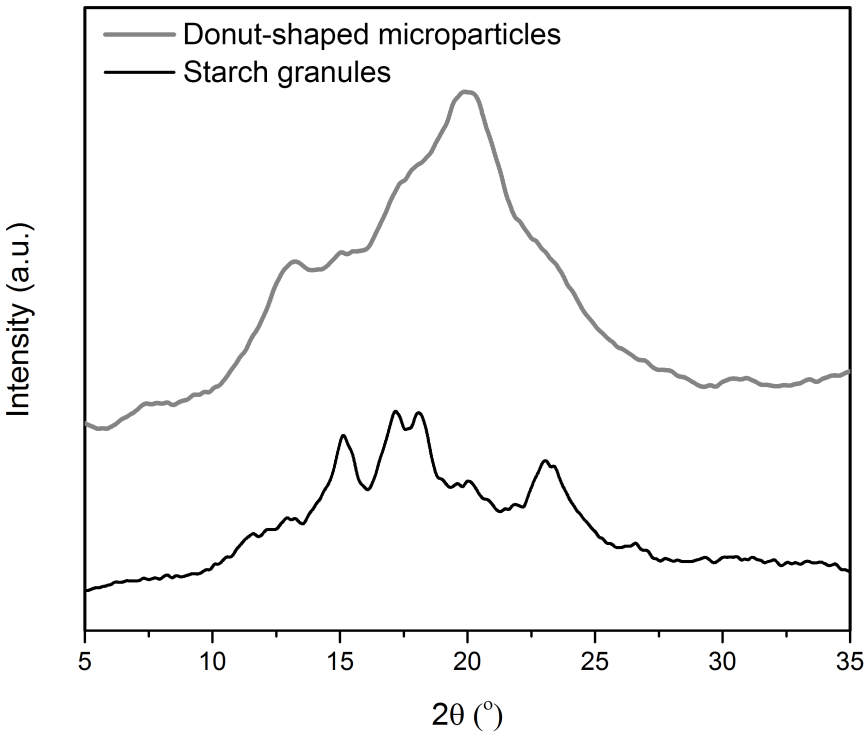


*Figure 4.34: XRD diffraction patterns of corn starch granules and donut-shaped microparticles.*

### *3.3. Differential scanning calorimetry (DSC)*

The DSC curves of the starch granules and the donut-shaped microparticles displayed typical endothermic peaks corresponding to the gelatinization of starch (Figure 4.35). The thermal parameters obtained for the starch granules [Table 4.9] were in the same range of other corn starch varieties (de La Rosa-Millán, Agama-Acevedo,

Jimenez-Aparicio, & Bello-Pérez, 2010). The donut microparticles exhibited a higher onset and gelatinization temperature, and a lower gelatinization enthalpy compared with the granules. The endothermic peak is attributed to the order-disorder phase transition during the gelatinization, where the double helices and crystalline lamellae are disrupted. In the gelatinization process the intra- and intermolecular bonds between starch macromolecules are broken. The energy required to gelatinize depends on the degree of hydrogen bonding (I. Tan, Wee, Sopade, & Halley, 2004). The lower energy required to disrupt the hydrogen bonding is an indicative of the lower proportion of this bonding within donut microparticles. The gelatinization temperatures are mainly due to the melting of crystalline lamella. The increase of gelatinization temperature suggests an increase in the ordered arrangement of the remaining helices within donut microparticles (Dries, Gomand, Goderis, & Delcour, 2014). Thus, the thermal treatment and subsequent ethanol precipitation distorted the supra-macromolecular packing of starch granules to form more perfect crystals compared to the native corn starch.

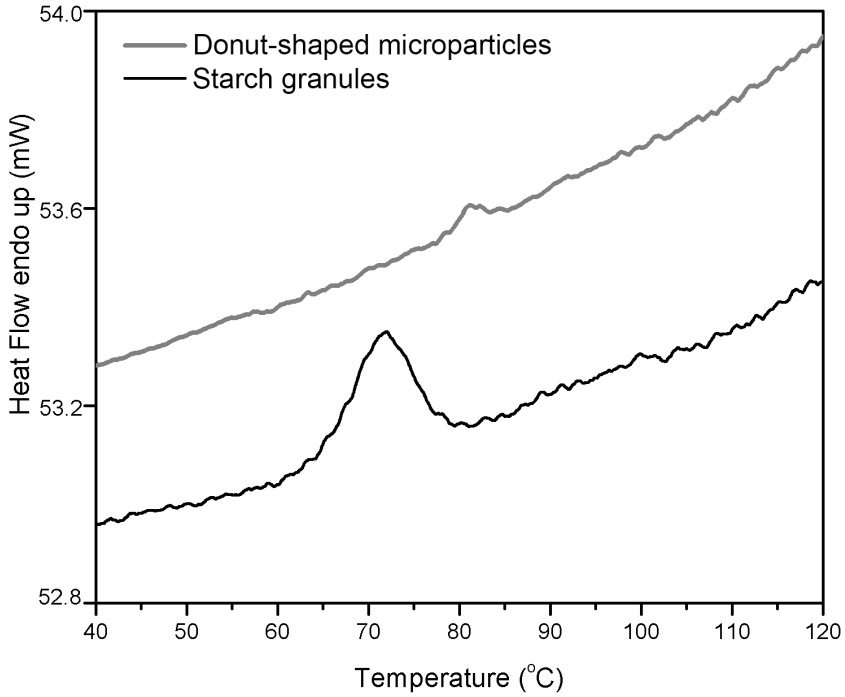


*Figure 4.35: DSC curves of corn starch granules and donut-shaped microparticles.*

*Table 4.9 Thermal properties, swelling power and solubility of corn starch and donut microparticles.*

| | **Donut microparticles** | **Starch granules** |
|---|---|---|
| **Thermal properties** | | |
| $T_o$ (ºC) | 78.0 | 60.6 |
| $T_g$ (ºC) | 81.2 | 71.8 |
| $T_c$ (ºC) | 85.8 | 81.5 |
| ΔHg (J/g) | 0.8 | 10.5 |
| **Hydration properties** | | |
| Swelling power (g/g of dry starch) | 6.0 | 2.3 |
| Solubility index (%) | 2.3 | 0.4 |

$T_o$, onset temperature; $T_g$, gelatinization temperature, $T_c$, conclusion temperature; $\Delta H_g$, enthalpy of gelatinization.

*3.4. Solubility and swelling properties*

The results summarized in Table 4.9 revealed an enhanced swelling capacity and solubility of the microparticles compared to the starch granules. The partial disruption of the supra-macromolecular structure, and consequently the distortion of the crystallinity within the granules and the conversion of the double helical order arrangement to a single helix, led to a more open structure where the water molecules could penetrate easier within the microparticles increasing substantially their solubility and swelling power.

Several steps are involved in the thermal treatment of starch in excess of water at a temperature between To and Tg: water uptake, granule swelling, leaching of amylose and finally partial destructuration of the granule. During the diffusion of water into the granules, the hydrogen bonds between starch macromolecules are broken and simultaneously starch macromolecules – water hydrogen bonds are formed. The granule swelling is accompanied by the leaching of amylose. (Ring, Lanson, Morris, L'Anson, & Morris, 1985) showed that the single helix chains of amylose of lower

molecular weight leached out just below of the gelatinization temperature. Although, the location of amylose is not complete elucidated, it is known that amylose concentrates rather at the periphery than at the inner part of the corn starch granule (Pan & Jane, 2000). It is proposed that the granule swelling and leaching out of amylose lead to a deformability of the granule and its surface. Upon addition of absolute ethanol to the starch slurry, an inclusion complex is formed in the swelling granule between starch macromolecules and ethanol (B. Zhang, Dhital, Haque, & Gidley, 2012). The ethanol replaces water and is enclosed in the internal cavity of the single helix of amylose and unwinds the large amylopectin. In the helices, the hydrophobic groups are directed outside and the hydrophilic to the inside, similar to the conformation of cyclodextrin (Rodríquez-Llamazares et al., 2007). The guest ethanol bonds via non-covalent interactions, mainly hydrophobic and van der Waals attraction, to the central cavity of the helix. At the same time, the addition of ethanol leads to the swelling of the granule which resembles a donut-shaped structure to reduce the contact between hydrophilic starch macromolecule conformation and free

ethanol molecules. The removal of ethanol on drying shrinks the granule and an anhydrous V-helices structure with an empty cavity is formed, resulting in a structure with more water affinity. The rough surface is due to shrinking by drying and leaching out of the peripheral amylose from the granule during heating. The association (entanglement) of amylose with amylopectin molecules preserves partially the integrity of the supra-macromolecular packing of the starch granule which is also stabilized by the inclusion complex between ethanol and the single helix of amylose and the large amylopectin.

## 4. Conclusions

Starch microparticles with donut-shaped morphology have been prepared via an aqueous–alcoholic treatment. The thermal treatment of the starch slurry and the addition of ethanol as precipitant led to the partial disruption of the supra-macromolecular structure and consequently distortion of the crystallinity within the starch granules. The double helical order arrangement of the granule is converted to a single helix, a more open structure where the water

molecules can penetrate easier. Thus, the donut microparticles showed higher solubility and swelling power and also higher gelatinization temperatures and a lower gelatinization enthalpy compared with the starch granules. The simplicity and the easiness of the preparation method and the remarkable stability of the donut-shaped microparticles of more than 18 month make it suitable for various applications such as a carrier for an active compound and fillers for food packaging applications.

## References

Castaño, J., Rodríguez-Llamazares, S., Contreras, K., Carrasco, C., Pozo, C., Bouza, R., … Giraldo, D. (2014). Horse chestnut (Aesculus hippocastanum L.) starch: Basic physico-chemical characteristics and use as thermoplastic material. Carbohydrate Polymers, 112, 677–685. http://doi.org/10.1016/j.carbpol.2014.06.046

Chen, J., & Jane, J. (1994). Preparation of granular cold-water-soluble starches by alcoholic-alkaline treatment. Cereal Chemistry, 71(6), 623–626.

Chen, J., & Jane, J. (1995). Effectiveness of granular cold-water-soluble starch as a controlled-release matrix. Cereal Chemistry, 72(3), 265–268.

de La Rosa-Millán, J., Agama-Acevedo, E., Jimenez-Aparicio, A. R., & Bello-Pérez, L. A. (2010). Starch characterization of different blue maize varieties. Starch - Stärke, 62(11), 549–557. http://doi.org/10.1002/star.201000023

Dries, D. M., Gomand, S. V., Goderis, B., & Delcour, J. A. (2014). Structural and thermal transitions during the conversion from native to granular cold-water swelling maize starch. Carbohydrate Polymers, 114, 196–205. http://doi.org/10.1016/j.carbpol.2014.07.066

El-Feky, G. S., El-Rafie, M., El-Sheikh, M., El-Naggar, M. E., & Hebeish, A. (2015). Utilization of Crosslinked Starch Nanoparticles as a Carrier for Indomethacin and Acyclovir Drugs. J Nanomed Nanotechnol, 6(1), 1–8. http://doi.org/10.4172/2157-7439.1000254

Gonçalves, P. M., Noreña, C. P. Z., da Silveira, N. P., & Brandelli, A. (2014). Characterization of starch nanoparticles obtained from Araucaria angustifolia seeds by acid hydrolysis and ultrasound. LWT - Food Science and Technology, 58(1), 21–27. http://doi.org/10.1016/j.lwt.2014.03.015

Jane, J., Craig, S. A. S., Seib, P. A., & Hoseney, R. C. (1986). Characterization of granular cold water-soluble starch. Starch - Stärke, 38(8), 258–263. http://doi.org/10.1002/star.19860380803

Lay Ma, U. V., Floros, J. D., & Ziegler, G. R. (2011). Formation of inclusion complexes of starch with fatty acid esters of bioactive compounds. Carbohydrate Polymers, 83(4), 1869–1878. http://doi.org/10.1016/j.carbpol.2010.10.055

Ma, X., Jian, R., Chang, P. R., & Yu, J. (2008). Fabrication and characterization of citric acid-modified starch nanoparticles/plasticized-starch composites. Biomacromolecules, 9(11), 3314–3320. http://doi.org/10.1021/bm800987c

Majzoobi, M., Kaveh, Z., Blanchard, C. L., & Farahnaky, A. (2015). Physical properties of pregelatinized and granular cold water swelling maize starches in presence of acetic acid. Food Hydrocolloids, 51, 375–382. http://doi.org/10.1016/j.foodhyd.2015.06.002

Pan, D. D., & Jane, J. (2000). Internal structure of normal maize starch granules revealed by chemical surface gelatinization. Biomacromolecules, 1(1), 126–132. http://doi.org/10.1021/bm990016l

Ring, S. G., Lanson, K. J., Morris, V. J., L'Anson, K., & Morris, V. J. (1985). Static and dynamic light-scattering studies of amylose solutions. Macromolecules, 18(2), 182–188. http://doi.org/10.1021/ma00144a013

Rodríquez-Llamazares, S., Yutronic, N., Jara, P., Englert, U., Noyong, M., & Simon, U. (2007). The structure of the first supramolecular α-cyclodextrin complex with an aliphatic monofunctional carboxylic acid. European Journal of Organic Chemistry, (26), 4298–4300. http://doi.org/10.1002/ejoc.200700454

Shi, L., Fu, X., Tan, C. P., Huang, Q., & Zhang, B. (2017). Encapsulation of ethylene gas into granular cold-water-soluble starch: structure and release kinetics. Journal of Agricultural and Food Chemistry, 65(10), 2189–2197.

http://doi.org/10.1021/acs.jafc.6b05749

Tan, I., Wee, C. C., Sopade, P. A., & Halley, P. J. (2004). Investigation of the starch gelatinisation phenomena in water-glycerol systems: Application of modulated temperature differential scanning calorimetry. Carbohydrate Polymers, 58(2), 191–204. http://doi.org/10.1016/j.carbpol.2004.06.038

Xie, F., Pollet, E., Halley, P. J., & Avérous, L. (2013). Starch-based nano-biocomposites. Progress in Polymer Science, 38(10–11), 1590–1628. http://doi.org/10.1016/j.progpolymsci.2013.05.002

Zhang, B., Dhital, S., Haque, E., & Gidley, M. J. (2012). Preparation and characterization of gelatinized granular starches from aqueous ethanol treatments. Carbohydrate Polymers, 90(4), 1587–1594. http://doi.org/10.1016/j.carbpol.2012.07.035

# 5. Starch edible films loaded with donut-shaped starch microparticles

## 1. Introduction

Biopolymers are being extensively studied by the scientific community with the aim of providing alternatives to the petroleum derived plastics which have many environmental and health hazard. Starch based materials provide good alternatives to the conventional polymers due to their intrinsic biodegradability and biocompatibility, they are even used as edible polymers in the food packaging industry (BeMiller & Whistler, 2009).

The use of biopolymers at industrial level is facing various challenges due to their poor thermal, barrier and mechanical properties. One of the common strategies to improve and tune the physical properties of the bioplastics is the addition of nano and microfillers to the polymer matrix (Fengge Gao, 2012). A wide variety of nano and microparticles were reported as fillers for starch matrices (Xie et al., 2013). For example, cellulose nanocrystals and microcrystals were reported to improve the mechanical properties of different starch thermoplastic films (Montero et al., 2016; Rico et al., 2016). Shi et. al. evaluated the effect of the incorporation of starch nanoparticles produced by spray drying within corn starch

films (A. M. Shi, Wang, Li, & Adhikari, 2013a; A. M. Shi et al., 2013b). However, to the best of our knowledge the effect of the incorporation of the unmodified chemically starch microparticles on properties of starch films was not reported.

In this work, starch microparticles with donut-shaped morphology from two different botanical sources, pea and corn, were prepared via a simple thermal aqueous–alcoholic treatment. The morphology, size, crystallinity, swelling and solubility properties of the microparticles were analysed. The produced microparticles were loaded to starch thermoplastic films from the same botanical origin. These films were prepared by solution casting method. The effect of the microparticles addition on the morphology, crystallinity, thermal stability, water vapour and oxygen permeability of the films were evaluated. The loaded films are of potential interest for food industry and food packaging applications.

## 2. Materials and methods

### *2.1. Materials and reagents*

Pea and corn starches were provided by Roquette Freres S. A. (France). The amylose content of the starches reported by the company was 35% and 25%, respectively. Absolute ethanol was purchased from Scharlau (Spain). Glycerol was purchased from Sigma Aldrich (Germany). Water was purified using a Milli-Q Ultrapure water-purification system (Millipore, France).

### *2.2. Preparation of starch microparticles.*

Donut-shaped starch microparticles were prepared by thermal aqueous-alcoholic treatment under the following procedure (Farrag et al., 2017). An amount of 8g of starch was added to 150 mL of Milli-Q water. The mixture was heated at 66 °C under constant stirring at 500 rpm during 1 h. Then 150 mL of absolute ethanol were added during 75 min (2 mL/min) using a diaphragm pump (SIMDOS 02, KNF Neuberger, Switzerland) to the starch slurry under the same stirring conditions without heating. When the

starch microparticles suspension was cooled to room temperature, another 150 mL of ethanol were added dropwise under constant stirring at a flow rate 3 mL/min. Finally, the suspension was centrifuged for 20 min at 4400 rpm, and washed several times with ethanol to remove water. After washing, the microparticles were dried in a forced air oven at 50 °C. The microparticles were prepared in triplicate.

### *2.3. Preparation of starch films loaded with donut-shaped starch microparticles*

The TPS films of corn and pea starches loaded with starch donut-shaped microparticles were prepared using the solution casting method (Montero et al., 2016). Native starches were suspended in 60 mL of glycerol and water solution. The suspensions were mixed and then heated in a microwave oven for 150 s. The suspensions were withdrawn each 30 s for mixing and then returned to the microwave oven. The gelatinized starch solutions were then stirred at 800 rpm using magnetic stirring till cooling down. The starch microparticles were added to the gelatinized starch solution

and homogenized using a T 25 digital ULTRA-TURRAX homogenizer at 5000 rpm for 10 min. The obtained suspensions were sonicated for degassing and then poured in a 20 cm diameter flat bottom petri dishes lined with teflon sheets. The petri dishes were dried in a forced air oven for 30 h at 30$^{o}$ C. The obtained films were reconditioned in a climate chamber at room temperature and at 40% relative humidity to insure the equilibration of the water in the films.

The total weight of dry starch (i.e. native starch weight + starch microparticles weight) was kept at 2.1 g. The starch microparticles were added in a percentage of 10 and 15% of the total dry starch content. The ratio between the native starch weight and the glycerol weight was 7:3.

*2.4. Scanning electron microscopy (SEM)*

The morphology of the donut-shaped starch microparticles was characterized using a Carl Zeiss ultra plus field emission scanning electron microscope (FESEM) operated at 3 kV (Carl Zeiss, Germany). The particles were previously sputter-coated with iridium using QUORUM Q150T-S turbo-pumped sputter coater

(Quorum Technologies Ltd, UK). The size of the microparticles was measured directly from the SEM micrographs using the ImageJ software (Schneider, Rasband, & Eliceiri, 2012).

*2.5. Solubility and swelling properties*

The solubility index and the swelling power of the starch microparticles were determined following the method reported by Castaño et al. (J. Castaño et al., 2014). Briefly, 1.25 g of the starch microparticles were suspended in 30 mL of deionized water. The suspensions were heated in a water bath for 30 min and then centrifuged at 4400 rpm for 30 min. The supernatant was separated and dried at 70 ºC overnight and the precipitated dried starch was weighed to determine the solubility index Equation 5.1.

$$Solubility\ index\ (\%) = \frac{Weight\ of\ the\ dried\ soluble\ starch}{Total\ weight\ of\ the\ starch} \times 100 \quad (5.1)$$

The solid residue of centrifugation was weighed to determine the swelling power using the following Equation 5.2.

$$Swelling\ power\ = \frac{The\ solid\ residue\ of\ centrifugation}{Total\ weight\ of\ the\ starch} \quad (5.2)$$

*2.6. X-ray diffraction (XRD)*

X-ray diffraction patterns were recorded in a diffractometer D5000 Siemens (Karlsruhe, Germany). The equipment operated at a voltage of 45 kV and a current of 30 mA and uses copper K-alpha (Cu Kα) radiation with an average wavelength of λ (Kα) = 0.15 nm (1.54 Å). The aperture used was 0.6 mm. Diffractograms were registered in the angular region of 2θ from 5° to 40°, at room temperature, with a step time of 4 s and an angular increment of 0.005°.

*2.7. Thermogravimetric analysis (TGA)*

Thermogravimetric analysis was performed using a PerkinElmer TGA-4000 microbalance with a ceramic sample pan (Massachusetts, USA). Approximately 10–15 mg of the TPS starch films were heated from 50 °C to 500 °C at 10 °C/min with a 20 mL/min oxygen flow.

*2.8. Water vapour transmission rate (WVTR)*

Water vapour transmission rate (WVTR) was measured with a Permatran-W, 1/50 G, Mocon equipment, (Mocon Inc., USA). Smooth and uniform parts of the starch film samples with thickness of 170 μm were selected. Masks with 5 $cm^2$ test area were used for putting samples in the cell of the equipment at 37.8 $^{\circ}C$. Relative humidity of 5% and 40% were applied in two sides of the films as driving force of the test. Water vapour transmission rate was calculated by counting passed molecules through the film every 30 min. Passed molecules were carried to counting part of the equipment by nitrogen carrying gas which was purged continuously during the test. Tests were done until obtain steady line for transmission rate under a continuous mode (WVTR, in g / ($m^2$.day)).

*2.9. Oxygen transmission rate (OTR)*

Oxygen transmission rate (OTR) was investigated with an OX-TRAN, 1/50 G, Mocon equipment (Mocon Inc., USA). Smooth and uniform parts of the starch film samples with thickness of 170 μm were selected. Masks with 5 $cm^2$ test area were used for putting

samples in the cell of equipment. Temperature of cell was 23 $^{\circ}$C. One side of the film was exposed to dry oxygen flow, relative humidity of 0.5%, with pressure of 27.7 psi. Then diffusion process of oxygen molecules to the film started. Oxygen transmission rate was calculated by counting passed molecules through the film every 30 min. Passed molecules were carried to counting part of the equipment by dry nitrogen carrying gas which was purged continuously with the pressure of 28.1 psi during the test. Tests were done until obtain steady line for transmission rate under continuous mode (OTR, in $cm^3/(m^2.day)$).

## 3. Results and discussion

### *3.1. Preparation and characterization of the donut-shaped starch microparticles*

#### *3.1.1. Morphology and size analysis*

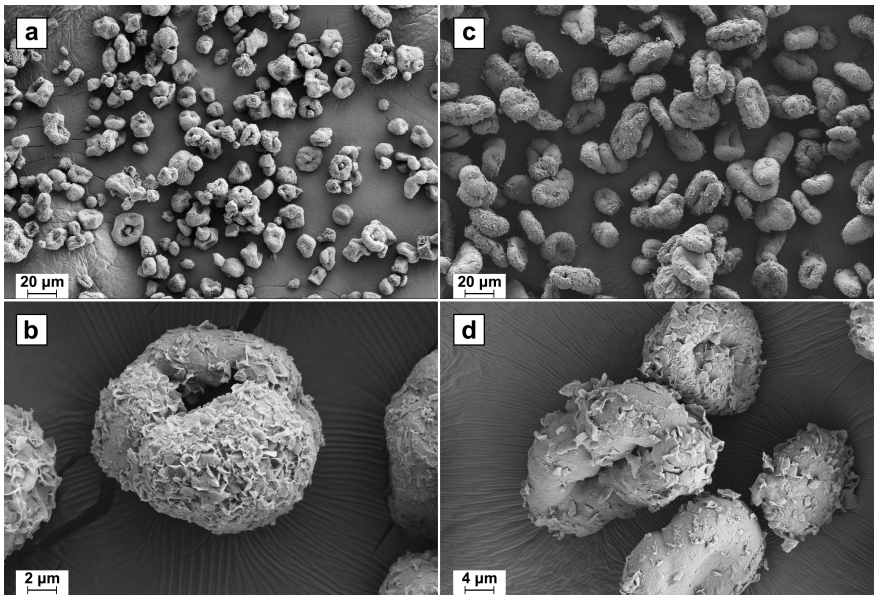


*Figure 5.36 SEM micrographs of donut-shaped microparticles of corn (a, b) and pea (c, d) starch.*

Figure 5.36 shows the morphology of the donut-shaped starch microparticles obtained from both corn and pea starches by thermal aqueous-alcoholic treatment. The surface of the donut-shaped microparticles appeared rough and irregular. The cavities in the middle were rounded for the small particles and elongated for the

big ones. These cavities disappeared for some of the big particles leaving a starch microparticles with a concave centre. The microparticles of pea starch showed bigger sizes than those of corn starch due to the bigger size of the pea starch granules as is shown in Table 5.10. The average size of the corn and pea starch microparticles was 14.01 ± 2.65 μm and 28.61 ± 6.84 μm, respectively. Analogous donut-shaped morphology was reported before for the hydroxypropylated potato starch (Kaur, Singh, & Singh, 2004) and for granular cold water soluble starch prepared by an alcoholic-alkaline method at ambient pressure (J. Jane et al., 1986; Majzoobi et al., 2015). The size of the obtained microparticles suggests that the supramolecular packing of the starch granules did not completely damaged.

*Table 5.10 Particle size analysis and solubility properties of the starch granules and their corresponding donut-shaped microparticles*

| | **Particle size analysis** | **Solubility properties** | |
|---|---|---|---|
| **Sample** | **Average diameter ± dev (µm)** | **Swelling power ± dev** | **Solubility index (%) ± dev** |
| Corn starch | 10.70 ± 3.20 | 2.32 ± 0.06 | 0.41 ± 0.05 |
| Corn microparticles | 14.01 ± 2.65 | 6.03 ± 0.05 | 2.27 ± 0.15 |
| Pea starch | 24.40 ± 5.50 | 3.76 ± 0.16 | 2.59 ± 0.21 |
| Pea microparticles | 28.61 ± 6.84 | 4.58 ± 0.01 | 2.43 ± 0.22 |

*3.1.2. X-ray diffraction analysis (XRD)*

The structural changes at supra-macromolecular level associated with the donut-shaped microparticles formation were analysed using XRD. As can be observed in Figure 5.37 a, the diffraction peaks at around 15°, 17°, 18° and 23° reveals the A-type crystallinity of the corn starch granules (J. Castaño et al., 2012). The formation of the corn donut-shaped microparticles led to disappearing of those diffraction peaks, and the formation of two broad peaks at 13° and 20° which are characteristics of a V-type crystalline structure (L. Shi et al., 2017). The diffraction pattern of the pea starch granules shows 2θ values at 15°, 17°, 20° and 23°

which indicate a mixture of A and B type polymorphism, i.e. a C-type crystal structure [Figure 5.37 b] (Qin, Liu, Jiang, Xiong, & Sun, 2016).

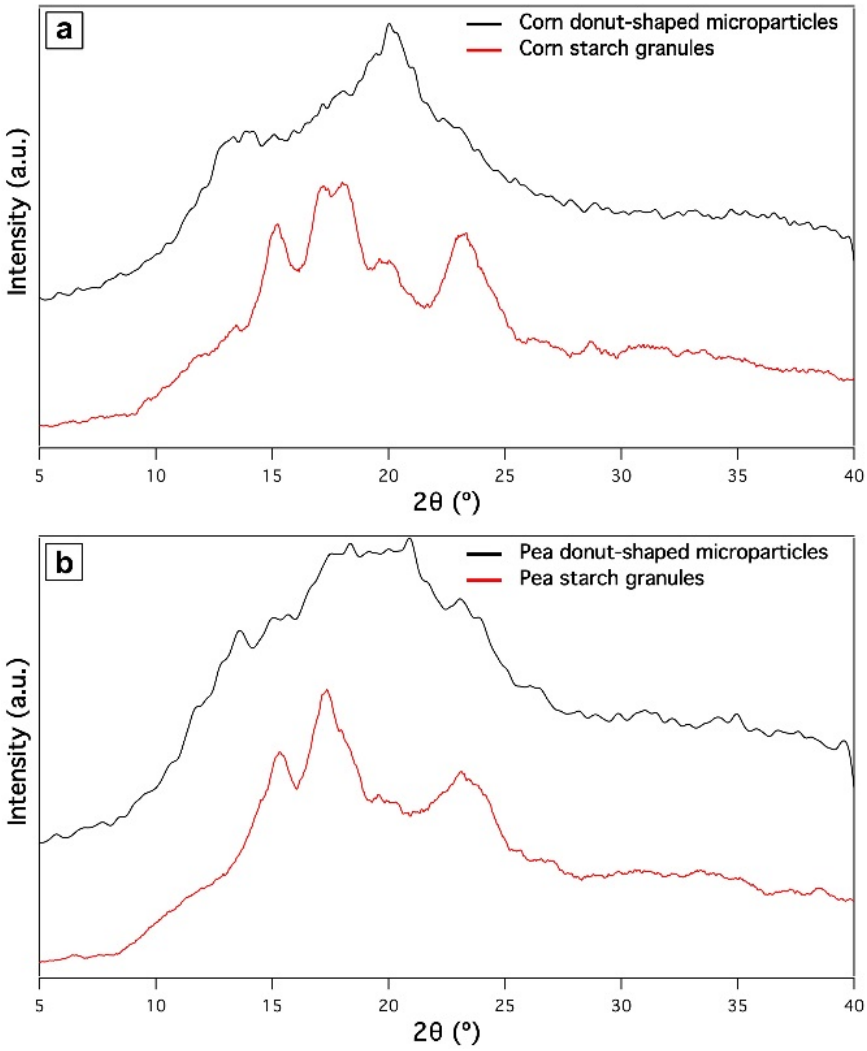


*Figure 5.37 XRD diffraction patterns of starch granules and their donut-shaped microparticles of corn (a) and pea (b).*

The pea donut-shaped starch microparticles showed also a V-type crystallinity without complete vanishing of the C-type crystal structure. Both A and B type crystals are double helical six folded structures. While the A-type crystalline structures are closely packed with water molecules between each double helical structure, B-type are more loose and open structures with a water molecules column located in the central cavity formed by six double helices (van Soest et al., 1996). Being a C-type crystal structure, pea starch granules possesses a more open crystalline structure due to the existence of the B-type crystals beside A-type ones.

*3.1.3. Solubility and swelling properties*

The results of swelling power and solubility index are summarized in Table 5.10 and revealed that hydration properties are higher for pea starch granules in comparison with corn granules that have the more packed A-type crystallinity. However, the swelling power of corn microparticles is higher than that of pea microparticles. The preparation of the donut-shaped microparticles includes several steps: water uptake, granule swelling, leaching of

amylose and finally partial destructuration of the granule. The partial disruption of the supra-macromolecular structure, and consequently the distortion of the crystallinity within the granules led to the conversion of the double helical order (A and B type crystals) arrangement to a single helix crystalline structure i.e. V type. The preparation starts with heating the starch in water to a temperature less than that of gelatinization ($T_g$). During this step, the water diffuses to the starch granules, the hydrogen bonds between starch macromolecules are broken and simultaneously starch macromolecules – water hydrogen bonds are formed. The granule swelling is accompanied by the leaching out of amylose just below of the gelatinization temperature as suggested by Ring et. al (Ring et al., 1985). The water diffusion, the granule swelling and the leaching out of amylose lead to a deformability of the granule and its surface. The subsequent addition of the absolute ethanol to the starch slurry results in the formation of inclusion complex in the swelled granules between starch macromolecules and ethanol (B. Zhang et al., 2012). The ethanol is enclosed in the internal cavity of the single helix of amylose replacing water and unwinding the large amylopectin

forming non-covalent interactions, mainly hydrophobic and van der Waals attraction with the central cavity of the helix. The addition of ethanol also leads to the dehydration of the granule which resembles a donut-shaped structure to reduce the contact between hydrophilic starch macromolecule and free ethanol molecules. In the final step, the starch microparticles were dried to remove the ethanol which lead to shrinking of the microparticles and the formation of anhydrous V-helices structure with an empty cavity and with more water affinity. The rough surface of the microparticles is due to shrinking by drying and leaching out of the peripheral amylose from the granule during heating. The increased water affinity is reflected in the enhanced swelling power of the donut-shaped microparticles compared to the starch granules as is shown in Table 5.10. To conclude, the thermal treatment of the starch slurry followed by the addition of ethanol cause a partial disruption of the supra-macromolecular structure, and consequently the distortion of the crystallinity within the granules and the conversion of the double helical order arrangement to a single helix, led to a more open structure where the water molecules could penetrate easier within

the microparticles increasing substantially their solubility and swelling power.

### *3.2. Characterization of the donut-shaped starch microparticles loaded TPS*

#### *3.2.1. Morphology*

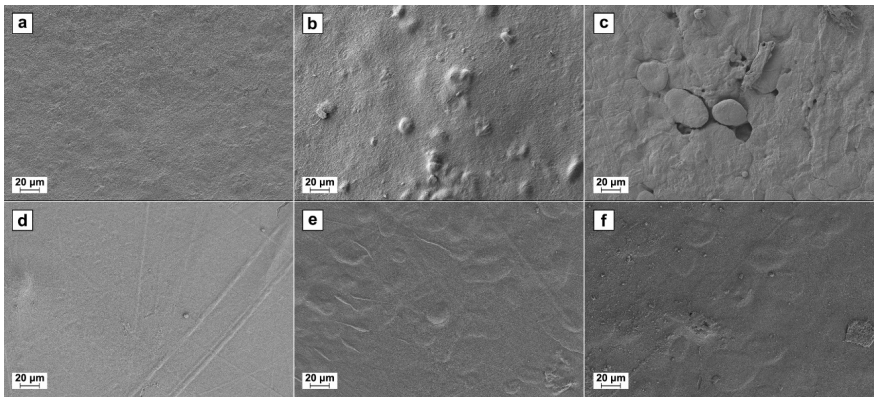


*Figure 5.38 SEM micrographs of the TPS surfaces: a) corn starch, b) corn starch + 10% microparticles, c) corn starch + 15% microparticles, d) pea starch, e) pea starch + 10% microparticles, f) pea starch + 15% microparticles.*

Figure 5.38 shows the SEM micrographs of the pea and corn starch TPS in addition to the films loaded with the donut-shaped microparticles of the same botanical origin. The surface of the corn films (CTPS) was continuous with no observed creases or starch aggregations which indicates that the plasticizer disrupted the

intermolecular and intramolecular hydrogen bonds of the corn starch completing the plasticization process (Montero et al., 2016). On the other hand, the pea starch film (PTPS) showed few creases along the matrix surface. When the donut-shaped starch microparticles are incorporated to the films, the loaded films exhibit a smooth surface in general. The microparticles can be distinguished through the starch matrix, however, they are completely covered and embedded in the films.

*3.2.2. X-ray diffraction analysis (XRD)*

The structure of the starch thermoplastic films was furtherly studied by analysing their X-ray diffraction patterns. In general, the observed crystallinity peaks of the starch films are mainly of two types: 1) residual crystallinity of A-, B- and C- types remaining from the original starch crystalline structures; 2) processing induced crystallinity during the plasticisation and the other preparation parameters. At supra-macromolecular level, the leaching of the amylose out of the starch granules and its recrystallization into a single helix is the main cause of the formation of three crystalline

structures of the processing induced crystallinity: $V_H$, $V_A$ and $E_H$ (Montero et al., 2016).

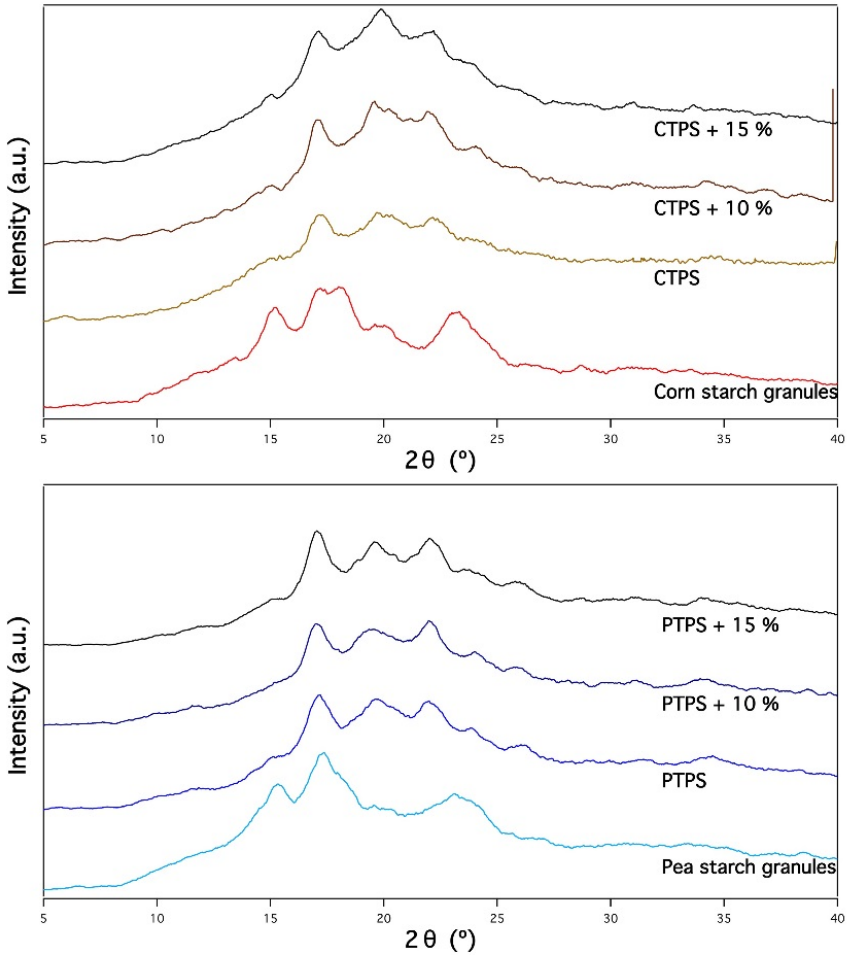


*Figure 5.39. XRD diffraction patterns of starch granules and their TPS of corn (a) and pea (b).*

Figure 5.39 shows the diffraction patterns of the donut-microparticles loaded TPS of both starch types: pea and corn, and

compares them with the original pattern of their granules and with the non-loaded TPS. All the TPS films showed strong peaks at 17°, 19.5°, 22.1° which corresponds to the processing induced $V_H$-type crystallinity (van Soest et al., 1996). These crystals are of 6-folded single helix amylose that are less contracted and have more water than the $V_A$-type crystals. The CTPS films (from corn starch) showed a weak peak at 15º which may correspond to a residual A-type crystallinity [Figure 5.39 a]. The peak at 17° for the PTPS films (from pea starch) were stronger than usual which may indicate an overlapping with the residual C-type crystals peak at 2θ value of 16.9°. Another weak peak was noticed for the PTPS films at 26º which may correspond to the processing induced $V_A$-type crystals. The addition of the donut- microparticles was accompanied with a little increase of the intensity at 20.0° that corresponds to the V-type crystalline structure of the microparticles. The peak at 20.0° overlaps with the $V_H$-type peak at 19.5° forming doublets in some XRD patterns.

*3.2.3. Thermogravimetric analysis (TGA)*

The thermo-oxidative degradation curves of the starch films plasticized with glycerol showed 4 degradation stages: 1) the mass loss attributed to the dehydration between 50 ºC and 120 ºC; 2) the main degradation stage showed between 150 ºC and 260 ºC is attributed to the glycerol-rich phase of the film (Montero et al., 2016); 3) the degradation stage of the starch-rich phase of the film between 260 ºC to 400 ºC; 4) the last degradation around 450 ºC represents the mass loss due to the oxidation of the residual organic matter. The addition of the starch microparticles to the PTPS increased its thermal stability as is seen in Figure 5.40 The thermal stability increases even more by elevating the percentage of the microparticles from 10% to 15 %. The mass loss in the glycerol-rich phase area was also lower for the films with higher microparticles contents which indicates less free glycerol chains. The CTPS did not show a noticeable change in the thermal stability at 10 % of microparticles, however, the thermal stability increased significantly by increasing the microparticles concentration to 15%.

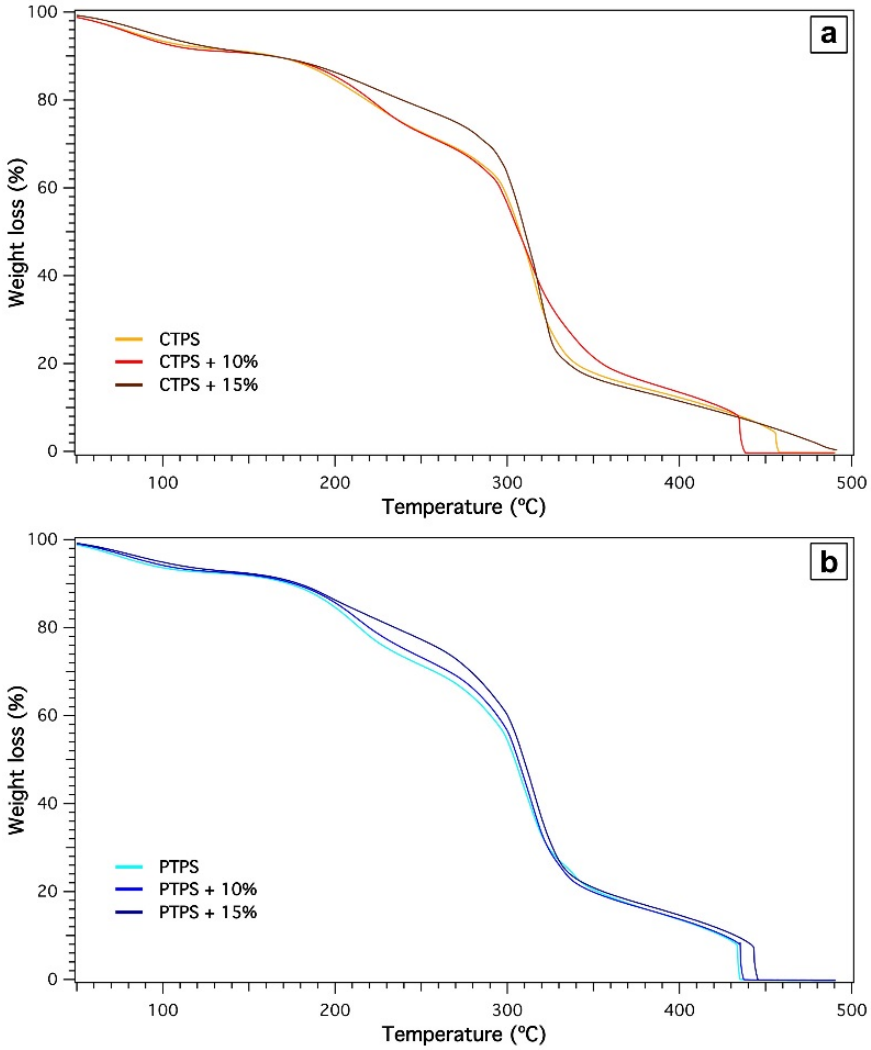


*Figure 5.40 TGA curves of the TPS films from corn (a) and pea (b).*

### *3.2.4. Water vapour and oxygen transmission rates*

*Table 5.11 Water vapour permeability and Oxygen permeability values for starch films*

| Sample | Water vapour transmission rate (gm/m$^2$.day) | Oxygen transmission rate (cc/m$^2$.day) |
|---|---|---|
| **CTPS** | 217.81 | 62.93 |
| **CTPS + 10%** | 203.37 | 15.62 |
| **CTPS + 15%** | 196.38 | 6.13 |
| **PTPS** | 200.01 | 276.23 |
| **PTPS + 10%** | 186.48 | 98.76 |
| **PTPS + 15%** | 160.31 | 11.40 |

Controlling the type and the amount of the gases passing through the packaging films are of great importance for maintaining the packaged food fresh and healthy as long as possible. For that, the microparticles are being added to the packaging films as fillers to adjust the adequate amount of water vapour and oxygen and therefore control the humidity content and the oxidation issues inside the package. The values of the water vapour and oxygen permeability of the different starch films are presented in Table 5.11. The addition of the microparticles to the pea thermoplastic starch films (PTPS) decreased the water vapour transmission rate significantly. However, the water vapour transmission rate of the CTPS was decreased slightly by increasing the microparticles

content within the films. This may be because the microparticles from corn origin have much more swelling capacity than those of pea origin as discussed before [Table 5.10] which make them less effective as water vapour barriers. The addition of the microparticles to the films from both origins decreased dramatically the oxygen permeability depending on the percentage of the microparticles in the film. The donut-starch microparticles embedded in the films may increase the compactness of the films and act as a barrier for the water vapour and oxygen molecules limiting their pathways.

## 4. Conclusions

Starch microparticles with donut-shaped morphology from two different botanical origins were prepared via a simple thermal aqueous–alcoholic treatment. The thermal treatment of the starch slurry and the addition of ethanol as precipitant led to the conversion of double helical order arrangement of the granule (A- and C-type for the corn and pea starch granules respectively) to the V-type crystalline structure. These crystals are of single helix and have more open structure where the water molecules can penetrate easier. Thus,

the donut-shaped microparticles showed higher swelling power compared with the starch granules. The simplicity and the easiness of the preparation method and the remarkable stability of the donut-shaped microparticles make it suitable for various applications such as fillers for food packaging applications. The donut-shaped microparticles were loaded to films of the same botanical origin to make TPS. The X-ray diffraction patterns showed both residual and processing induced crystallinity of the (TPS) films. The addition of the microparticles increases the thermal stability of the produced films. Moreover, tuning the percentage of the microparticles in the thermoplastic films allows delivering the desired amount of the oxygen and water vapour to the packaged food. This is of a great importance for maintaining the packaged food fresh and healthy as long as possible.

## References

BeMiller, J. N., & Whistler, R. L. (Eds.). (2009). Starch: chemistry and technology (Third edit). Academic Press.

Castaño, J., Bouza, R., Rodríguez-Llamazares, S., Carrasco, C., & Vinicius, R. V. B. (2012). Processing and characterization of starch-based materials from pehuen seeds (Araucaria araucana (Mol) K. Koch). Carbohydrate Polymers, 88(1), 299–307. http://doi.org/10.1016/j.carbpol.2011.12.008

Castaño, J., Rodríguez-Llamazares, S., Contreras, K., Carrasco, C., Pozo, C., Bouza, R., … Giraldo, D. (2014). Horse chestnut (Aesculus hippocastanum L.) starch: Basic physico-chemical characteristics and use as thermoplastic material. Carbohydrate Polymers, 112, 677–685. http://doi.org/10.1016/j.carbpol.2014.06.046

Castaño, J., Rodríguez-Llamazares, S., Sepúlveda, E., Giraldo, D., Bouza, R., & Pozo, C. (2017). Morphological and structural changes of starch during processing by melt blending. Starch - Stärke, 68, 1–9. http://doi.org/10.1002/star.201600247

Chin, S. F., Pang, S. C., & Tay, S. H. (2011). Size controlled synthesis of starch nanoparticles by a simple nanoprecipitation method. Carbohydrate Polymers, 86(4), 1817–1819. http://doi.org/10.1016/j.carbpol.2011.07.012

Farrag, Y., Sabando, C., Rodríguez-Llamazares, S., Bouza, R., Rojas, C., & Barral, L. (2017). Preparation of donut-shaped starch microparticles by aqueous-alcoholic treatment. Food Chemistry, Submitted Manuscript.

Fengge Gao (Ed.). (2012). Advances in polymer nanocomposites : types and applications. Elsevier.

Jane, J., Craig, S. A. S., Seib, P. A., & Hoseney, R. C. (1986). Characterization of granular cold water-soluble starch. Starch - Stärke, 38(8), 258–263. http://doi.org/10.1002/star.19860380803

Jane, J. lin. (2009). Structural features of starch granules II. Starch: Chemistry and Technology (Third Edit). Elsevier Inc.

http://doi.org/10.1016/B978-0-12-746275-2.00006-9

Kaur, L., Singh, N., & Singh, J. (2004). Factors influencing the properties of hydroxypropylated potato starches. Carbohydrate Polymers, 55(2), 211–223. http://doi.org/10.1016/j.carbpol.2003.09.011

Kim, H. Y., Park, S. S., & Lim, S. T. (2015). Preparation, characterization and utilization of starch nanoparticles. Colloids and Surfaces B: Biointerfaces, 126, 607–620. http://doi.org/10.1016/j.colsurfb.2014.11.011

Lamanna, M., Morales, N. J., Garcia, N. L., & Goyanes, S. (2013). Development and characterization of starch nanoparticles by gamma radiation: Potential application as starch matrix filler. Carbohydrate Polymers, 97(1), 90–97. http://doi.org/10.1016/j.carbpol.2013.04.081

Majzoobi, M., Kaveh, Z., Blanchard, C. L., & Farahnaky, A. (2015). Physical properties of pregelatinized and granular cold water swelling maize starches in presence of acetic acid. Food Hydrocolloids, 51, 375–382. http://doi.org/10.1016/j.foodhyd.2015.06.002

Montero, B., Rico, M., Rodríguez-Llamazares, S., Barral, L., & Bouza, R. (2016). Effect of nanocellulose as a filler on biodegradable thermoplastic starch films from tuber, cereal and legume. Carbohydrate Polymers. http://doi.org/10.1016/j.carbpol.2016.10.073

Qin, Y., Liu, C., Jiang, S., Xiong, L., & Sun, Q. (2016). Characterization of starch nanoparticles prepared by nanoprecipitation: Influence of amylose content and starch type. Industrial Crops and Products, 87, 182–190. http://doi.org/10.1016/j.indcrop.2016.04.038

Rico, M., Rodríguez-Llamazares, S., Barral, L., Bouza, R., & Montero, B. (2016). Processing and characterization of polyols plasticized-starch reinforced with microcrystalline cellulose. Carbohydrate Polymers, 149, 83–93. http://doi.org/10.1016/j.carbpol.2016.04.087

Ring, S. G., Lanson, K. J., Morris, V. J., L'Anson, K., & Morris, V. J. (1985). Static and dynamic light-scattering studies of amylose solutions. Macromolecules, 18(2), 182–188. http://doi.org/10.1021/ma00144a013

Schneider, C. A., Rasband, W. S., & Eliceiri, K. W. (2012). NIH Image to ImageJ: 25 years of image analysis. Nat Meth, 9(7), 671–675. Retrieved from http://dx.doi.org/10.1038/nmeth.2089

Shi, A. M., Wang, L. J., Li, D., & Adhikari, B. (2013a). Characterization of starch films containing starch nanoparticles. Part 2: Viscoelasticity and creep properties. Carbohydrate Polymers, 96(2), 602–610. http://doi.org/10.1016/j.carbpol.2012.10.064

Shi, A. M., Wang, L. J., Li, D., & Adhikari, B. (2013b). Characterization of starch films containing starch nanoparticles Part 1: Physical and mechanical properties. Carbohydrate Polymers, 96(2), 593–601. http://doi.org/10.1016/j.carbpol.2012.12.042

Shi, L., Fu, X., Tan, C. P., Huang, Q., & Zhang, B. (2017). Encapsulation of ethylene gas into granular cold-water-soluble starch: structure and release kinetics. Journal of Agricultural and Food Chemistry, 65(10), 2189–2197. http://doi.org/10.1021/acs.jafc.6b05749

Srichuwong, S., Sunarti, T. C., Mishima, T., Isono, N., & Hisamatsu, M. (2005). Starches from different botanical sources I: Contribution of amylopectin fine structure to thermal properties and enzyme digestibility. Carbohydrate Polymers, 60(4), 529–538. http://doi.org/10.1016/j.carbpol.2005.03.004

van Soest, J. J. G., Hulleman, S. H. D., de Wit, D., & Vliegenthart, J. F. G. (1996). Crystallinity in starch bioplastics. Industrial Crops and Products, 5(1), 11–22. http://doi.org/10.1016/0926-6690(95)00048-8

Xie, F., Pollet, E., Halley, P. J., & Avérous, L. (2013). Starch-based nano-biocomposites. Progress in Polymer Science, 38(10–11), 1590–1628.

http://doi.org/10.1016/j.progpolymsci.2013.05.002

Young, A. H. (1984). Chapter VIII – Fractionation of starch. In Starch: Chemistry and Technology (Second edi, pp. 249–283). http://doi.org/10.1016/B978-0-12-746270-7.50014-8

Zhang, B., Dhital, S., Haque, E., & Gidley, M. J. (2012). Preparation and characterization of gelatinized granular starches from aqueous ethanol treatments. Carbohydrate Polymers, 90(4), 1587–1594. http://doi.org/10.1016/j.carbpol.2012.07.035

# 6. Starch edible films loaded with donut-shaped starch-quercetin microparticles: characterization and release kinetics

## 1. Introduction

The scientific and the industrial communities are becoming more and more concerned about the environmental and the health issues caused by the petroleum derived plastics. For that, biopolymers are being extensively studied in the last years to evaluate their possible applications as replacement of the conventional plastics (Chandra & Rustgi, 1998). Biopolymers have found their ways to be applied in the fields of drug delivery, tissue engineering, biomedical scaffolds and stents and in the packaging industry (Bai et al., 2015; Malmir et al., 2017; Vilos et al., 2013; Williams et al., 1999). However, more research is required to provide more characterization and improvement of their properties to adapt the desired applications.

The starch films can be produced either by melt processing or by solution casting in the presence of water (A. M. Shi et al., 2013b). A suitable plasticizer must be added to the starch which normally improves the mechanical properties of the starch films (Chang et al., 2010; Rico et al., 2016). Different fillers can be added to modify the starch film properties such as nanoparticles and

microparticles of biopolymers (Le Corre et al., 2010; Ma et al., 2008). Additional functional ingredients such as antimicrobials, antioxidants or other nutritional supplements can be added to the biofilms to obtain active packaging materials (Arrieta et al., 2014; Cheng, Wang, & Weng, 2015). The incorporation of an antioxidant in the packaging film provides a strategy to overcome the oxidation issue of the packed food and participate in the food preservation. However, the antioxidant must be non-toxic for the consumer and have no negative effect on the food quality (Benbettaïeb et al., 2016). Quercetin (3,3',4',5,7-pentahydroxyflavone) is a natural flavonoid which is found in many leaves, fruits and vegetables such as onions, apples and tea among other plants. It is known for its strong antioxidant activity and was reported to have anti-inflammatory and anti-cancer activities (Bose et al., 2013).

In this work, a combined strategy for modifying the starch films was applied. Donut-shaped starch microparticles from cereal and legume origins loaded with quercetin were produced by thermal aqueous-alcoholic treatment. The morphology, the thermal stability, the quercetin loading percentage and the antioxidant activity of the

donut-shaped microparticles were analyzed. The quercetin loaded microparticles were introduced to films of starches of the same botanical origin in two different amounts. The thermal stability of the films was evaluated. The release kinetics of the quercetin from the starch films were evaluated and compared for films from both origins.

## 2. Materials and methods

### *2.1. Materials and reagents*

Pea and corn starches were provided by Roquette Freres S. A. (France). The amylose content of the starches reported by the company was 35% and 25% respectively. Absolute ethanol was purchased from Scharlau (Spain). Quercetin (purity ≥95%), glycerol and DPPH (1,1-diphenyl-2-picrylhydrazyl) radical were purchased from Sigma Aldrich (Germany). Water was purified using a Milli-Q Ultrapure water-purification system (Millipore, France).

*2.2. Preparation of starch-quercetin microparticles.*

Starch microparticles were prepared by thermal aqueous-alcoholic treatment under the following procedure (Farrag et al., 2017). An amount of 8 g of starch was added to 150 mL of Milli-Q water. The mixture was heated at 66 °C under constant stirring at 500 rpm during 1 h. Then, 150 mL of 12 mg/mL quercetin solution in absolute ethanol were added during 75 min (2mL/min) using a diaphragm pump (SIMDOS 02, KNF Neuberger, Switzerland) to the starch slurry under the same stirring conditions without heating. When the starch microparticles suspension was cooled to room temperature, another 150 mL of 12 mg/mL quercetin solution in absolute ethanol were added dropwise under constant stirring at a flow rate 3mL/min. Finally, the suspension was centrifuged for 20 min at 4400 rpm, and washed with ethanol to remove water and the excess quercetin. After washing, the microparticles were dried in a forced air oven at 50 °C. The microparticles were prepared in triplicate.

*2.3. Preparation of starch films loaded with donut-shaped starch-quercetin microparticles*

The films of corn and pea starches that contain starch donut-shaped microparticles loaded with quercetin were prepared using the solution casting method (Montero et al., 2016). Native starches were suspended in 60 mL of glycerol and water solution. The suspensions were mixed and then heated in a microwave oven for 150 s. The suspensions were withdrawn each 30 s for mixing and then returned to the microwave oven. The gelatinized starch solutions were then stirred at 800 rpm using magnetic stirring till cooling down. The starch-quercetin microparticles were added to the starch solution and homogenized using a T 25 digital ULTRA-TURRAX homogenizer at 5000 rpm for 10 min. The obtained suspensions were sonicated for degassing and then poured in a 20 cm diameter flat bottom petri dishes lined with Teflon sheets. The petri dishes were dried in a forced air oven for 30 h at $30^{o}$ C. The obtained films were reconditioned in a climate chamber at room temperature and at 40% relative humidity to insure the equilibration of the water in the films.

The total weight of dry starch (i.e. native starch weight + donut-shaped starch-quercetin microparticles weight) was kept at 2.1 g. The starch-quercetin microparticles were added in a percentage of 10 and 15% of the total dry starch content. The ratio between the native starch weight and the glycerol weight was 7:3.

*2.4. Scanning electron microscopy (SEM)*

The morphology of the starch-quercetin microparticles was characterized using a Carl Zeiss ultra plus field emission scanning electron microscope (FESEM) operated at 3 kV (Carl Zeiss, Germany). The particles were previously sputter-coated with iridium using QUORUM Q150T-S turbo-pumped sputter coater (Quorum Technologies Ltd, UK). The size of the microparticles was measured directly from the SEM micrographs using ImageJ software (Schneider et al., 2012).

*2.5. Determination of quercetin loading percentage*

2 mg of the dried starch-quercetin microparticles were accurately measured and suspended in 1.5 mL of methanol. The

suspensions were shaken and left overnight to allow the complete release of the loaded quercetin. Afterwards, the suspensions were centrifuged at 14500 rpm for 5 min and the absorbance of the quercetin in the supernatant was determined using an UV-vis spectrophotometer SPECORD 200 PLUS (Analytikjena, Germany) at a wavelength of 372 nm. A series of standard solutions of quercetin in methanol were used for obtaining the calibration curve. The absorbance of the quercetin in the supernatants was measured after further dilution and then compared to the corresponding calibration curve. The measurements were performed in triplicate.

The loading of quercetin was calculated according to Equation 6.1 (Papadimitriou & Bikiaris, 2009).

$$Drug\ loading\ (\%) = \frac{weight\ of\ drug\ released}{weight\ of\ microparticles} \times 100 \quad (6.1)$$

*2.6. Antioxidant activity*

The antioxidant activities of the starch-quercetin microparticles were determined by the DPPH method (Villaño, Fernández-Pachón, Moyá, Troncoso, & García-Parrilla, 2007). This experiment is based on measuring the scavenging capacity of the

antioxidant toward the stable DPPH radical. The freeze-dried starch-quercetin microparticles were suspended in methanol in a concentration of 1mg/mL. The suspensions were incubated overnight to insure the complete release of the quercetin from the particles. The suspensions were centrifuged and aliquots of 20 µL of each supernatant were added to 1.5 mL of 0.1 mM DPPH solution in methanol. The total volume of each solution was completed to 2 mL using methanol. The mixture was shaken and then allowed to stand for 30 min at room temperature away from light. A solution of 0.05 mg/mL quercetin in methanol was used as positive control. The absorbance of the DPPH radical at 517 nm was measured. The antioxidant activity was calculated according Equation 6.2

$$Antioxidant\ activity\ (\%) = \frac{A_0 - A_s}{A_o} \times 100 \quad (6.2)$$

Where $A_0$ is the absorbance of the DPPH in the absence of the antioxidants, $A_s$ is the absorbance of the samples. All the steps of the experiment were done away from light and using amber glassware. All the measurements were performed in triplicate.

*2.7. Thermogravimetric analysis (TGA)*

Thermogravimetric analysis was performed using a PerkinElmer TGA-4000 microbalance with a ceramic sample pan (Massachusetts, USA). Approximately 20–25 mg of material were heated from 50°C to 500°C at 10°C/min with a 20 mL/min oxygen flow. The TG curves and their first derivatives, the DTG curves, were recorded in each test.

*2.8. In-vitro release in water/ethanol medium*

Pieces of the starch films of dimensions 1x1 $cm^2$ were cut. The thickness of each film was measured using a Digital Thickness Gauge (Baxlo precision, 4050, Barcelona, Spain) and then weighed. Each piece of film was placed in an amber glass container, then 10 mL of 35% (v/v) ethanol solution in water were added and the film container was maintained firmly closed at room temperature with continuous stirring at 300 rpm. The amount of the quercetin in the release medium was determined periodically using UV-vis spectrophotometer at a wavelength 372 nm. A series of standard solutions of quercetin in 35% (v/v) ethanol in water were used for

calibration. The absorbance of the supernatant samples were measured after further dilution if needed and then compared to the standard curve. The cumulative quercetin release was calculated. The experiment was repeated 3 times for each sample of the starch films. Samples were analysed to determine the quercetin quantity released till the equilibrium. The concentration of the quercetin was assumed to be uniform in all parts of the film.

*2.9. Statistical analysis*

Statistical analysis was performed basically by means of Igor Pro 6.37 software. The Add-in program DDSolver was used for making the fitting calculations and for the calculation of the coefficient of determination $R^2$ and the AIC (Akaike's information criterion) (Y. Zhang et al., 2010).

**3. Results and discussion**

*3.1. Preparation and characterization of the starch-quercetin microparticles*

The donut-shaped starch microparticles loaded with quercetin were prepared by thermal aqueous-alcoholic treatment.

The morphology obtained suggests that the supramolecular packing of the starch granules was not completely damaged. Figure 6.41 shows the morphology of the donut-shaped starch microparticles prepared from corn and pea starches. The diameter of the particles from corn starch was 17.0 ± 2.7 µm while the microparticles from pea starch showed bigger particle size (32.3 ± 6.8 µm). The difference in the particle size is more likely due to the initial granule size of starches from different origins (10.7 ± 3.2 µm and 24.4 ± 5.5 µm for the corn and pea granules, respectively). Crystals of quercetin seem to be adsorbed to the surface of the pea-starch microparticles which is less observed for the corn-starch ones.

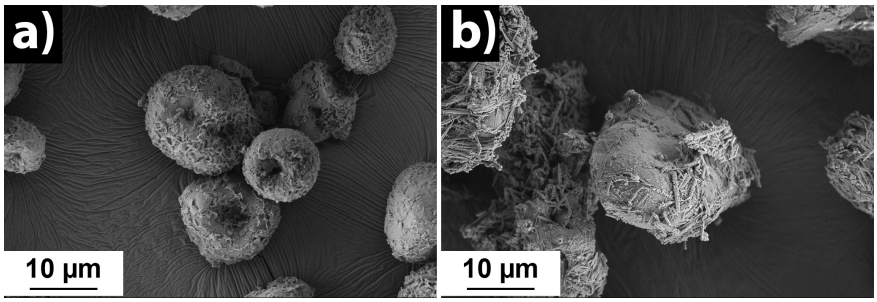


*Figure 6.41 SEM micrographs of the starch-quercetin donut shaped microparticles of corn (a) and pea (b) starches.*

The heating of the aqueous starch suspension just below the gelatinization temperature caused the diffusion of water into the

starch granules, breaking of the hydrogen bonds between starch macromolecules and simultaneously lead to the formation of starch macromolecules – water hydrogen bonds. The granule swelling was accompanied by the leaching out of amylose just below of the gelatinization temperature as suggested by Ring et. al (Ring et al., 1985). Ethanol was previously reported to be used to produce starch nanoparticles in addition to being a good solvent for the quercetin which has a limited solubility in water (Chebil et al., 2007; Chin et al., 2011). By starting to drop the quercetin ethanolic solution on the starch solution, the quercetin precipitated due to the excess water in the medium. The solubility of the quercetin was increased by dropping more ethanol in the medium, therefore, the precipitated quercetin was re-dissolved and started to diffuse to the swelled starch particles. The continuous increase of the ethanol concentration in the preparation medium resulted in the formation of inclusion complex in the swelled granules between starch macromolecules and ethanol (B. Zhang et al., 2012). The addition of ethanol also is thought to lead to dehydration of the granule which resembles a donut-shaped structure to reduce the contact between

hydrophilic starch macromolecules and free ethanol molecules. The drying process of the produced donut-shaped starch-quercetin microparticles has led to the removal of ethanol, shrinking of the microparticles and precipitation of some quercetin crystals on the surface of the starch-microparticles.

*3.2. Loading percentage and antioxidant activity*

The loading percentage of the quercetin calculated by applying Equation 6.1 was found to be different for the microparticles from each starch origin. Starch from legume origin has a loading percentage of 13.2 ± 0.2 % in comparison with 5.7 ± 0.1 % for the microparticles from cereal origin. This difference in the loading percentages for both starches might be due to the different composition of each starch type. The pea starch was reported to have an amylose and amylopectin of higher molecular weights than that of the starch obtained from corn (Young, 1984).

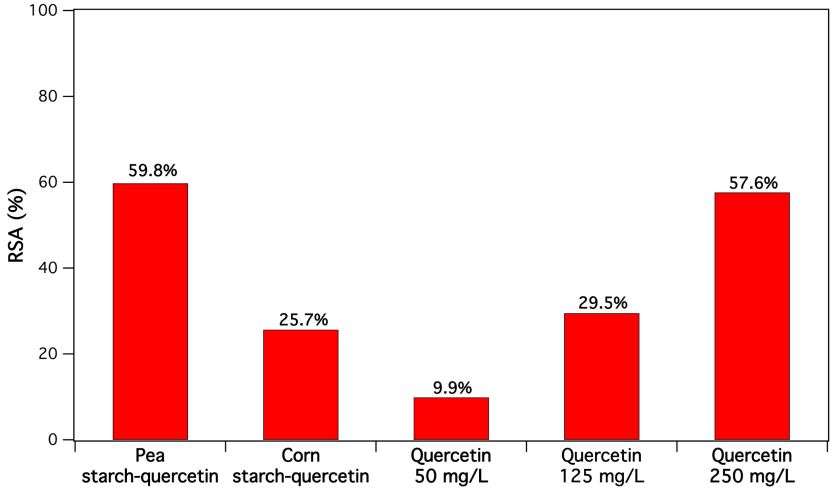


*Figure 6.42 Antioxidant activity of the starch-quercetin microparticles and quercetin standard solutions.*

Figure 6.42 shows the radical scavenging activity (RSA%) of both types of donut-shaped starch-quercetin microparticles compared to the RSA of the row quercetin in various concentrations. The pea starch-quercetin microparticles showed an antioxidant activity of 59.8% which is slightly higher than that of 250 mg/L of row quercetin when using the same volume (20 µL). This is quite higher than the antioxidant activity of the corn starch-quercetin microparticles (25.7%). The antioxidant activity of the starch-quercetin microparticles is related to the quercetin loading percentage. Comparing the RSA values of the starch-quercetin

microparticles to those of the row quercetin-methanolic solution allows the quantification of the quercetin released from the microparticles. This provides another way for the evaluation of the quercetin loading percentage. The calculated loading percentages of the quercetin for pea and corn starch microparticles were 13.1 ± 0.2 % and 5.7 ± 0.2 % respectively which are equal to the values obtained by the loading percentage experiment previously discussed.

### *3.3. Thermogravimetric analysis (TGA)*

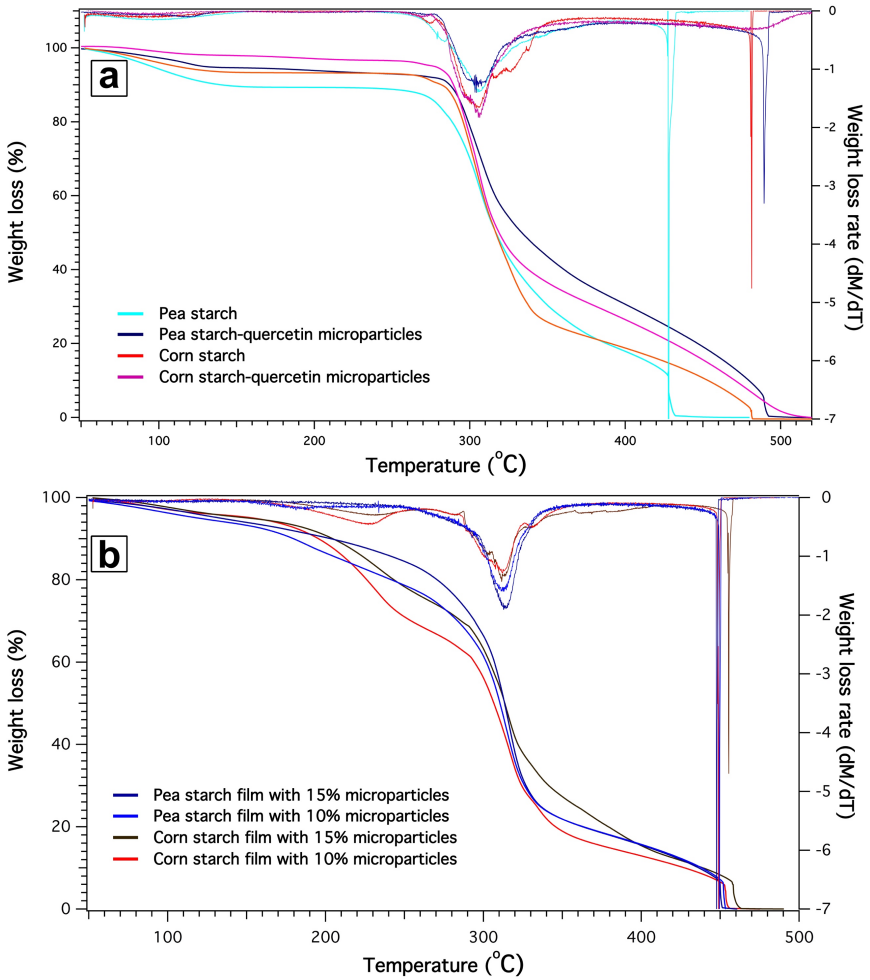


*Figure 6.43 TGA and DTG curves of the starch-quercetin microparticles and the starch granules (a) and of the starch films containing starch-quercetin microparticles (b).*

The thermogravimetric (TG) and the derivative thermogravimetric (DTG) curves of the starch-quercetin donut-shaped microparticles and the pea and corn starch granules are

presented in Figure 6.43 a. The starch-quercetin microparticles resulted to be slightly more thermally stable than their original granules. The thermo-oxidative degradation of the pea starch-quercetin microparticles started at 280 °C in comparison with 269 °C for the pea starch granules. The same increase in the onset degradation temperature was noted for the corn starch-quercetin microparticles when compared to that of the corn starch granules (278 °C and 269 °C, respectively). The degradation of the microparticles were significantly slower than for their original starch granules.

The amount of the starch-quercetin within the film also showed an impact on the thermal stability of the films as presented in Figure 6.43 b. The thermo-oxidative degradation curves of the starch films plasticized with glycerol showed 3 degradation stages in addition to the mass loss attributed to the dehydration between 50 ºC and 120 ºC. The main degradation stage showed between 150 ºC and 260 ºC is attributed to the glycerol-rich phase of the film (Montero et al., 2016). The degradation stage of the starch-rich phase of the film occurs between 260 ºC to 400 ºC. The last degradation

peaks showed around 450 ºC represent the mass loss due to the oxidation of the residual organic matter. The films with more amount of starch-quercetin microparticles showed higher degradation onset temperature for the glycerol-rich phase area. The mass loss in the glycerol-rich phase area was also lower for the films with higher microparticles contents which indicates less free glycerol chains.

*3.4. Quercetin release kinetics from the starch films*

The release kinetics of quercetin from the starch films loaded with starch-quercetin donut-shaped microparticles are shown in Figure 6.44. Each film was loaded with starch-quercetin microparticles from the same botanical origin. The release behaviour of quercetin was noted to be different for each starch origin. The films based on corn starch showed faster release kinetics of quercetin than those based on pea starch [Figure 6.44 a].

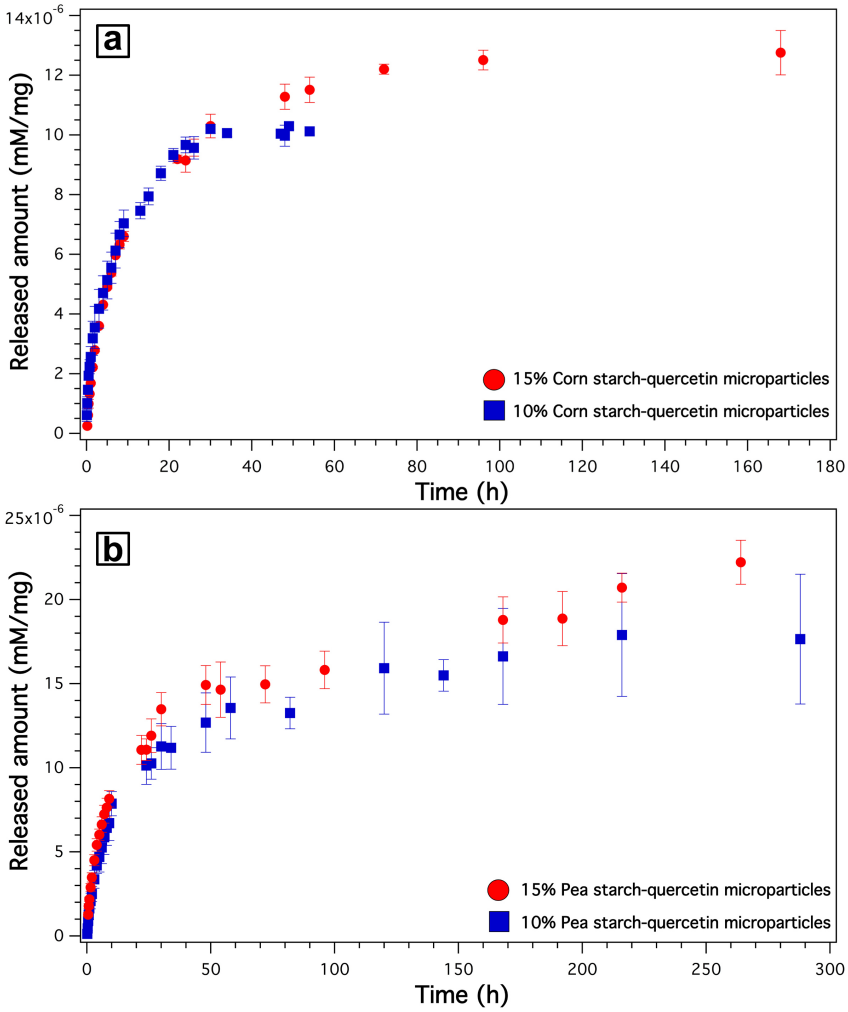


*Figure 6.44 Release kinetics of quercetin from starch films loaded with starch-quercetin microparticles of the same botanical origin (corn (a) and pea (b)).*

While the equilibrium was reached after 1 day and 4 days for the corn starch based films containing 10% and 15% of starch-quercetin microparticles respectively; it took 9 days for the pea

starch based films containing 10% of starch-quercetin microparticles to achieve the equilibrium. The pea starch based film that contains 15% starch-quercetin microparticles continued to release for more than 10 days [Figure 6.44 b]. However, the in-vitro release experiment was terminated after 11 days as the UV-Vis spectrum shows a new peak at a wavelength of 295 nm [Figure 6.45]. This peak indicates the loss of conjugation of the chromophore, i.e. the degradation of the quercetin (Dall'Acqua, Miolo, Innocenti, & Caffieri, 2012).

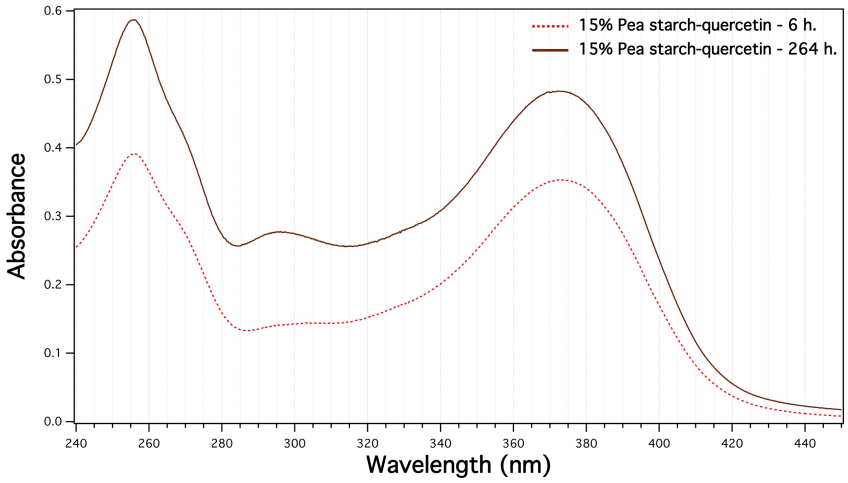


*Figure 6.45 Absorbance graphs of the pea starch film containing 15% pea starch-quercetin microparticles at 6 h and 264 h. The absorbance at 264 h was recorded after dilution.*

When comparing the films made of the same starch botanical origin, they were found to have very similar release kinetics for at least the first day of the in-vitro release experiment independently on the amount of the starch-quercetin microparticles contained. In addition, the amounts of the quercetin released till at least the first 60% of the released fraction were quite similar. This suggests that the release of the quercetin could be controlled mainly by non-concentration dependent diffusion.

For a better understanding of the release mechanism, the experimental release data were fitted to Peppas-Sahlin model. This model is a semi-empirical model that describes the drug release kinetics from hydrophilic polymers and is applicable for different geometric shapes. The model considers the release kinetics to be affected by two additive transport mechanisms: Fickian diffusional release and case-II relaxational contribution as illustrated in Equation 6.3 (Peppas & Sahlin, 1989; Siepmann & Peppas, 2001).

$$\frac{M_T}{M_\infty} = k_1(T)^m + k_2(T)^{2m} \quad (6.3)$$

Where $M_T$ is the amount of drug released at time T, $M_\infty$ is the maximum amount of the drug released measured at the

equilibrium, $k_1$ and $k_2$ are the release constants and m is the release exponent. This equation can be applied for $M_T/M_\infty < 0.6$ (Peppas & Sahlin, 1989). A further modification was necessary Equation 6.4 to incorporate the lag period ($T_{lag}$) to the equation for providing a better fitting and a more accurate description of the release kinetics (Ford et al., 1991).

$$\frac{M_T}{M_\infty} = k_1(T - T_{lag})^m + k_2(T - T_{lag})^{2m} \quad (6.4)$$

Where $T_{lag}$ is the time during which the release was delayed. The first term of the right hand of Equation 6.4 represents the fickian diffusion contribution where the second term represents the case-II relaxational contribution associated with relaxation in hydrophilic polymers which undergoes swelling in water (Peppas & Sahlin, 1989).

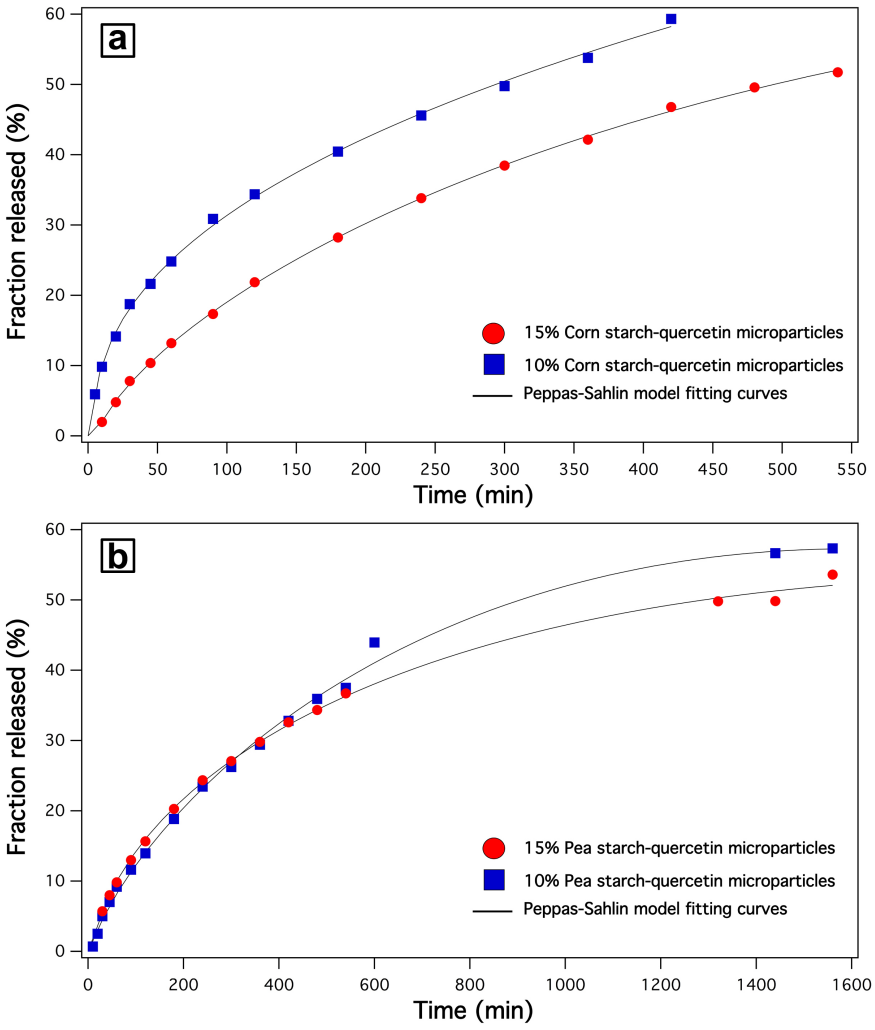


*Figure 6.46 Fit of the Peppas-Sahlin model to the experimental release data of quercetin from films of starches from different botanical origin (corn (a) and pea (b)).*

*Table 6.12 Parameters obtained by fitting the quercetin release profiles to Peppas-Sahlin model.*

| Parameter | Corn starch film + 10% starch-quercetin microparticles | Corn starch film + 15% starch-quercetin microparticles | Pea starch film + 10% starch-quercetin microparticles | Pea starch film + 15% starch-quercetin microparticles |
|---|---|---|---|---|
| $R^2$ | 0.999 | 0.999 | 0.998 | 0.999 |
| AIC | 28.799 | 10.161 | 55.691 | 34.935 |
| $k_1$ | 4.421 | 0.775 | 0.391 | 0.986 |
| $k_2$ | -0.007 | -0.002 | -0.001 | -0.005 |
| m | 0.431 | 0.724 | 0.770 | 0.614 |
| $T_{lag}$ (min) | 3.152 | 6.323 | 5.468 | 13.077 |

The calculated model parameters of the different films in addition to the coefficient of determination R2 and the AIC are summarized in Table 6.12. The experimental data for the first 60% of the amount of the released quercetin showed good fitting with Peppas-Sahlin model as is shown in [Figure 6.46]. The fractions of the quercetin released from the corn starch films containing 15% microparticles after 9 h were about 52% in comparison with 59% in 7 h for the films that contain 10% microparticles. Films from pea starch containing both concentrations of microparticles released 60% of the total quercetin released in more than 1 day. As is shown in Table 6.12, the values of the coefficient of determination R2 were equal or above 0.998 for all the films. Films based on pea starch

showed higher lag time than corn starch based films at the same microparticles concentration. This might be because of the higher rigidity of the pea starch films (Montero et al., 2016). The lag periods are thought to be the time required for the film surfaces to hydrate and start the diffusion process (Ford et al., 1991). The lag time increases when the microparticles amount loaded in the films increases. The values of the case II relaxational contribution constants, k2, were very small and have negative signs for all the films. Those values indicate that the case II relaxation has no significant contribution in the release process (Aguirre et al., 2016; Altimari et al., 2012; Maghsoodi & Barghi, 2011). The values of the fickian diffusion contribution constants k1 were higher than k2. This support the previously mentioned suggestion that the release of the quercetin from the starch films is mainly controlled by diffusion.

## 4. Conclusions

A completely biodegradable and biocompatible edible starch films loaded with donut-shaped starch-quercetin microparticles in different amounts were produced from pea and corn starch. The origin of the starch was found to have a significant impact on the characteristics of the starch microparticles as well as the starch films. At the microparticles level, the starch from cereal origin showed lower loading percentage and thus lower antioxidant activity than the microparticles of legume origin. The starch-quercetin microparticles also showed higher thermal stability than the starch granules. The films based on cereal starch seem to be suitable for very short term release applications due to the fast rate of the release of quercetin (1 to 4 days depending on the microparticles concentration). On the other hand, films based on legume starch continued to release for longer periods making them suitable for quercetin release applications during 1 week or a little more. The mechanism of release for all the films seemed to be non-concentration dependent diffusion for at least the first 60% of released quercetin. This was confirmed by fitting the experimental

release data of the first 60% of released quercetin to the Peppas-Sahlin model taking into consideration the lag time required to start the release process. The films with more microparticles content showed higher thermal stability. The produced biofilms can be utilized mainly for active food packaging applications.

## References

Aguirre, G., Villar-Alvarez, E., González, A., Ramos, J., Taboada, P., & Forcada, J. (2016). Biocompatible stimuli-responsive nanogels for controlled antitumor drug delivery. Journal of Polymer Science, Part A: Polymer Chemistry, 54(12), 1694–1705. http://doi.org/10.1002/pola.28025

Altimari, I., Spizzirri, U. G., Iemma, F., Curcio, M., Puoci, F., & Picci, N. (2012). pH-sensitive drug delivery systems by radical polymerization of gelatin derivatives. Journal of Applied Polymer Science, 125(4), 3006–3013. http://doi.org/10.1002/app.36234

Arrieta, M. P., Castro-López, M. del M., Rayón, E., Barral-Losada, L. F., López-Vilariño, J. M., López, J., … Manuel, J. (2014). Plasticized poly(lactic acid) − poly(hydroxybutyrate) (PLA − PHB) blends incorporated with catechin intended for active food-packaging applications. Journal of Agricultural and Food Chemistry, 62(41), 10170–10180. http://doi.org/10.1021/jf5029812

Bai, J., Dai, J., & Li, G. (2015). Electrospun composites of PHBV/pearl powder for bone repairing. Progress in Natural Science: Materials International, 25(4), 327–333. http://doi.org/10.1016/j.pnsc.2015.07.004

BeMiller, J. N., & Whistler, R. L. (Eds.). (2009). Starch: chemistry and technology (Third edit). Academic Press.

Benbettaïeb, N., Chambin, O., Karbowiak, T., & Debeaufort, F. (2016). Release behavior of quercetin from chitosan-fish gelatin edible films influenced by electron beam irradiation. Food Control, 66, 315–319. http://doi.org/10.1016/j.foodcont.2016.02.027

Bose, S., Du, Y., Takhistov, P., & Michniak-Kohn, B. (2013). Formulation optimization and topical delivery of quercetin from solid lipid based nanosystems. International Journal of Pharmaceutics, 441(1–2), 56–66. http://doi.org/10.1016/j.ijpharm.2012.12.013

Castaño, J., Bouza, R., Rodríguez-Llamazares, S., Carrasco, C., & Vinicius, R. V. B. (2012). Processing and characterization of

starch-based materials from pehuen seeds (Araucaria araucana (Mol) K. Koch). Carbohydrate Polymers, 88(1), 299–307. http://doi.org/10.1016/j.carbpol.2011.12.008

Castaño, J., Rodríguez-Llamazares, S., Contreras, K., Carrasco, C., Pozo, C., Bouza, R., … Giraldo, D. (2014). Horse chestnut (Aesculus hippocastanum L.) starch: Basic physico-chemical characteristics and use as thermoplastic material. Carbohydrate Polymers, 112, 677–685. http://doi.org/10.1016/j.carbpol.2014.06.046

Chandra, R., & Rustgi, R. (1998). Biodegradable polymers. Progress in Polymer Science, 23(7), 1273–1335. http://doi.org/10.1016/S0079-6700(97)00039-7

Chang, P. R., Jian, R., Zheng, P., Yu, J., & Ma, X. (2010). Preparation and properties of glycerol plasticized-starch (GPS)/cellulose nanoparticle (CN) composites. Carbohydrate Polymers, 79(2), 301–305. http://doi.org/10.1016/j.carbpol.2009.08.007

Chebil, L., Humeau, C., Anthoni, J., Dehez, F., Engasser, J.-M., & Ghoul, M. (2007). Solubility of flavonoids in organic solvents. Journal of Chemical & Engineering Data, 52(5), 1552–1556. http://doi.org/10.1021/je7001094

Cheng, S. Y., Wang, B. J., & Weng, Y. M. (2015). Antioxidant and antimicrobial edible zein/chitosan composite films fabricated by incorporation of phenolic compounds and dicarboxylic acids. LWT - Food Science and Technology, 63(1), 115–121. http://doi.org/10.1016/j.lwt.2015.03.030

Chin, S. F., Pang, S. C., & Tay, S. H. (2011). Size controlled synthesis of starch nanoparticles by a simple nanoprecipitation method. Carbohydrate Polymers, 86(4), 1817–1819. http://doi.org/10.1016/j.carbpol.2011.07.012

Chiu, C. wai, & Solarek, D. (2009). Modification of Starches. Starch (Third Edit). Elsevier Inc. http://doi.org/10.1016/B978-0-12-746275-2.00017-3

Dall'Acqua, S., Miolo, G., Innocenti, G., & Caffieri, S. (2012). The

photodegradation of quercetin: Relation to oxidation. Molecules, 17(8), 8898–8907. http://doi.org/10.3390/molecules17088898

Farrag, Y., Sabando, C., Rodríguez-Llamazares, S., Bouza, R., Rojas, C., & Barral, L. (2017). Preparation of donut-shaped starch microparticles by aqueous-alcoholic treatment. Food Chemistry, Submitted Manuscript.

Ford, J. L., Mitchell, K., Rowe, P., Armstrong, D. J., Elliott, P. N. C., Rostron, C., & Hogan, J. E. (1991). Mathematical modelling of drug release from hydroxypropylmethylcellulose matrices: Effect of temperature. International Journal of Pharmaceutics, 71(1–2), 95–104. http://doi.org/10.1016/0378-5173(91)90071-U

Jane, J. lin. (2009). Structural features of starch granules II. Starch: Chemistry and Technology (Third Edit). Elsevier Inc. http://doi.org/10.1016/B978-0-12-746275-2.00006-9

Lamanna, M., Morales, N. J., Garcia, N. L., & Goyanes, S. (2013). Development and characterization of starch nanoparticles by gamma radiation: Potential application as starch matrix filler. Carbohydrate Polymers, 97(1), 90–97. http://doi.org/10.1016/j.carbpol.2013.04.081

Le Corre, D., Bras, J., & Dufresne, A. (2010). Starch nanoparticles : A review. Biomacromolecules, 11(5), 1139–1153. http://doi.org/10.1021/bm901428y

Ma, X., Jian, R., Chang, P. R., & Yu, J. (2008). Fabrication and characterization of citric acid-modified starch nanoparticles/plasticized-starch composites. Biomacromolecules, 9(11), 3314–3320. http://doi.org/10.1021/bm800987c

Maghsoodi, M., & Barghi, L. (2011). Polymer percolation threshold in multi-component HPMC matrices tablets. Advanced Pharmaceutical Bulletin, 1(1), 27–33. http://doi.org/10.5681/apb.2011.004

Malmir, S., Montero, B., Rico, M., Barral, L., & Bouza, R. (2017). Morphology, thermal and barrier properties of biodegradable films of poly (3-hydroxybutyrate-co-3-hydroxyvalerate) containing cellulose nanocrystals. Composites Part A: Applied Science and

Manufacturing, 93, 41–48. http://doi.org/10.1016/j.compositesa.2016.11.011

Mason, W. R. (2009). Starch Use in Foods. Starch (Third Edit). Elsevier Inc. http://doi.org/10.1016/B978-0-12-746275-2.00020-3

Montero, B., Rico, M., Rodríguez-Llamazares, S., Barral, L., & Bouza, R. (2016). Effect of nanocellulose as a filler on biodegradable thermoplastic starch films from tuber, cereal and legume. Carbohydrate Polymers. http://doi.org/10.1016/j.carbpol.2016.10.073

Papadimitriou, S., & Bikiaris, D. (2009). Novel self-assembled core-shell nanoparticles based on crystalline amorphous moieties of aliphatic copolyesters for efficient controlled drug release. Journal of Controlled Release, 138(2), 177–184. http://doi.org/10.1016/j.jconrel.2009.05.013

Peppas, N. A., & Sahlin, J. J. (1989). A simple equation for the description of solute release. III. Coupling of diffusion and relaxation. International Journal of Pharmaceutics, 57(2), 169–172. http://doi.org/10.1016/0378-5173(89)90306-2

Rico, M., Rodríguez-Llamazares, S., Barral, L., Bouza, R., & Montero, B. (2016). Processing and characterization of polyols plasticized-starch reinforced with microcrystalline cellulose. Carbohydrate Polymers, 149, 83–93. http://doi.org/10.1016/j.carbpol.2016.04.087

Ring, S. G., Lanson, K. J., Morris, V. J., L'Anson, K., & Morris, V. J. (1985). Static and dynamic light-scattering studies of amylose solutions. Macromolecules, 18(2), 182–188. http://doi.org/10.1021/ma00144a013

Schneider, C. A., Rasband, W. S., & Eliceiri, K. W. (2012). NIH Image to ImageJ: 25 years of image analysis. Nat Meth, 9(7), 671–675. Retrieved from http://dx.doi.org/10.1038/nmeth.2089

Shi, A. M., Wang, L. J., Li, D., & Adhikari, B. (2013). Characterization of starch films containing starch nanoparticles Part 1: Physical and mechanical properties. Carbohydrate Polymers, 96(2), 593–601.

http://doi.org/10.1016/j.carbpol.2012.12.042

Siepmann, J., & Peppas, N. A. (2001). Modeling of drug release from delivery systems based on hydroxypropyl methylcellulose (HPMC). Advanced Drug Delivery Reviews, 48(2–3), 139–157. http://doi.org/10.1016/j.addr.2012.09.028

Villaño, D., Fernández-Pachón, M. S., Moyá, M. L., Troncoso, A. M., & García-Parrilla, M. C. (2007). Radical scavenging ability of polyphenolic compounds towards DPPH free radical. Talanta, 71(1), 230–235. http://doi.org/10.1016/j.talanta.2006.03.050

Vilos, C., Morales, F. A., Solar, P. A., Herrera, N. S., Gonzalez-Nilo, F. D., Aguayo, D. A., … Velasquez, L. A. (2013). Paclitaxel-PHBV nanoparticles and their toxicity to endometrial and primary ovarian cancer cells. Biomaterials, 34(16), 4098–4108. http://doi.org/10.1016/j.biomaterials.2013.02.034

Williams, S. F., Martin, D. P., Horowitz, D. M., & Peoples, O. P. (1999). PHA applications: addressing the price performance issue: I. Tissue engineering. International Journal of Biological Macromolecules, 25(1), 111–121. http://doi.org/10.1016/S0141-8130(99)00022-7

Young, A. H. (1984). Chapter VIII – Fractionation of starch. In Starch: Chemistry and Technology (Second edi, pp. 249–283). http://doi.org/10.1016/B978-0-12-746270-7.50014-8

Zhang, B., Dhital, S., Haque, E., & Gidley, M. J. (2012). Preparation and characterization of gelatinized granular starches from aqueous ethanol treatments. Carbohydrate Polymers, 90(4), 1587–1594. http://doi.org/10.1016/j.carbpol.2012.07.035

Zhang, Y., Huo, M., Zhou, J., Zou, A., Li, W., Yao, C., & Xie, S. (2010). DDSolver: an add-in program for modeling and comparison of drug dissolution profiles. The AAPS Journal, 12(3), 263–271. http://doi.org/10.1208/s12248-010-9185-1

# 7. General conclusions

In this thesis nano and microparticles of PHBV and different starch types were prepared by different techniques. The emulsification/solvent evaporation technique used for the preparation of the particles of PHBV provided control over the morphology and the size of the nano and microparticles by controlling the preparation parameters. Nanoprecipitation was found to be an easy way for obtaining PHBV nanoparticles. Controlling the polarity of the anti-solvent was found crucial for obtaining the spherical morphology of the nanoparticles.

Nanoparticles of starches from different botanical origin were prepared by nanoprecipitation using 0.1 M hydrochloric acid as non-solvent. The nanoparticles were spherical and their sizes vary depending on the origin and the concentration of the starch solution. Nanoparticles from different starches loaded with quercetin have been produced. The starch origin affects the quercetin loading percentage, the release kinetics and the antioxidant activity of the produced nanoparticles. The release kinetics of quercetin seemed to be controlled mainly by Fickian diffusion which have been revealed fitting the release data to the Peppas-Sahlin model.

Thermal aqueous–alcoholic treatment is an easy way for the preparation of donut-shaped starch microparticles from two different origins. The simplicity and the easiness of the preparation method and the remarkable stability of the donut-shaped microparticles of more than 18 month make it suitable for various applications such as fillers for food packaging applications. The addition of the microparticles increases the thermal stability of the produced films. Moreover, tuning the percentage of the microparticles in the thermoplastic films allows delivering the desired amount of the oxygen and water vapour to the packaged food.

The donut-shaped starch microparticles can act as a carrier for delivering a specific substrate through a biopolymeric film. The starch microparticles were loaded with quercetin and were used as fillers for starch thermoplastic films made from the same type of starch. The films based on cereal starch seem to be suitable for very short term release applications due to the fast rate of the release of quercetin (1 to 4 days depending on the microparticles concentration). On the other hand, films based on legume starch continued to release for longer periods making them suitable for

quercetin release applications during 1 week or a little more. The produced biofilms can be utilized mainly for active food packaging applications.

In conclusion, nano and microparticles from two different biopolymers have been produced by easy techniques. The incorporation of some of these particles into biopolymeric films led to significant improvements of some properties of the films especially the barrier properties. Some of the produced particles also showed capacity for active delivery function during reasonable periods. These promising results opens the door for many possibilities for improving some properties of more types of biopolymeric films with potential applications in the area of food packaging and other areas like biomedical and pharmaceutical applications.

# Anexo I: Resumen

## Introducción

La producción y la demanda de plásticos a nivel mundial se ha incrementado en los últimos 65 años. En 2015, la producción global de plásticos de origen fósil fue de alrededor de 400 millones de toneladas, en comparación con los 300 millones de toneladas en 2005. En el año 2015 el mayor mercado de plásticos correspondió al envase y embalaje con alrededor del 36%. Sin embargo, el sector del envase y embalaje generó cerca de un 47% del total de desperdicios plásticos en el mismo año, al tratarse de productos de uso y desecho rápido. Entre 1950 y 2015, se produjeron más de 8300 millones de toneladas de plásticos, de los cuales sólo el 10% fueron reciclados y el 9% han sido incinerados. Alrededor del 60% de dichos plásticos (4900 millones de toneladas) fueron desechados y acumulados en vertederos o distribuidos en la naturaleza (Geyer et al., 2017). Los rayos solares fragmentan dichos desechos plásticos en pequeñas partículas de pocos milímetros o micrómetros, que se propagan por el planeta alcanzando incluso los océanos, amenazando así los ecosistemas marinos (Andrady, 2015). Estos hechos generan mayor

concienciación tanto en la comunidad científica como en la industrial sobre el impacto de los plásticos derivados del petróleo en el medio ambiente y la salud. Además de las cuestiones medioambientales, los plásticos convencionales tienen el inconveniente a largo plazo de estar producidos mediante fuentes limitadas, como son el petróleo y el gas natural. Varias estrategias han sido aplicadas para solventar dichas cuestiones, así como para gestionar los desperdicios plásticos, que incluyen el reciclaje de plásticos y su uso en procesos de recuperación de energía.

Los plásticos bio-basados están siendo extensamente estudiados en los últimos años para evaluar su posible aplicación como sustitución sostenible a los plásticos convencionales (Chandra & Rustgi, 1998). Además, constituyen una alternativa de fuentes renovables mientras que los recursos fósiles son limitados. Algunos bioplásticos, que son producidos por plantas o bacterias, tienen el potencial de reducir la emisión de gases de efecto invernadero (GHG) por la fijación y eliminación temporal del $CO_2$ de la atmósfera. El $CO_2$ fijado es liberado al final del ciclo de vida de los bioplásticos dejando valiosas biomasas que pueden ser reutilizadas

para el crecimiento de otras plantas, lo que cierra el ciclo energético y lo hace más eficiente.

La incorporación de los biopolímeros y de los polímeros bio-basados y biodegradables en el mercado está afrontando algunas limitaciones, especialmente en su procesado y en su comportamiento (Rhim et al., 2013). La mayoría de los biopolímeros presentan limitadas propiedades mecánicas y baja temperatura de distorsión por calor. Las propiedades barrera de estos polímeros son también bajas especialmente para vapor de agua (Mihindukulasuriya & Lim, 2014). Una de las estrategias prometedoras para mejorar y afinar las propiedades físicas de los biopolímeros consiste en la adición de rellenos en la matriz del polímero. Una amplia variedad de materiales han sido usados como relleno en los plásticos produciendo mejoras en sus propiedades mecánicas, tales como negro de carbono, talco, vidrio y sílice (Andrady, 2015). Recientemente se han relatado mejoras en el comportamiento mecánico y en las propiedades barrera de diferentes filmes biopoliméricos a través de la adición de rellenos de nano y micropartículas. Por ejemplo, los nanocristales y microcristales de

celulosa, nanopartículas metálicas y nanoarcillas (Montero et al., 2016; Rhim et al., 2013; Rico et al., 2016).

El principal objetivo de este trabajo es la preparación y caracterización de nano y micropartículas de biopolímeros seleccionados y dirigidos al envase y embalaje alimentario convencional y activo. Las partículas obtenidas se pretenden incluir en los filmes biopoliméricos produciendo nuevos materiales biocompuestos con mejores propiedades y funciones activas. Dos biopolímeros han sido seleccionados para la preparación de nano y micropartículas. El primer biopolímero es poli(3-hidroxibutirato-co-3-hidroxivalerato) (PHBV), que es uno de los polímeros más prometedores de la familia de los polihidroxialcanoatos (PHAs), especialmente por sus mejores propiedades mecánicas y térmicas. El segundo biopolímero seleccionado es el almidón, que es uno de los biopolímeros más abundantes en la tierra, y ha sido utilizado ya en el sector del envase y embalaje alimentario, sobre todo mezclado con otros polímeros y biopolímeros.

El poli(3-hidroxibutirato-co-3-hidroxivalerato) (PHBV) es un copolímero de hidroxibutirato (HB) y hidroxivalerato (HV) hidrofóbico en diferentes proporciones molares (Bakare et al. 2016) [Figura 1.5]. Este pertenece a la familia de los polihidroxialcanoatos (PHAs) de poliésteres alifáticos que son productos naturales principalmente sintetizados por algunas bacterias como una fuente de carbono y energía (Laycock et al., 2014). Es un biopolímero completamente biodegradable (Bordes et al. 2009; Wang et al. 2013) y biocompatible (Shishatskaya et al. 2004), que es producido tanto por microorganismos como por plantas genéticamente modificadas (Baran et al. 2002). El PHBV es soluble a temperatura ambiente en cloroformo y diclorometano. También es soluble en tolueno y dimetilformamida a altas temperaturas (80 ºC- 90 ºC). Tiene muchas aplicaciones en el sector de la medicina (Meng et al. 2008), ingeniería tisular (Williams et al. 1999; Bai et al. 2015), como vehículo para la administración de fármacos (Durán et al. 2008; Vilos et al. 2013) y en la industria del envase y embalaje alimentario como sustituto de los plásticos no biodegradables tradicionales

(Chandra and Rustgi 1998; Bittmann et al. 2013; Farmahini-Farahani et al. 2015; Pawar et al. 2015).

El almidón es el segundo biopolímero más abundante en el planeta después de la celulosa. Se produce por la mayoría de las plantas verdes para almacenar energía. Su bajo coste y su amplia disponibilidad le sitúa como uno de los candidatos más interesantes entre los polímeros naturales biocompatibles y biodegradables. El almidón se está utilizando ampliamente en la industria alimentaria, industria del papel y como excipiente en la industria farmacéutica (Chiu & Solarek, 2009; Mason, 2009). Además, el almidón está llamando mucho la atención en la industria del envase y embalaje alimentario por sus potenciales aplicaciones en dicho sector, filmes comestibles y en envases compuestos (J. Castaño et al., 2014, 2012). Los almidones derivados de distintos orígenes botánicos tienen distintas proporciones y distintas masas moleculares de amilosa y amilopectina y diferentes estructuras cristalinas. Esto da como resultado diferentes propiedades físicas, así como diferente procesabilidad y posibles aplicaciones (Johanna Castaño et al., 2017; Kim et al., 2015; Srichuwong et al., 2005; Young, 1984).

A nivel molecular el almidón es principalmente un polímero de unidades de glucosa que están conectadas formando dos macromoléculas: amilosa, que está formada por unidades D-glucosa conectadas por enlaces helicoidales α-(1-4) [Figura 1.6]; y amilopectina, que es una macromolécula altamente ramificada de unidades D-glucosa conectada por enlaces α-(1-4) unidas frecuentemente a puntos de ramificación de enlaces α-(1-6) [Figura 1.7].

La quercetina [Figura 1.8] (3,3',4',5,7-pentahidroxiflavonol; nombre IUPAC: 2-(3,4-dihydroxyphenyl)-3,5,7-trihydroxy-4H-chromen-4-one) es el flavonoide natural más representativo entre la subclase de los flavonoles (H. Li et al., 2009). Se encuentra en numerosas hojas, frutos y verduras como las cebollas, las manzanas y el té, entre otras plantas (Bose et al., 2013; Jeszka-Skowron et al., 2015). La quercetina, entre otros flavonoides, ha sido extensamente estudiada a lo largo de los últimos años por sus propiedades antioxidantes, antiinflamatorias y anticancerígenas (Guazelli et al., 2013; H. Li et al., 2009; Lightfoot Vidal et al., 2016; Mohan et al., 2016; G. Wang et al., 2016). Este flavonoide natural presenta muy

baja solubilidad en agua, pero sí es soluble en etanol y en la mayoría de los solventes orgánicos. Del mismo modo es soluble en soluciones alcalinas acuosas pero sufre degradación en medios alcalinos, especialmente bajo luz (Dechene, 1951; Jurasekova et al., 2014). La quercetina tiene una máxima absorbancia en una longitud de onda de 372 nm, que puede ser detectada por espectroscopia ultravioleta-visible.

## Objetivos de la tesis

El objetivo general de esta tesis es la síntesis y caracterización de nano y micropartículas de biopolímeros obtenidos de recursos naturales para su uso en envase y embalajes alimentarios. Para alcanzar este objetivo, se han desarrollado los siguientes objetivos específicos:

1. Seleccionar una técnica sencilla y adecuada para la obtención de nano y micropartículas a partir de PHBV, así como de almidones de diferentes origenes botánicos.
2. Caracterización de las nano y micropartículas obtenidas a partir de los citados biopolímeros.
3. Estudiar la posibilidad de cargar algunas de las nano y micropartículas con antioxidantes naturales. Evaluar el porcentaje de carga, la actividad antioxidante y la cinética de la liberación.
4. Incorporación de algunas de las nano y micropartículas en filmes biopoliméricos. Estudiar los efectos de esta incorporación en las propiedades de los filmes buscando su aplicación en la industria de envase y embalaje alimentario.

**Resultados**

Se han preparado nano y micropartículas de PHBV utilizando las técnicas de la emulsificación/evaporación de solventes y nanoprecipitación. La morfología y el tamaño de las partículas obtenidas fueron controladas variando las condiciones del procedimiento. En el caso de la técnica de emulsificación/evaporación de solventes, los resultados fueron nano y micropartículas esféricas y porosas con un rango de tamaño de 300 nm hasta 20 μm. A través del control del tipo de surfactante, su concentración, la concentración del polímero, y el método de la emulsificación se consigue modificar la porosidad y la distribución del tamaño de las partículas obtenidas. Disminuyendo la concentración de la solución del polímero o aumentando la concentración del surfactante se obtienen micropartículas de tamaño inferior con menor rango de distribución de tamaños. La concentración del surfactante tienen mayor influencia sobre el tamaño de las partículas cuanto mayor sea la concentración de la solución del polímero. Se establece una comparación entre los efectos de los dos surfactantes que han sido utilizados (SDS y PVA).

Se concluye que con una concentración alta de PVA (10%) se obtienen micropartículas de menor tamaño y más homogéneas. Sin embargo, cuando se utilizó el SDS en la misma concentración se han podido conseguir nanopartículas y micropartículas simultáneamente. Se alcanzan mayores porcentajes de nanopartículas incrementando la concentración de SDS y/o disminuyendo la concentración de la solución del polímero. Para conseguir únicamente nanopartículas simplemente se debe filtrar la mezcla obtenida de nano y micropartículas. Utilizando SDS con baja concentración (5%) se producían partículas de menor dimensión y con rangos de distribución de tamaño más ajustados. En la mayoría de los casos fue necesaria la ultrasonicación para obtener las nanopartículas.

Se han logrado obtener nano y micropartículas de menor dimensión mediante la técnica de nanoprecipitación, lo que no ha sido reportado para este tipo de polímeros. La interacción entre los solventes y los antisolventes juega un papel crucial en la morfología de las partículas preparadas. Cuando se ha utilizado el etanol como antisolvente, el resultado fue de nanopartículas heterogéneas con

morfología laminar con tendencia a formar agregados. Por el contrario, para alcanzar nanopartículas de morfología esférica y micropartículas de menor tamaño, además de partículas ovaladas no uniformes, ha sido necesario hacer uso de soluciones con antisolventes de 80% de etanol y 20% de agua. El aumento de la proporción del agua en el antisolvente dio como resultado nanopartículas de morfología esférica mejor definida y separada además de menores cantidades de micropartículas de inferiores dimensiones. La mejora en la esfericidad de las nanopartículas es alcanzada con ultrasonicación en lugar de la tradicional agitación mecánica. Se han obtenido resultados similares sustituyendo el etanol por metanol.

Generalmente el control de la polaridad del antisolvente es fundamental si se quieren obtener nano y micropartículas esféricas. El porcentaje de agua se debe ajustar para garantizar la miscibilidad entre el solvente y el antisolvente. Se logró obtener nanopartículas de PHBV utilizando DMF como solvente y agua como antisolvente, teniendo en cuenta que la polaridad del agua se ha reducido gracias al aumento de la fuerza iónica con la adición de sal. La técnica de la

nanoprecipitación en la preparación de las nanopartículas de PHBV ha favorecido su producción por ser más simple, barata y requerir menor tiempo, logrando así alto rendimiento.

Se utilizaron almidones de diferente origen botánico para preparar nanopartículas de almidón, utilizando la técnica de nanoprecipitación. Dichas nanopartículas fueron esféricas y su tamaño y polidispersidad aumenta con el incremento de la concentración del almidón. El origen del almidón tiene un efecto significativo sobre el comportamiento de estas nanopartículas a nivel nanométrico, ya que diferentes almidones presentan diferentes masas moleculares y diferente proporción amilosa/amilopectina. Se produjeron nanopartículas de distintos almidones cargados con quercetina. La capacidad de carga y el comportamiento de la liberación de la quercetina sobre la nanopartícula, y como consecuencia su actividad antioxidante, cambia con el origen del almidón. Las nanopartículas de almidón de maíz – quercetina son las que menor porcentaje de carga de quercetina presentaban, y por lo tanto menor actividad antioxidante y menor cantidad de liberación. Las nanopartículas de almidón de patata mostraban un ligero

aumento de la capacidad de carga frente a las nanopartículas de almidón de guisante. Esta diferencia puede deberse al mayor contenido de amilopectina que presenta el almidón de patata, lo que le aporta mayor eficiencia en la inmovilización de la molécula de la quercetina, caso contrario a la amilosa, molécula de morfología lineal, extensa y rígida. Las nanopartículas de almidón de patata y guisante mostraban una fracción similar de liberación de la quercetina, más alta que en las nanopartículas de almidón de maíz. La cinética de la liberación de la quercetina sobre las nanopartículas de almidón – quercetina parece ser controlada principalmente por la difusión de Fickian, lo que sido revelado aplicando el modelo de Peppas–Sahlin.

Se prepararon micropartículas de almidón con forma de donut a través de tratamiento acuoso – alcohólico. El tratamiento térmico de la suspensión del almidón y la adición del etanol como precipitado conduce a la ruptura parcial de la estructura supra-macromolecular y por consiguiente la distorsión de la cristalinidad dentro de los gránulos del almidón. La disposición doble helicoidal de los gránulos se convierte en una única hélice, donde podrá

penetrar más fácilmente el agua cuanto más abierta sea su estructura. De este modo las micropartículas con forma de donut mostraban mayor solubilidad y capacidad de hinchamiento, así como temperatura de gelatinización más alta y menor entalpía de gelatinización, comparada con los gránulos de almidón. La facilidad y simplicidad del método de preparación, y la notable estabilidad de las micropartículas con forma de donut durante los 18 meses de estudio, lo sugiere adecuado para preparar micropartículas que actúen como vehículos portadores de compuestos activos y como relleno para varias aplicaciones en el sector del envase y embalaje de alimentos.

Las micropartículas con forma de donut preparadas a partir de dos orígenes botánicos diferentes fueron cargadas en filmes del mismo origen botánico para hacer TPS. Los patrones de difracción de rayos X mostraban tanto cristalinidad residual como inducida por el procesado de los (TPS) filmes. La incorporación de las micropartículas aumenta la estabilidad térmica de los filmes generados. Además, la estabilidad térmica se incrementa aún más aumentando el porcentaje de las micropartículas de 10% a 15%. La

adición de micropartículas de guisante en filmes de almidón termoplásticos (PTPS) hace disminuir significativamente la tasa de transmisión de vapor de agua. Sin embargo, la tasa de transmisión de vapor de agua en filmes termoplásticos de almidón de maíz (CTPS) descendió ligeramente al aumentar el contenido de micropartículas dentro del film. Esto puede ser debido a que las micropartículas procedentes del maíz presentan mayor capacidad de hinchamiento frente a las procedentes del guisante, que tienen menor eficacia como barrera de vapor de agua, como se expone en el capítulo 5. La incorporación de las micropartículas en los filmes de ambos orígenes hizo descender considerablemente la permeabilidad de oxígeno, en función del porcentaje de estas. Ajustar el porcentaje de las micropartículas en los filmes termoplásticos permite dejar pasar la cantidad deseada de oxígeno y vapor de agua en el envase alimentario. Esto es de vital importancia para conservar los alimentos envasados de forma fresca y sana el máximo tiempo posible.

Se han producido filmes de almidón proveniente de guisante y maíz, cargado de micropartículas de almidón – quercetina con

forma de donut, en diferentes proporciones, completamente biodegradable, biocompatible y comestible. Se ha hallado que el origen del almidón tiene un impacto importante en la caracterización de este tipo de micropartículas así como en los filmes. A nivel de micropartículas, el almidón procedente del cereal mostraba menor porcentaje de carga de quercetina, lo que hace disminuir la actividad antioxidante frente a las micropartículas cuyo origen es la legumbre. Las micropartículas de almidón–quercetina resultantes eran ligeramente más estables térmicamente que los gránulos originales. La degradación térmica oxidativa en las micropartículas de almidón de guisante – quercetina se inicia a 280 ºC frente a 269 ºC en gránulos del mismo almidón. Esto ocurre de manera similar en el caso de las micropartículas de almidón de maíz – quercetina (278 ºC) frente a los gránulos del mismo (269 ºC). Los filmes basados en almidón de cereal parecen ser adecuados a muy corto plazo en aplicación de liberación de compuestos activos debido al rápido ritmo de liberación de la quercetina (de 1 a 4 días en función de la concentración de las micropartículas). Por otra parte, los filmes basados en almidón de legumbre continúan la liberación durante

periodos más largos, haciéndolos adecuados para aplicaciones en las que la quercetina requiere para su liberación de más de 1 semana. Los filmes de almidón de guisante que contienen un 15% de micropartículas de almidón – quercetina continúan la liberación más de 10 días [Figura 6.44]. Sin embargo, Los experimentos de liberación in-vitro se finalizaron después de 11 días, debido a que la espectroscopia ultravioleta visible mostró un nuevo máximo en una longitud de onda de 295 nm [Figura 6.45]. Este dato indica la pérdida de la conjugación del cromóforo, es decir, la degradación de la quercetina (Dall'Acqua et al., 2012). El mecanismo de liberación de todos los filmes parece ser debido a difusión no dependiente de la concentración. Esto ha sido confirmado adecuando los datos de liberación experimental del primer 60% de la fracción de quercetina liberada en el modelo de Peppas-Sahlin, tomando en consideración el tiempo de retraso requerido para comenzar el proceso de liberación. Los filmes que contienen mayor cantidad de micropartículas mostraban una mayor estabilidad térmica. Los biofilmes producidos pueden ser utilizados principalmente en aplicaciones de envase y embalaje alimentario activo.

## Conclusión

Se han producido nanopartículas y micropartículas procedentes de dos diferentes biopolímeros de recursos naturales a través de técnicas sencillas. La incorporación de algunas de estas partículas en filmes biopoliméricos lleva a mejoras significativas en las propiedades de dichos filmes, especialmente las propiedades barrera. Algunas de las partículas producidas también muestran la capacidad de liberación de compuestos activos durante periodos de tiempo razonables. Estos resultados prometedores abren la puerta a varias posibilidades, entre ellas, la mejora de las propiedades de más tipos de filmes biopoliméricos, con potenciales aplicaciones en el sector del envase y embalaje alimentario convencional y activo.

**Referencias**

Andrady, A. L. (2015). Plastics and Environmental Sustainability. Plastics and Environmental Sustainability. http://doi.org/10.1002/9781119009405

Bose, S., Du, Y., Takhistov, P., & Michniak-Kohn, B. (2013). Formulation optimization and topical delivery of quercetin from solid lipid based nanosystems. International Journal of Pharmaceutics, 441(1–2), 56–66. http://doi.org/10.1016/j.ijpharm.2012.12.013

Castaño, J., Bouza, R., Rodríguez-Llamazares, S., Carrasco, C., & Vinicius, R. V. B. (2012). Processing and characterization of starch-based materials from pehuen seeds (Araucaria araucana (Mol) K. Koch). Carbohydrate Polymers, 88(1), 299–307. http://doi.org/10.1016/j.carbpol.2011.12.008

Castaño, J., Rodríguez-Llamazares, S., Contreras, K., Carrasco, C., Pozo, C., Bouza, R., … Giraldo, D. (2014). Horse chestnut (Aesculus hippocastanum L.) starch: Basic physico-chemical characteristics and use as thermoplastic material. Carbohydrate Polymers, 112, 677–685. http://doi.org/10.1016/j.carbpol.2014.06.046

Castaño, J., Rodríguez-Llamazares, S., Sepúlveda, E., Giraldo, D., Bouza, R., & Pozo, C. (2017). Morphological and structural changes of starch during processing by melt blending. Starch - Stärke, 68, 1–9. http://doi.org/10.1002/star.201600247

Chandra, R., & Rustgi, R. (1998). Biodegradable polymers. Progress in Polymer Science, 23(7), 1273–1335. http://doi.org/10.1016/S0079-6700(97)00039-7

Chiu, C. wai, & Solarek, D. (2009). Modification of Starches. Starch (Third Edit). Elsevier Inc. http://doi.org/10.1016/B978-0-12-746275-2.00017-3

Dall'Acqua, S., Miolo, G., Innocenti, G., & Caffieri, S. (2012). The photodegradation of quercetin: Relation to oxidation. Molecules, 17(8), 8898–8907. http://doi.org/10.3390/molecules17088898

Dechene, E. B. (1951). The relative stability of rutin and quercetin in alkaline solution. Journal of the American Pharmaceutical Association., 40(10), 495–497. http://doi.org/10.1002/jps.3030401005

Geyer, R., Jambeck, J. R., & Law, K. L. (2017). Production, use, and fate of all plastics ever made. Science Advances, 3(7), e1700782. http://doi.org/10.1126/sciadv.1700782

Guazelli, C. F. S., Fattori, V., Colombo, B. B., Georgetti, S. R., Vicentini, F. T. M. C., Casagrande, R., … Verri, J. W. A. (2013). Quercetin-loaded microcapsules ameliorate experimental colitis in mice by anti-inflammatory and antioxidant mechanisms. Journal of Natural Products, 76(2), 200–208. http://doi.org/10.1021/np300670w

Jeszka-Skowron, M., Krawczyk, M., & Zgoła-Grześkowiak, A. (2015). Determination of antioxidant activity, rutin, quercetin, phenolic acids and trace elements in tea infusions: Influence of citric acid addition on extraction of metals. Journal of Food Composition and Analysis, 40, 70–77. http://doi.org/10.1016/j.jfca.2014.12.015

Jurasekova, Z., Domingo, C., Garcia-Ramos, J. V, & Sanchez-Cortes, S. (2014). Effect of pH on the chemical modification of quercetin and structurally related flavonoids characterized by optical (UV-visible and Raman) spectroscopy. Physical Chemistry Chemical Physics, 16(25), 12802–12811. http://doi.org/10.1039/c4cp00864b

Kim, H. Y., Park, S. S., & Lim, S. T. (2015). Preparation, characterization and utilization of starch nanoparticles. Colloids and Surfaces B: Biointerfaces, 126, 607–620. http://doi.org/10.1016/j.colsurfb.2014.11.011

Laycock, B., Halley, P., Pratt, S., Werker, A., & Lant, P. (2014). The chemomechanical properties of microbial polyhydroxyalkanoates. Progress in Polymer Science, 39(2), 397–442. http://doi.org/10.1016/j.progpolymsci.2013.06.008

Li, H., Zhao, X., Ma, Y., Zhai, G., Li, L., & Lou, H. (2009).

Enhancement of gastrointestinal absorption of quercetin by solid lipid nanoparticles. Journal of Controlled Release, 133(3), 238–244. http://doi.org/10.1016/j.jconrel.2008.10.002

Lightfoot Vidal, S., Rojas, C., Bouza Padin, R., Perez Rivera, M., Haensgen, A., Gonzalez, M., & Rodriguez-Llamazares, S. (2016). Synthesis and characterization of polyhydroxybutyrate-co-hydroxyvalerate nanoparticles for encapsulation of quercetin. Journal of Bioactive and Compatible Polymers, 31(5), 439–452. http://doi.org/10.1177/0883911516635839

Mason, W. R. (2009). Starch Use in Foods. Starch (Third Edit). Elsevier Inc. http://doi.org/10.1016/B978-0-12-746275-2.00020-3

Mihindukulasuriya, S. D. F., & Lim, L. T. (2014). Nanotechnology development in food packaging: A review. Trends in Food Science and Technology, 40(2), 149–167. http://doi.org/10.1016/j.tifs.2014.09.009

Mohan, L., Anandan, C., & Rajendran, N. (2016). Drug release characteristics of quercetin-loaded TiO nanotubes coated with chitosan. International Journal of Biological Macromolecules, 4–9. http://doi.org/10.1016/j.ijbiomac.2016.04.034

Montero, B., Rico, M., Rodríguez-Llamazares, S., Barral, L., & Bouza, R. (2016). Effect of nanocellulose as a filler on biodegradable thermoplastic starch films from tuber, cereal and legume. Carbohydrate Polymers. http://doi.org/10.1016/j.carbpol.2016.10.073

Rhim, J.-W., Park, H.-M., & Ha, C.-S. (2013). Bio-nanocomposites for food packaging applications. Progress in Polymer Science, 38(10–11), 1629–1652. http://doi.org/10.1016/j.progpolymsci.2013.05.008

Rico, M., Rodríguez-Llamazares, S., Barral, L., Bouza, R., & Montero, B. (2016). Processing and characterization of polyols plasticized-starch reinforced with microcrystalline cellulose. Carbohydrate Polymers, 149, 83–93. http://doi.org/10.1016/j.carbpol.2016.04.087

Srichuwong, S., Sunarti, T. C., Mishima, T., Isono, N., &

Hisamatsu, M. (2005). Starches from different botanical sources I: Contribution of amylopectin fine structure to thermal properties and enzyme digestibility. Carbohydrate Polymers, 60(4), 529–538. http://doi.org/10.1016/j.carbpol.2005.03.004

Wang, G., Wang, J. J., Chen, X. L., Du, L., & Li, F. (2016). Quercetin-loaded freeze-dried nanomicelles: Improving absorption and anti-glioma efficiency in vitro and in vivo. Journal of Controlled Release, 235, 276–290. http://doi.org/10.1016/j.jconrel.2016.05.045

Young, A. H. (1984). Chapter VIII – Fractionation of starch. In Starch: Chemistry and Technology (Second edi, pp. 249–283). http://doi.org/10.1016/B978-0-12-746270-7.50014-8